CHALMERS

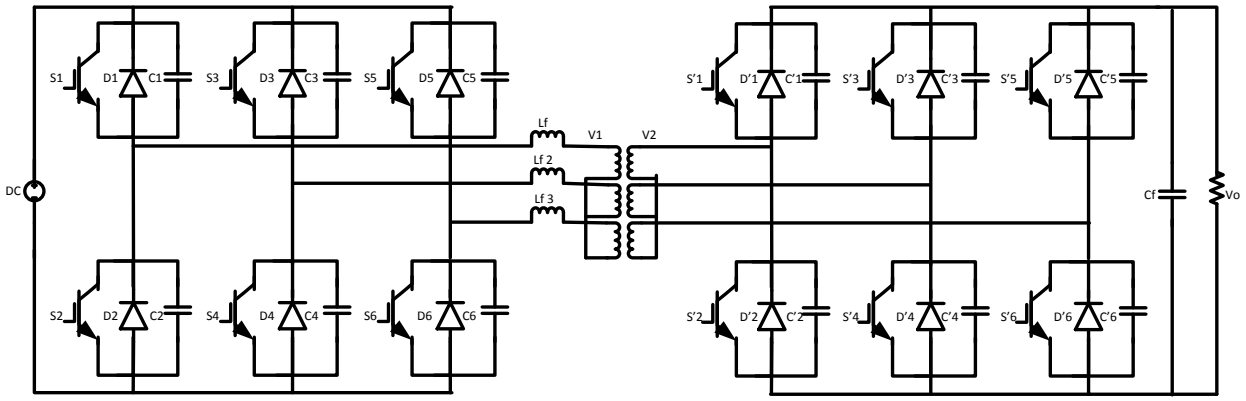

Design and implementation of a proper modulation and control scheme for a single and three phases Dual Active Bridge Converter

Mohammad Sadegh Moeinian

Department of Energy and Environment
Division of Electric Power Engineering
CHALMERS UNIVERSITY OF TECHNOLOGY
Göteborg, Sweden, 2014

Design and implementation of a proper modulation and control scheme for a single and three phase Dual Active Bridge Converter

Mohammad Sadegh Moeinian

Examiner: Torbjörn Thiringer

Supervisor: Mohammad Amin Bahmani

Technical Report 2014:1
Department of Energy and Environment
Division of Electric Power Engineering
CHALMERS UNIVERSITY OF TECHNOLOGY
SE-41296 Göteborg
Sweden

To my lovely father,

Mohammad Reza Moeinian

Abstract

In this master thesis, the aim is to implement the single and three phase Dual Active Bridge converter both with simulation and experimentally. In the first phase of the thesis, as a case study, the single and three phase DAB converter are simulated in the PLECS software. The phase shift method has been implemented in order to control the converter. The operation frequency of the simulation is 5 KHz and the input and output voltage of the converters are 3KV and 6KV respectively. The transmitted power is 2MW. In the second phase of the project, the single phase dual active bridge has been implemented in the laboratory by using the dSPACE controller. The DAB converter has been tested for the frequencies of 50, 500 Hz and 1 KHz and for the maximum power of 0.5 KW. The maximum input and output voltage is 80 and 144 volts respectively. All tests for different voltage levels and frequencies have been done by simulation as well and the simulation results have been verified by the experimental results. The same tests also have been done for the three phase DAB converter which is implemented in the laboratory. These tests have been done for the frequency of 55 and 555 Hz and for the maximum power of 1.5 KW. The simulation results are also verified by the experimental results. In the last phase of the thesis, soft switching has been implemented by using snubber capacitors on both the single and three phase DAB converter and the results have been compared with the previous results.

The highest possible frequency for the Single phase dual active bridge used in this thesis is 1 KHz and the highest possible frequency for the three phase case is 555 KHz by using the digital implementation of the dSPACE controller. The accuracy of the phase shift for the single phase DAB converter for the frequency of 1 KHz is 3.6 degrees and for the three phase DAB converter for the frequency of 555 Hz is 2 degrees.

Loss calculation also has been done theoretically, for the simulation and also for the experimental tests. The results show that the implemented DAB converter has higher losses for higher frequencies. The implemented three phase DAB converter also has higher losses than the single phase one in this thesis due to the higher cabling and switching losses.

Keywords

Single phase dual active bridge, three phase dual active bridge, dSPACE controller

Acknowledgment

I would like to take this opportunity to thank my examiner Torbjörn Thiringer for his great support, encouragement and for giving me the opportunity to do my master thesis in the Division of Electric Power Engineering in Chalmers University. I really appreciate it.

I would like to thank Mahsa Abbasian, my wife, for her patience, support and love. She really encouraged me to do my master thesis in the field which I liked it but left it for some years.

My special thanks go to Amin Bahmani, my supervisor, for his time, constant guidance and patience. He really gave me calmness during the project.

My thanks go to the other people who helped me in this thesis, Saeid Haghbin, Ali Rabiei and my lovely cousin Alireza Abbasian.

Last but not least, I would like to thank my mother Zahra, my sister Maryam, my brother Ahmad and friends who support and motivate me during my whole life.

Mohammad Sadegh Moeinian

Göteborg, May 2014

Preface

This work was done as an M.Sc thesis for Linköping University. However, the work itself was conducted at Chalmers University of technology with the supervisors Torbjörn Thiringer and Mohammad Amin Bahmani.

Table of Contents

Contents

1. Introduction 1

1.1. Problem Background 1

1.2. Previous Work 1

1.3. Purpose 2

2. Collection of known usable Theory 3

2.1. Dual Active Bridges Converter 3

2.2. Phase shift control 4

2.2.1 Single phase Dual active bridge 5

2.2.2 Three phase Dual active bridge 5

2.3. dSPACE controller 6

2.3.1 dSPACE board 7

2.3.2 RTI interface 8

2.3.3 Digital implementation limitation 9

2.4. Soft Switching 10

2.4.1 Snubber capacitor 11

2.5. Loss calculation 12

2.5.1 IGBT and diode losses 12

2.5.1.1 Conduction losses 12

2.5.1.2 Switching losses 13

2.5.1.3 Transformer calculation 14

3. Case Set-Up 15

3.1. Component selections of DAB Converter 15
3.1.1 IGBT 15
3.1.2 Diode 17
3.1.3 Transformer 17
3.1.4 Snubber capacitor setup 21
3.2. Modeling of the Dual Active Bridges in software 23
3.3. Experimentaly Implementation of the Dual Avtive Bridge 26
3.3.1 dSPACE controller setup 26
3.3.2 Dual Active Bridge converter setup 28
4. Analysis 31
4.1. Analysis of Simulations Results 31
4.1.1 Single phase dual active bridge simulation 31
4.1.2 Three phase dual active bridge simulation 35
4.2. Analysis of Experimental Results 37
4.2.1 Single phase dual active bridge experimental results 37
A. Analysis of the single phase DAB at 50 Hz 39
B. Analysis of the single phase DAB at 100 Hz 41
C. Analysis of the single phase DAB at 500 Hz 42
D. Analysis of the single phase DAB at 1 KHz 43
4.2.2 Three phase dual active bridge experimental results 44
A. Analysis of the three phase DAB at 50 Hz 45
B. Analysis of the three phase DAB at 100 Hz 46
C. Analysis of the three phase DAB at 500 Hz 46
4.2.3 Analysis of the DAB converter by using the snubber capacitor 47
4.3 Loss calculation for both the single and three phase DAB converter 52

4.3.1 Loss calculation for the first test of the single phase DAB converter 53
4.3.2 Loss calculation for the second test of the single phase DAB converter 57
4.3.3 Loss calculation for the third test of the single phase DAB converter 59
4.3.4 Loss calculation for the fourth test of the single phase DAB converter 61
4.3.5 Loss calculation for the fifth test of the single phase DAB converter 64
4.3.6 Loss calculation for the first test of the three phase DAB converter 66
4.3.7 Loss calculation for the second test of the three phase DAB converter 69
4.3.8 Loss calculation for the third test of the three phase DAB converter 71
4.4 Comparison between Simulation and Experimental Results 74
4.4.1 Single phase dual active bridge 74
4.4.2 Three phase dual active bridge 78
5. Conclusion 81
6. Future work 82
7. References 83
8. Appendix 84

1. Introduction

1.1.Problem Background

Nowadays, the world moving toward using more renewable resources. Many researches, much investment and annually progress rate of wind energy which is about 30 percent show that wind power has a potential to become one of the most important supplying energy resources in the next decades. Some researchers like Mark Z. Jacobson and Mark A. Delucchi accessed that the wind energy with solar and water energy could supply more than the whole of the world demanding energy by 2030. According to them, there isn't any problem to reach this point in terms of technology and economy but the problem is more politically and socially. In their points of view, the solar energy has peak production during the daytime and this energy and wind energy can supply 90 percent of the worldwide demanding energy complementary. Hydropower can supply the gap and also tidal and geothermal energy can complement it. The main problem here is the long distance between the locations where the offshore wind turbine and solar power plants are installed and consumer's location. In this point of view, the transmission loss of electricity plays an important role in order to reach this goal to connect the wind energy production and solar energy production. The HVDC transmission lines have significantly lower transmission losses in comparison to the conventional AC transmission lines for a long distance which gives them the opportunity to be used instead of AC transmission lines. One of the main devices in HVDC transmission installation is the DC-DC converter which is used to replace the bulky conventional transformer as voltage level adjusting element. One of the promising topologies in this case is dual active bridge converters which can decrease the losses by using soft switching modulation schemes.

1.2.Previous Work

Due to the importance of this issue, many investigations have been done on DC-DC converters and also on the SAB and DAB converters. The DAB topology is one of the isolated bidirectional dc-dc converter (IBDC) topologies. The dual fly back, forward fly back, dual push pull, full bridge forward and half full bridge are examples of the IBDC topologies with two till six switches in their circuits respectively. The Dual active bridge topology with eight and twelve switches was proposed by Doncker in 1991[1]. Both single-phase and triple-phase DAB converters were presented for high-power density high-power applications and they operated in a soft-switching manner in order to decrease the switching losses. However, due to the performance limitation of power devices, the power losses of DAB converters were high and the efficiency was low. Moreover, the DAB topology did not reach the new stage of development and just some few studies had been done on it on that time. Development of the power devices and magnetic materials (especially the SiC- and GaN-based power devices and iron-based nano-crystalline soft magnetic) in recent years, make the DAB converter feasible for replacing the bulky and heavy 50/60 Hz transformer. So, the

DAB topology is become interesting for many researchers nowadays. The researches on the DAB converter are mainly focus on basic principle, control method, soft-switching solution and hardware design and optimization. [5]

1.3.Purpose

The purpose of this master thesis is to design and implement a proper modulation and control scheme for a medium frequency transformer based Dual Active Bridge Converter. Since this converter is missing at Chalmers University of Technology, the main part of the thesis is to implement the DAB converter in the laboratory. The first preliminary aim is to implement a suitable control scheme for the single phase DAB converter. The second aim is to implement it experimentally and make comparisons between simulated and experimental results. In the next step, the tree-phase DAB converter is going to be implemented both by simulation and in the laboratory and make comparison between them. The comparison will be done as well between the single-phase and triple-phase dual active bridges.

2. Collection of known usable Theory

2.1 Dual Active Bridge Converter

These days there are many topologies of DC-DC converters and the different variants have advantages and disadvantages. One of topology which was first introduced by Doncker is the Dual Active Bridge converter. There are two types of DAB converters, the single-phase and three-phase. This converter consists of one Inverter Bridge which converts the DC voltage to AC voltage and one Rectifier Bridge which converts the AC voltage to DC voltage and the two bridges are connected to each other by a transformer. The inverter bridge in the single-phase DAB has four switches and diodes, the same as the rectifier bridge while in the three-phase DAB, each bridge has six switches. The advantages which can be mentioned are electrical insulation of the DAB converter and soft switching possibility in both the primary and secondary circuits of the converter. Disadvantage of the DAB converter is that, many switches are used in the converter which makes it expensive and also lead to complex control.

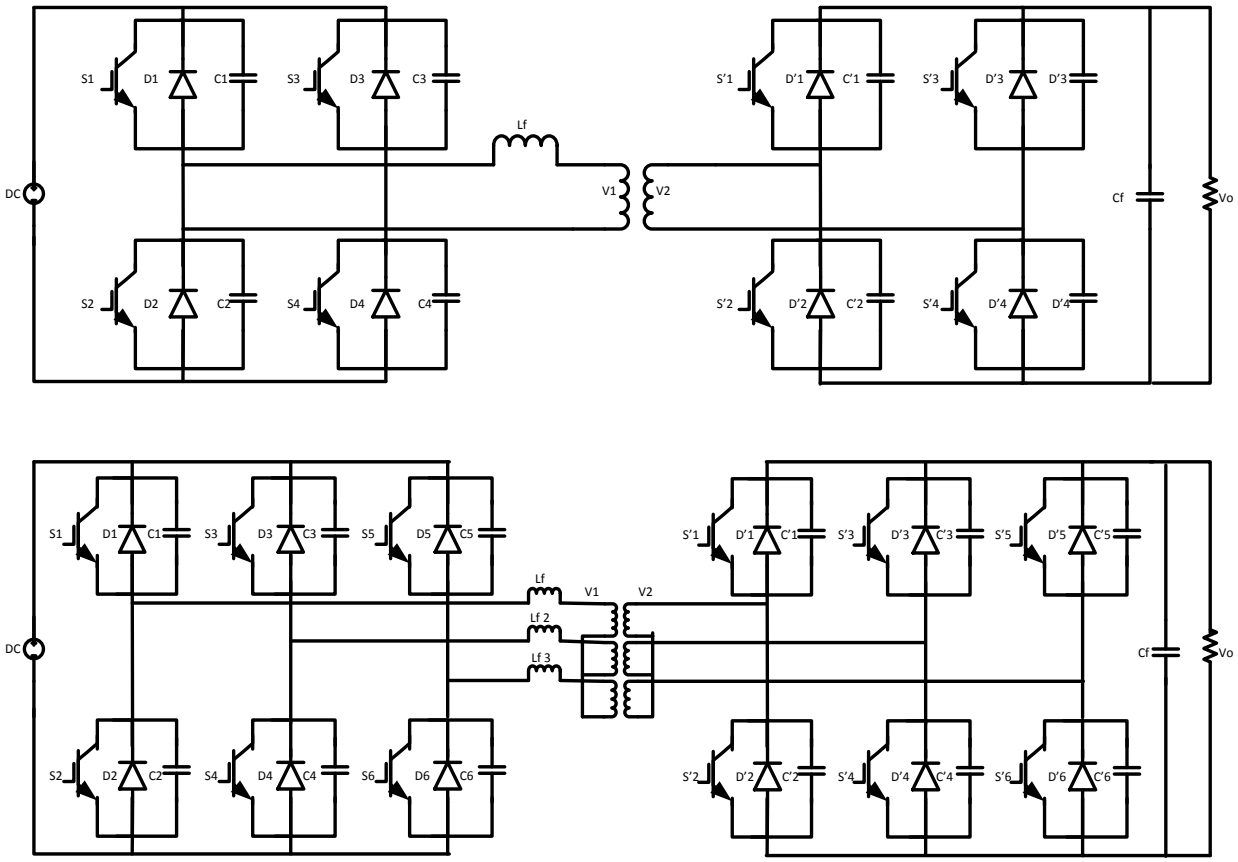

Fig. 2.1 Dual Active Bridge Converter (single phase & three phase)

Soft switching can also be lost in a high load and there is high ripple current in the output capacitor filter as well. The scheme of a single-phase and a triple-phase DAB converter can be seen in figure 2.1.

There are several methods to control the Dual active bridge switches. One of the traditional control methods which are going to be implemented in this thesis is phase shift controlling of the switches and making phase shift between bridges of the converter. This will be explained in the next section.

2.2 Phase shift control

There are some different modulation methods in order to control the switches of the dual active bridge converter which have different properties. One of these methods is the phase shift control. In this method, each diagonal pair of switches in both the inverter and rectifier bridge of the DAB converter are operating during 50 percent of the period but with a specified phase shift, which should be defined, between the inverter and rectifier bridges. In the following section, the phase shift control is explained for both the single and three phase DAB converter. Figure 2.2 shows the control method for both converters.

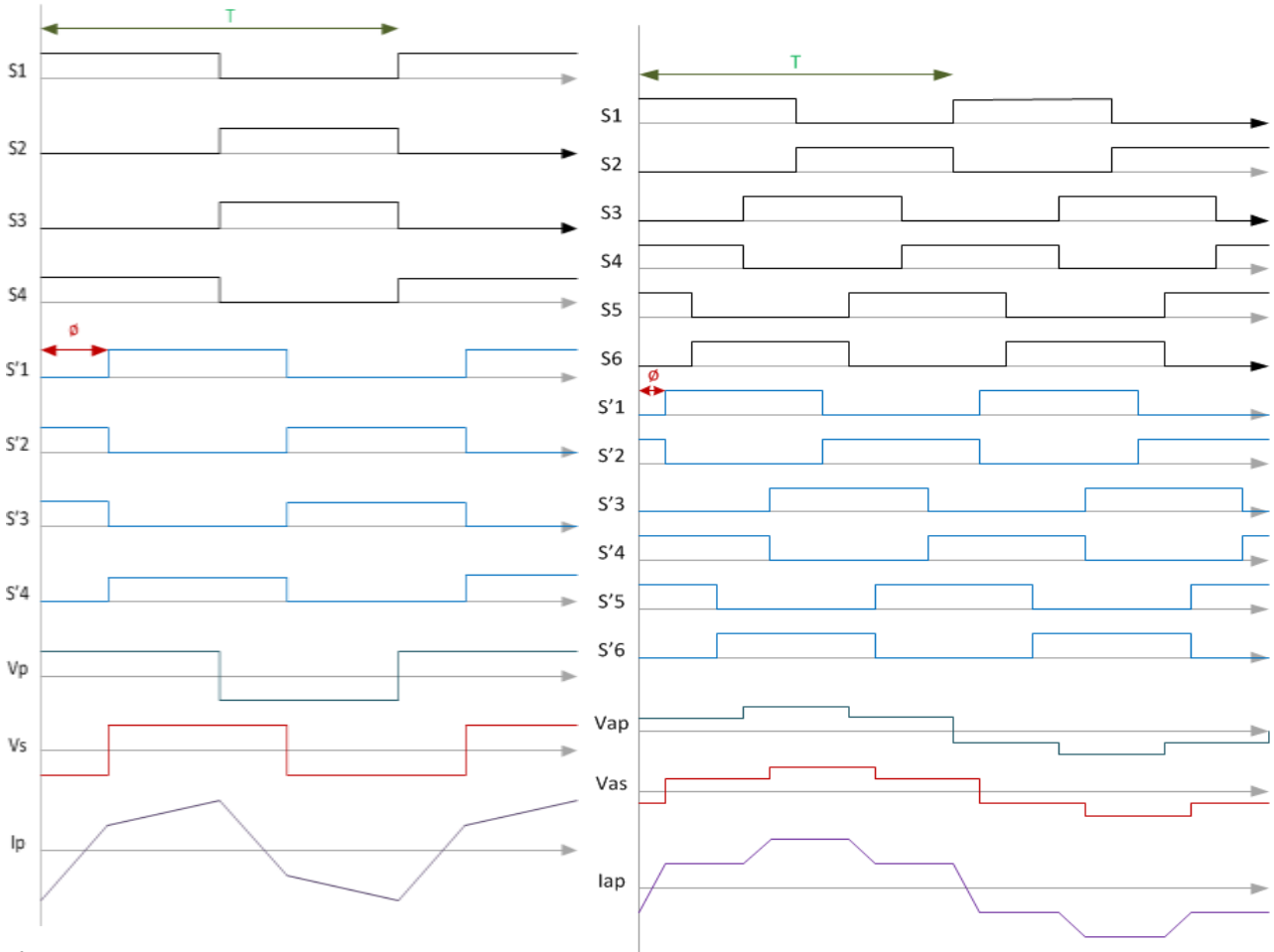

Fig. 2.2: *Phase shift control for the single (left) and three (right) phase dual active bridge converter*

2.2.1 Single phase Dual Active Bridge

In order to implement the phase shift control in the single phase DAB converter, switches S1 and S4 are conducting for half of the period and switches S2 and S3 are conducting for the other half of the period. At the same time with a specified delay and phase shift, switches S'1 and S'4 are operating for one half period and Switches S'2 and S'3 are operating for the other half of the period. By shifting the phase between the inverter and rectifier bridge, the transferred power can be controlled. The relation between the phase shift angle ***(ø),*** input and output voltage (V_{in} & V_{out}), output power (P_o), operation frequency of the converter *(f)* and the transformer ratio of converter *(n)* is given by

$$P_o = \frac{V_i^2}{\omega L} d\emptyset \left(1 - \frac{\emptyset}{\pi}\right) \tag{2.1}$$

where *d* can be calculated by

$$d = \frac{\mathrm{V_o}}{nV_i} \tag{2.2}$$

where *n* is defined as the ratio of the transformer in the converter. According to the equation, it can be seen that the maximum value of output power can be reached when the phase shift control ***(ø)*** is equal to $\frac{\pi}{2}$.

2.2.2 Three phase Dual Active Bridge

In the three phase dual active bridge, the same as in the single phase DAB, a phase shift should be implemented between the inverter and rectifier bridges. Each switch in both bridges is conducting with the duty cycle of 50 % but with different phases. The switches S1, S3 and S5 are conducting with a 120 degrees phase shift with each other. The switches S2, S4 and S6 are conducting with 120 degree phases shift with each other and also 180 degree phase shift with switches S1, S3 and S5 respectively. The switches S'1-S'6 are conducting in the same way as the switches S1-S6 but by considering the implemented phase

shift between the two bridges. Table 2.1 shows the switching schema for the inverter bridge of the three phase DAB converter. Figure 2.2 also shows the switching in a perfect way.

Table 2.1 The switching schema of the inverter bridge of three phase DAB converter

period	$0-\frac{\pi}{3}$	$\frac{\pi}{3}-\frac{2\pi}{3}$	$\frac{2\pi}{3}-\pi$	$\pi-\frac{4\pi}{3}$	$\frac{4\pi}{3}-\frac{5\pi}{3}$	$\frac{5\pi}{3}-2\pi$
Triggered switches	S1,S4,S5	S1,S4,S6	S1,S6,S3	S6,S3,S2	S3,S2,S5	S2,S5,S4

The rectifier bridge switches S'1-S'6 are triggered in the same way as of the switches of the inverter bridge but with the defined phase shift of $\emptyset$. For example the switch S'1 is triggered at the phase of $0+\emptyset$ and become off at a phase of $\pi+\emptyset$. The relation between the phase shift angle (**ø**), input and output voltage (V_{in} & V_{out}), output power (P_o), operation frequency of the converter (f) and transformer ratio of the three phase DAB converter (n) is given by

$$P_o=\frac{V_i^2}{\omega L}d\emptyset\left(\frac{2}{3}-\frac{\emptyset}{2\pi}\right) \qquad for \qquad 0\le\emptyset\le\frac{\pi}{3} \tag{2.3}$$

and,

$$P_o=\frac{V_i^2}{\omega L}d\left(\emptyset-\frac{\emptyset^2}{\pi}-\frac{\pi}{18}\right) \qquad for \qquad \frac{\pi}{3}\le\emptyset\le\frac{2\pi}{3} \tag{2.4}$$

According to the equations, it can be seen that the maximum value of output power can be reached when the phase shift control (**ø**) is equal to $\frac{\pi}{2}$, the same as the single phase dual active bridge.

2.3 dSPACE controller

dSPACE is a hardware and software package. The idea of this package is to use MatLab and especially Simulink in real-time applications. In order to do it in a simple way, the special hard- and software have been developed with a control system called dSPACE. By using this controller, it is possible to construct block diagrams in Simulink as controller and then send signals to the real system by using the dSPACE interface. The procedure is: The constructed block diagrams in Simulink that are translated to C-codes by the Matlab toolbox Real-Time Workshop. The dSPACE real-time interface (RTI) compiles these C-codes into the digital signal processor (DSP). When codes are set on the DSP and are loaded into the software which is called Control Desk, then it is possible to create virtual instrument panels. This software makes it easy to change the parameters in real-time. Moreover, during the simulation, data can be stored in the software and be analyzed later in MatLab. The DSP board communicates with the real system via an I/O board with different connectors. Figure 2.3 shows and explain the whole procedure.

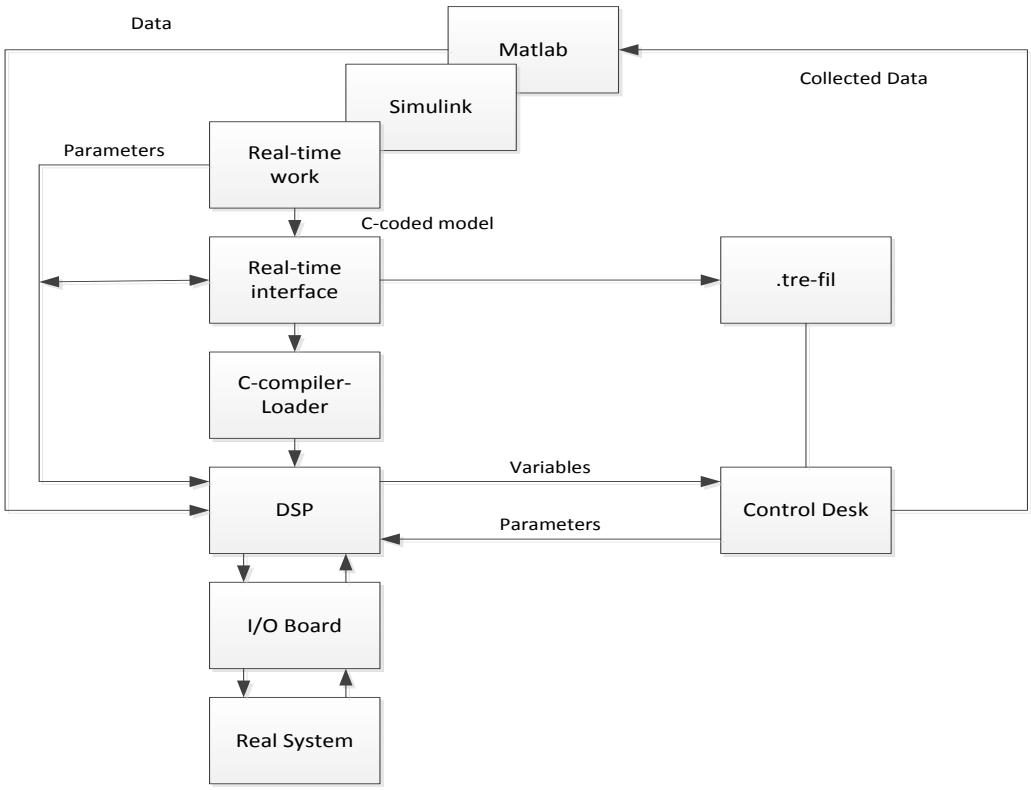

Fig. 2.3: *Function diagram for dSPACE and MatLab.*

2.3.1 dSPACE boards

There are many dSPACE boards with different specifications. Some types are the single board hardware like DS1103 and DS 1104. The other types are modular hardware like DS 1005 and DS 1006 and many other types. The one which is used in this thesis is the DS1103 PPC controller Board. This controller is the single-board system with real time processors and has high I/O speed and accuracy. This board is designed to meet the requirements of modern rapid control prototyping and suitable for applications such as: Robotics, induction motor control, automotive controllers and so on. "It provides different interfaces like 50-bit I/O channels, 36 A/D channels, and 8 D/A channels. For additional I/O tasks, a DSP controller unit built around Texas instruments' TM320F240 DSP is used as a subsystem". (dSPACE Catalog-2013). The dSPACE I/O Board has many input and output connectors for different measurements and controlling signals. In this thesis just the digital connectors have been used. Different digital signals such as serial communication and encoders can also be handled. The analogue signals can vary between +/-10 V if they

are connected to the right input channels. The technical details of the DS1103 are given in Appendix 1. Figure 2.4 shows the dSPACE board of the controller.

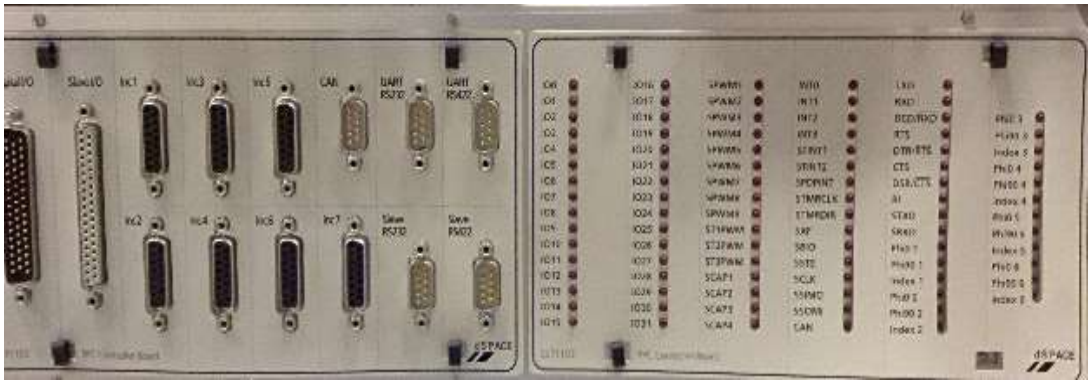

Fig. 2.4: *The dSPACE board that handles input and output signals between the computer and the real system.*

2.3.2 RTI interface

By using the RTI interface, the controller board is programmable from Simulink block diagram environments. There is a possibility to configure all I/O channels by using the RTI. In order to connect the real-time simulation to the real physical world, there is a need to introduce the I/O interfaces into the Simulink models. This allows replacing parts of the simulation model with the real physical hardware. In RTI, the channels of the I/O board are supported by the I/O libraries which are including the corresponding I/O blocks. The various RTI blocks (I/O blocks) allow accessing the dSPACE hardware. Figure 2.5 shows the library of the rtilib1103. There are two ways to get these blocks, both by using the Simulink library browsers or the RTI block libraries. The RTI manages continues-time, discrete-time and multi rate system. Depending on the I/O hardware, different channels of the board can be used with different sample rates and also in several subsystems.

The master PPC on the DS1103 controls a bit I/O unit with the following characteristics: 32-bit digital I/O, ±10 mA maximum output current and TTL voltage range for input and output.

The I/O unit is organized in four 8-bit groups (bits 0…7, 8…15, 16…23, 24…31)). Each group can be configured for input or output. If a group is configured for input, it's not possible to write on it. In this thesis, the second groups of 8-bits (8…15) has been used for the one-phase dual active bridge. The bits pins number can be seen in Figure 2.6.

The master PPC library contains several blocks for programming the digital I/O unit.

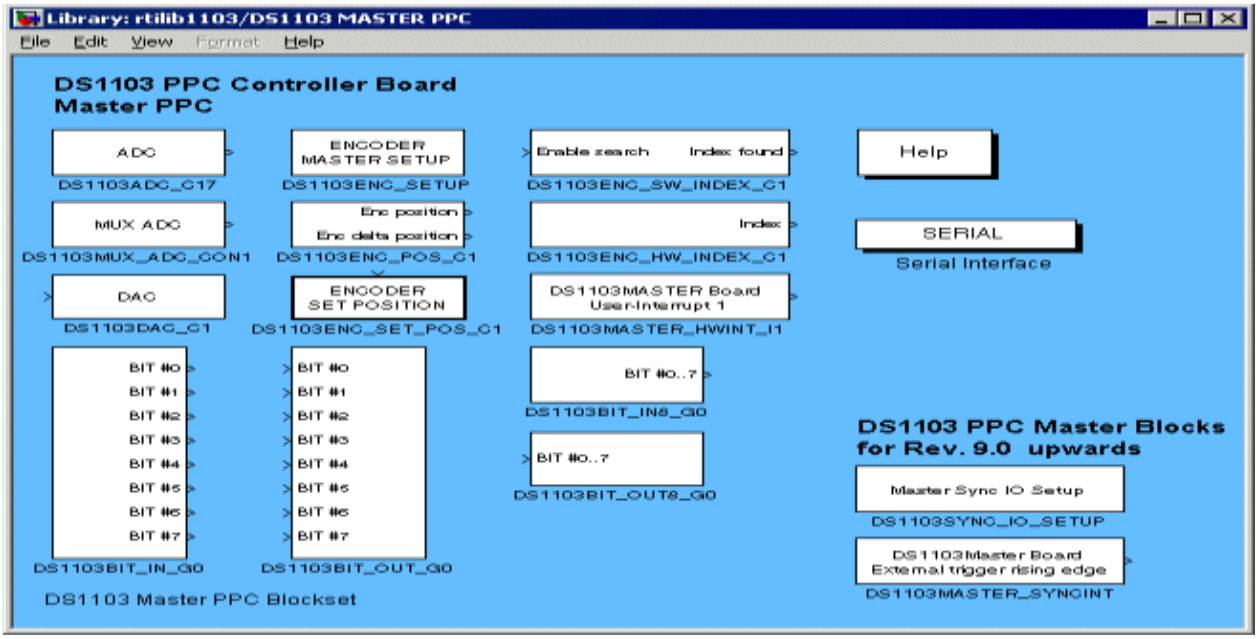

Fig. 2.5: The Library: rtilib1103/DS1103 MASTER PPC window

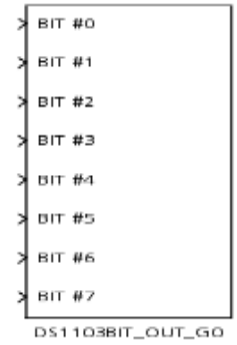

Fig. 2.6: Single bit from an 8-bit group of the 32-bit digital input

2.3.3 Digital implementation limitation

As mentioned in the previous section, the 8-bit digital I/O has been used to generate signals for the single phase DAB converter. (12-bit digital I/O has been used to generate signals for the three phase DAB converter). As can be seen in the catalog of the DS 1103, the settling time of the D/A converter of this board are five microseconds when the 14 bits have been used at the same time. It means that the time steps of the Simulink software should be set on the 5 microseconds so the Simulink blocks can be programmed and realized by the RTI. With too low step times, an overrun situation will happen and the RTI cannot translate the Simulink code into the C-codes for the dSPACE controller. This can be the limitation for the phase shift implementation of less than 5 microseconds in this thesis.

2.4 Soft Switching

Hard switching in the converters can give several problems of which the main is the switching losses due to the finite duration of the switching transient and the electromagnetic compatibility (EMC) problems due to the high voltage derivative with respect to time. By increasing the switching frequencies, there is a possibility to reduce the output current harmonic content and passing over the audible noise. The problem here is that by increasing the switching frequency, the switching losses are also increased especially when IGBT technology is employed. In this case, in order to have a high switching frequency and low switching loss at the same time, it is necessary to have a soft switching which can be achieved by implementing zero voltage switching in the converter. In order to make it more clear, it is necessary to mention that the power is dissipated in the switches because there is both voltage and current across the switches in a switching period which can be seen in Figure 2.7. This leads to that the power loss is equal to the multiplication of the voltage and current. However, if the voltage across the switches become zero or low before the switches begins to conduct then there will be no or low power loss due to the switching. This can be seen in Figure 2.7. Soft switching can be implemented in both the turning on and turning off period of the switches.

One method to have such a soft switching is using the snubber capacitor in resonant switch converters such a full bridge and dual active bridge converters.

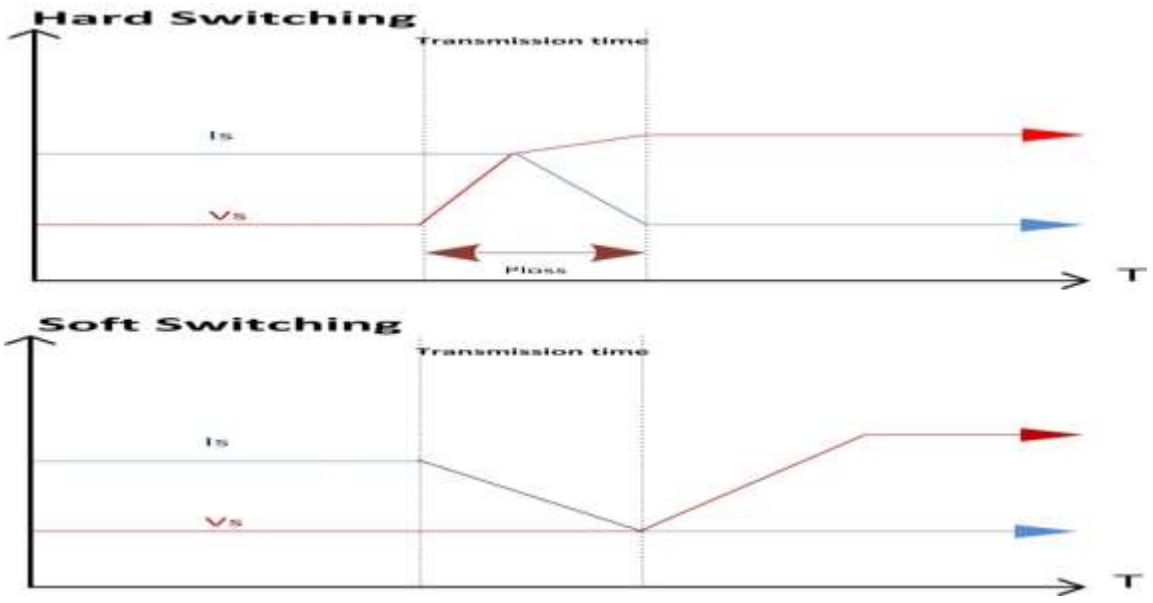

Fig. 2.7 Conceptual model of the voltage and current waveforms control by hard (up) and soft switching (down)

2.4.1 Snubber capacitor

A Snubber capacitor is usually used to protect the transistors by improving their switching trajectory. There are different types of snubber capacitors like turn-on, turn-off and overvoltage capacitor. By using a snubber capacitor in parallel with the switches, the switching overvoltage can be removed or reduced significantly. The turn-off snubber decreases the switching losses by increasing the voltage rise time of the IGBT. The designing of the snubber capacitor for DAB converters will be discussed in the Section 3.1.4.

2.5 Loss calculation

In this project, the loss has been calculated theoretically, based on the simulation results and also for the experimental results. The main part of losses in the Dual active bridge belongs to the IGBTs, diodes and transformer losses which are going to be explained.

2.5.1 IGBT and Diode Losses

The losses in the IGBT and diodes can be categorized into three parts: Conduction, Switching and blocking (leakage) losses, The last one can normally be neglected.

2.5.1.1 Conduction losses

This losses can be calculated by using an IGBT approximation with an in series DC voltage source (U_{CE0}) that representing IGBT on-state zero current collector-emitter voltage and a collector-emitter on-state resistance (r_c).

$$u_{CE}(i_C) = u_{CE0} + r_C i_C \tag{2.5}$$

The same approximation can be used for the diode,

$$u_D(i_D) = u_{D0} + r_D\, i_D \tag{2.6}$$

These parameters can be read from the data sheet of switch. The instantaneous value of the IGBT conduction losses can be calculated by

$$P_{CT}(t) = u_{CE}(t) i_C(t) = u_{CE0}.\, i_C(t) + r_C.\, i_C^2(t) \tag{2.7}$$

So, the average losses based on the IGBT current value I_{cav}, and the rms value of IGBT current I_{crms} can be expresses as

$$P_{CT} = \frac{1}{T_{sw}} \int_0^{Tsw} (u_{CE0}.\, i_C(t) + r_C.\, i_C^2(t))dt \; = u_{CE0}.\, I_{cav} + r_C.\, I_{crms}^2 \tag{2.8}$$

And in the same way, for the diode in one switching period can be calculated by

$$P_{CT} = \frac{1}{T_{sw}} \int_0^{Tsw} (u_{D0}.\, i_D(t) + r_D.\, i_D^2(t))dt \; = u_{D0}.\, I_{Dav} + r_D.\, \mathrm{I}_{\mathrm{Drms}}^2 \tag{2.9}$$

2.5.1.2 Switching losses

The internal diode of the IGBT is used as a free-wheeling diode, since in the majority of applications such as full-bridge DC-DC converter; the power electronics converter has some IGBT-based half-bridges. The calculation is also valid if an external freewheeling diode is used in parallel to the IGBT. The turn-on energy losses in IGBT (E_{onT}) can be calculated by

$$E_{onT} = \int_0^{tri+tfu} u_{CE}(t) i_C(t) dt = E_{onMi} + E_{onMrr} \quad (2.10)$$

Switch-on energy losses (the losses in the diode during the turn-on time of the IGBT) in the diode are mostly the reverse-recovery energy (E_{onD}) and can be calculated by

$$E_{onD} = \int_0^{tri+tfu} u_D(t) i_D(t) dt = E_{onDrr} = \frac{1}{4} Q_{rr} U_{Drr} \quad (2.11)$$

where U_{Drr} is the voltage across the diode during reverse recovery time. In the worst situation, this voltage can be equal to the supply voltage ($U_{Drr} = V_i$).

The switch-off energy losses in the IGBTs can be calculated in the same way. The switch-off losses in the diodes are normally neglected ($E_{offD} \approx 0$). So,

$$E_{offT} = \int_0^{tru+tfi} u_{CE}(t) i_C(t) dt \quad (2.12)$$

The switching losses of the IGBT and diodes can be calculated by multiplication of the switching energies and the switching frequency (f_{sw}).

$$P_{swM} = (E_{onM} + E_{offM}) f_{sw} \quad (2.13)$$

$$P_{swD} = (E_{onD} + E_{offD}) f_{sw} = E_{onD} f_{sw} \quad (2.14)$$

Total power losses in the IGBT and diode can be calculated as the sum of the conduction and switching losses.

$$P_T = V_{CE0} I_{Cav} + r_c I_{crms}^2 + (E_{offT} + E_{onT}) f_{sw} \quad (2.15)$$

$$P_D = V_{D0} I_{Dav} + r_D I_{Drms}^2 + E_{onD} f_{sw} \quad (2.16)$$

2.5.2 Transformer losses

The transformer loss consists of the copper loss and the iron loss. Transformer copper loss can be calculated by:

$$P_{CU} = RI_{rms}^2 \tag{2.17}$$

And the transformer iron loss can be expressed by

$$e = N\frac{d\Phi}{dt}$$

For square wave voltage: $V_{dc}.\Delta\, T = N.\Delta\, \Phi \rightarrow V_{dc}\frac{T}{2} = 2N\Phi_{max}$

$$\rightarrow V_{dc} = 4Nf\Phi_{max} \rightarrow \Phi_{max} = \frac{V_{dc}}{4Nf}$$

$$P_{core} = \eta f {B_{max}}^{1.6} + \frac{\pi^2 A\sigma}{6l} f^2 {\Phi_{max}}^2 \tag{2.18}$$

As it can be seen, the iron loss calculation is so complex. In this case, usually the core losses (R_C) can be calculated by using the open circuit transformer test. The value can be calculated by

$$R_C = \frac{{V_{oc}}^2}{P_{oc}} \tag{2.19}$$

Core losses are mostly caused by hysteresis and eddy current effect in the core.

Case Set-Up

3.1 Component selections of Dual Active Bridges Converter

As mentioned, the purpose of the project is to simulate and implement the dual active bridge with the available converters in the laboratory. In parallel, due to the limitation of the available converters, one DAB converter with the desired characteristics is also simulated and analyzed as a case study. In this section, the different components of the available Dual active bridge converter and the components for the case study DAB converter are mentioned.

3.1.1 IGBT

IGBT is the abbreviation of insulated gate bipolar transistor. This type of transistor has a high impedance gate which requires just a small amount of power to switch the device, just as for a MOSFET. It can also be designed to block negative voltages in the same way as the GTO. In the same way as a BJT, it has also a small on-state voltage drop when conducted even in devices with large blocking voltage rating. It has also an excellent safe operating area. The symbol of the IGBT can be seen in Figure 3.1. [4]

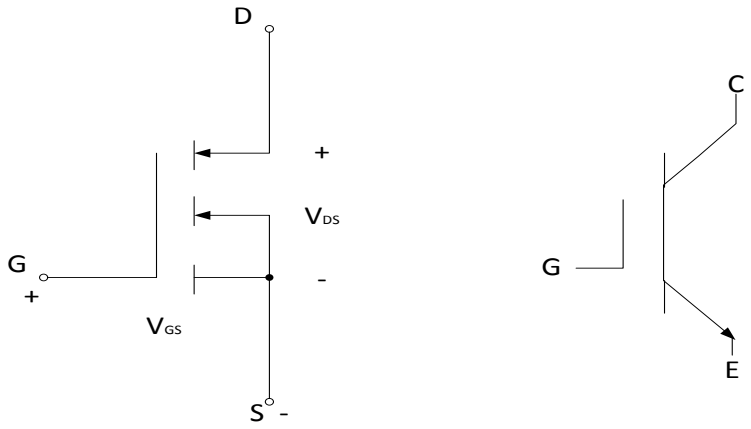

Fig. 3.1: IGBT symbols

The available converters in the laboratory have a kind of ultra-fast IGBT modules. Each module consists of two IGBTs which are connected to each other in series and each one is connected to one diode in parallel. Figure 3.2 shows the IGBT module of the DAB converter.

Fig. 3.2: The symbols and picture of the IGBT modules of the DAB converter

The characteristics of the IGBTS can be seen in Table 3.1.

Table 3.1: The characteristics of the SEMIKRON IGBT

SEMIKRON	V_{CES}	V_{CEO}	I_C	$t_{d(on)}$	$T_{(off)}$	Eon	R_{CE}
300GB125D	1200 V (T=25 C)	20	300 (T case=25 C)	130 ns	460 ns	16 mj	10 mΩ

The characteristic of the IGBT which has been used in the case study test is given in Table 3.2.

Table 3.2: The characteristics of the ABB HighPack IGBT

ABB HiPak	V_{CES}	V_{GES}	I_C	$t_{d(on)}$	$T_{(off)}$	$R_{CC'+EE'}$
5SNA 0750G650300	6500 V	20	750 A (T case=85 C)	1060 ns	4950 ns	0.07 mΩ

The case study test has been done for the input and output voltage of 3KV and 6KV respectively and for maximum possible power. The allowed current and voltage should be about the half of which is written in the catalogue ((Fazli and Mobarrez, 2012: 40). So, the two in-series IGBT have been used as switches in the rectifier bridge (for the output voltage of 6KV) and the two in-parallel IGBT have been used in the inverter bridge of the DAB (for the high current in the primary side).

3.1.2 Diodes

The diodes which are used in the converters are included in the IGBT module packages. As mentioned earlier, each IGBT package has two inverse diodes. The characteristics of diodes can be seen in Table 3.3.

Table 3.3: The characteristics of the SEMIKRON diode

SEMIKRON	I_F	R_F	V_F
300GB125D	260A(T=25 C)	1 mΩ	2 V (T=25)

More technical details regarding the IGBT module package can be found in the Appendix 2.

The characteristic of the diode which has been used in the case study test is given in Table 3.4.

Table 3.4: The characteristics of the ABB HiPak diode

ABB HiPak	I_F	V_F
5SNA 0750G650300	750A(T=25 C)	1.75 V (T=25)

3.1.3 Transformers

The transformer which is used for the single phase dual active bridge is a 50 Hz, 110/220 V single-phase transformer (a 50Hz, 127/220 three phase transformer is used for the three phase DAB converter). In the simulation, an ideal transformer has been used, meaning that it doesn't have any losses, and that the voltages are transformed in the direct ratio of the turns. In a real transformer some of the flux in the primary side don't linked to the secondary side which is called leakage flux and can be represented as an additional inductance in series with the primary side of the transformer which is done in the simulation as well. Figure 3.3 shows this in-series leakage inductance.

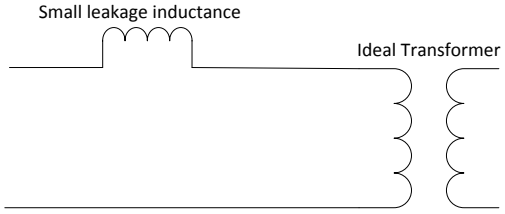

Fig. 3.3: Real transformer showing leakage inductance

Since the amount of leakage inductance is important as an integral part of the circuit and also provides an energy storage medium, it should be measured accurately to achieve the correct operation of the converter. In order to calculate the leakage inductance of the transformer, three methods have been used which are as follows.

A. With LCR meter

When the LCR meter is connected to the primary side of the transformer with open circuit secondary side, the value of the inductance which is shown in the LCR meter is the total amount of leakage inductance and primary inductance which can be seen in Figure 3.4. .

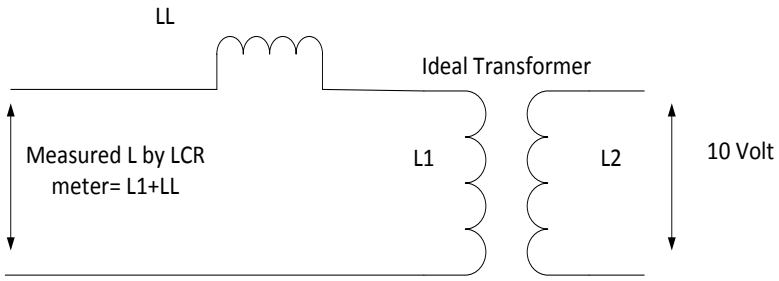

Fig. 3.4: The value of total inductance in the open circuit transformer

Since the leakage inductance is a function within the transformer, it can be measured directly. So In order to measure the leakage inductance of the transformer by an LCR meter, it is needed to make a short circuit on the secondary side of the transformer as shown in Figure 3.5.

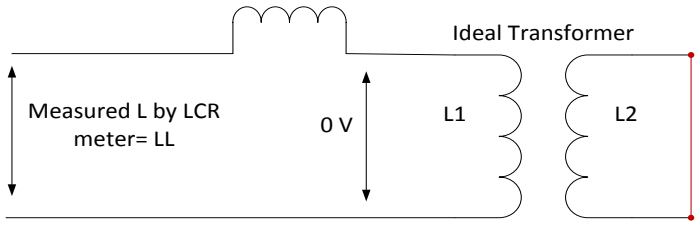

Fig. 3.5: The value of total inductance in the short circuit secondary side transformer

Due to the zero voltage on the output of the secondary side, the voltage of the primary side is zero as well, so the total inductance value which the LCR meter shows is the amount of the leakage inductance of the transformer. The value measured by the LCR meter is 3.7 mH for this transformer.

B. With the AC source, multi-meter and oscilloscope

Due to the reason that the LCR meter operates at the frequency 1 KHz frequency to measure the inductance; the other method has also been used in order to measure the leakage inductance.

In this method, firstly the primary side of the transformer is connected to the auto-transformer which produces a voltage of 3.2 V while the secondary side of the transformer is short-circuited.

The current and voltage has been measured by multi-meters and calculation is as follows:

$$Z = \frac{V}{I} = \frac{3.2}{2.6} = 1.2307\ \Omega \cong 1.24 \tag{3.1}$$

Then, the current and voltage have been measured by an oscilloscope in order to measure the phase shift between the current wave and voltage wave which is 72 degree. According to the following calculation the leakage inductance has been measured

$$\tan 72 = \frac{XL}{R} = 3.0776 \tag{3.2}$$

$$\cos 72 = \frac{R}{Z} = \frac{R}{1.24} = 0.31 \xrightarrow{yields} R = 0.3831 \tag{3.3}$$

By (3.2) and (3.3) the XL value becomes 1.179Ω.

Since the input voltage of the auto-transformer is the local electricity the frequency is 50 Hz. So,

$$XL = 2\pi f L \xrightarrow{yields} L = 3.75\ mH \tag{3.4}$$

As can be seen the value is almost the same as the value which has been calculated by method one.

C. With Bode 100

The other method has been used for the three phase transformer of the three phase DAB converter in order to measure the leakage inductance with higher accuracy. In order to measure the leakage inductance and internal resistance of the three phase transformer, the Bode 100 has been used. The Bode 100 is the Multifunctional measurement tool which works as an impedance meter, gain phase meter and etc.

Figure 3.6 shows the connection between the three phase transformer and the Bode 100. The Bode 100 should be calibrated first and then it can be used. After calibration, the inductance and resistance of the cabling is measured separately in order to remove their effects on the measurement results.

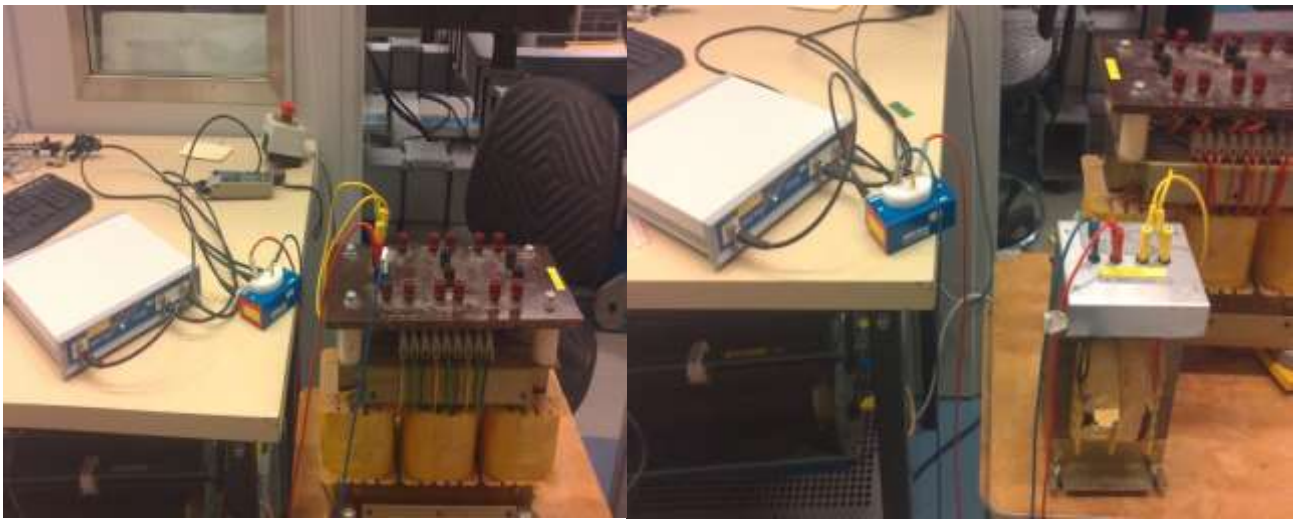

Fig. 3.6: leakage inductance measurement of the single and three phase transformers by using Bode 100

The results are shown in Table 3.5 for the different frequency.

Table 3.5: The three phase transformer characteristic (measured by Bode 100)

	Cables (2m)		Transformer (after removing cable effects)	
frequency	55 Hz	555 Hz	55 Hz	555 Hz
L_s	3.878 µH	4.808 µH	550 µH	545 µH
R_s	50 mΩ	55 mΩ	500 mΩ	525 mΩ

The same measurement has also been done for the single phase DAB converter in order to validate the results which are given by using other measurements methods. The results are given in Table 3.6.

Table 3.6: The single phase transformer characteristic (measured by Bode 100)

	Single phase transformer (after removing cable effects)		
frequency	50 Hz	500 Hz	1 kHz
L_s	3.716 mH	3.65 mH	3.57 mH
R_s	310 mΩ	1.34 Ω	2.1 Ω

As can be seen in the tables, the leakage inductance has been decreased for both transformers by increasing the frequency from 50 Hz to 1 KHz while the in-series resistance has been increased. It should be noted that due to the magnetic effect of the transformer core, the calculated R_s is not accurate for the high frequency.

The other parameter which is needed in this project is the core resistance and core losses of the transformer. In order to calculate the R_c which is the core resistance of the transformer, the open circuit test should be done on the transformer. By using one Wattmeter and the multi meter and (2.19), the value for both the single and three phase transformers is calculated which is shown in Table 3.7.

Table 3.7: The R_c Value for both the single and three phase transformers

	Single phase transformer	Three phase transformer
R_C *(Ω)*	516	601.4

3.1.4 Snubber capacitor setup

The snubber capacitor is not installed on the available converters in the laboratory. Implementation of the snubber capacitor on the DAB converters has been done in the final phase of the project. The reason is the switching overvoltage which was detected in the voltage waveforms of the transformer and can damage the switches. In order to choose the proper snubber capacitor, the minimum and maximum value of it has been calculated by using (Fazli and Mobarrez, 2012: 45).

$$C_{min} = \frac{i_{in}\Delta t}{V_d} \tag{3.5}$$

$$C_{max} = \frac{L{i_{in}}^2}{{V_d}^2} \tag{3.6}$$

i_{in} is the input current, Δt is the t_{fi} of the IGBT, V_d is the input voltage and L is the leakage inductance of the transformer. The first formula given from the voltage formula of the capacitor and the reasoning is that the capacitor is charged during the falling time of the current in the IGBT in the turn-off switching. The second formula has been reached by reasoning that a maximum value for the capacitors can be obtained by putting the energy stored in the leakage inductance of the transformer equal to the energy which is stored in the capacitor. Based on this formula, the range for the single phase DAB and three phase DAB converter are as given in Table 3.8.

Table 3.8: the minimum and maximum possible snubber capacitor for single and three phase DAB converters

Single phase dual active bridge	Three phase dual active brdige
1 nF- 6 µF	1 nF – 1 µF

Due to the reason that different tests with different parameter values are going to be done on DAB converters, the parameters in (3.5) and (3.6) are selected in such a way that the minimum and maximum range for the snubber capacitor can support all tests with different parameter values. For example in calculating the minimum snubber capacitor, the lowest possible i_{in} is selected according to the parameters of all tests and for calculating of the maximum capacitor, the minimum possible V_d is selected based on the parameters of the tests. The installed snubber capacitor can be seen in the Figure 3.7.

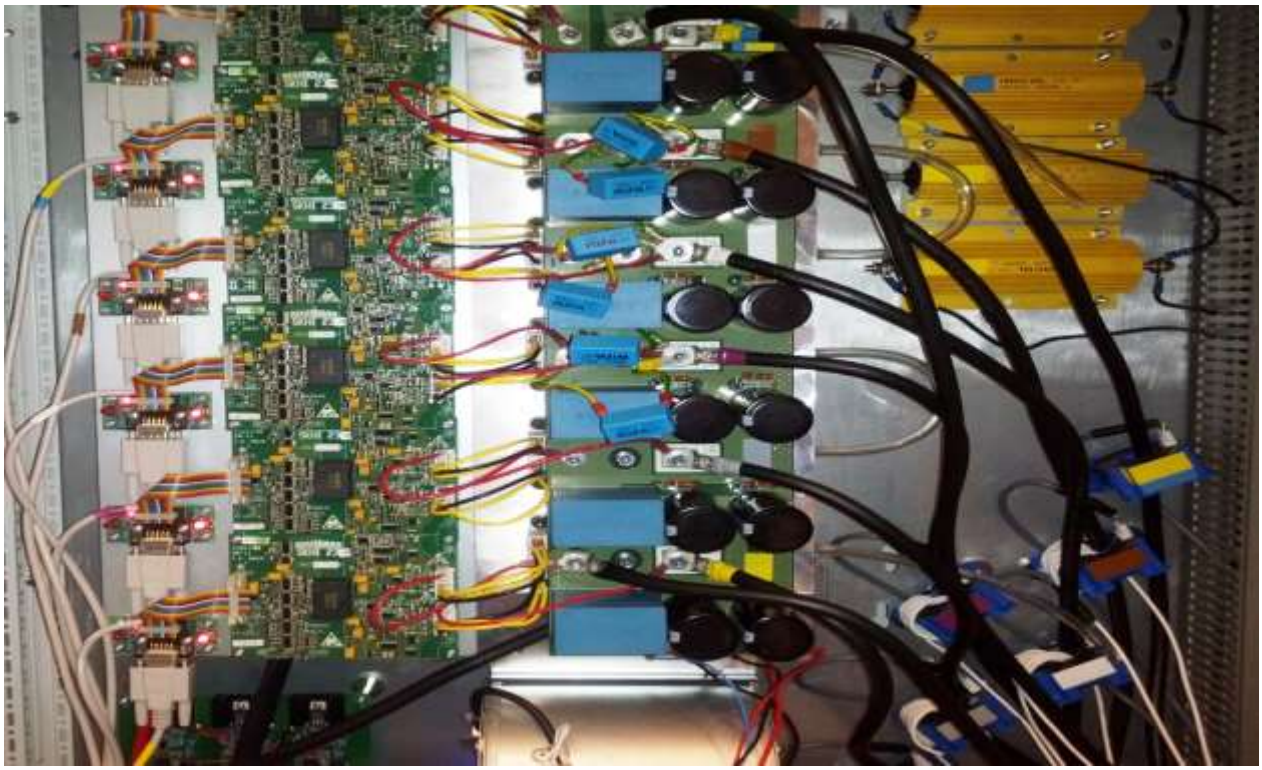

Figure 3.7: Installed snubber capacitor on the DAB converter

3.2 Modeling of the Dual Active Bridges in PLECS software

In this project, the simulation has been done by using the PLECS toolbox which can operate under Simulink. The modelling of both single and three phase Dual active bridge converters are presented in the following sections. It should be noted that, in addition to the converter which has been used in this project, the simulation has been done for one case study DAB converter as well.

The single and three phase dual active bridge converters have been modeled as shown in Figure 3.8 and Figure 3.9. The characteristics of IGBTS and diodes which are modeled are according to the SEMIKRON Switches which are used in the available converters in the laboratory. The ideal single phase and three phase transformer have been used as well, but the leakage inductance of the transformer is considered in series with the primary side of the transformer. The on-stage voltage drop has been considered for IGBTs and diodes but due to the limitation of the PLECS the switching losses is ignored. In terms of resistors, the internal resistance of the transformer is also considered in the primary side of it which was calculated for different transformer and frequencies in previous sections. The switching method of IGBTs in the DAB converter is explained in the theoretical chapter. The data which are given in Table 3.9 can be different for different tests but the most common data are given.

Table 3.9: The characteristics of the available single and three phase DAB converter components

	Single phase DAB	***Three phase DAB***
Component	***Data***	***Data***
IGBT switches	R=0.005, V_{CEO} =0.9 V	R=0.005, V_{CEO} =0.9 V
Diode	R=0.001 , V_F =1.1 V	R=0.001 , V_F =1.1 V
Output capacitor	C=2.25e-3	C=2.25e-3
Input capacitor	C=2.25e-3	C=2.25e-3
Transformer	[1 1.8], L=3.75e-3	[127 220], L=5.5-4
Rout	It depends on the needed power,	It depends on the needed power,

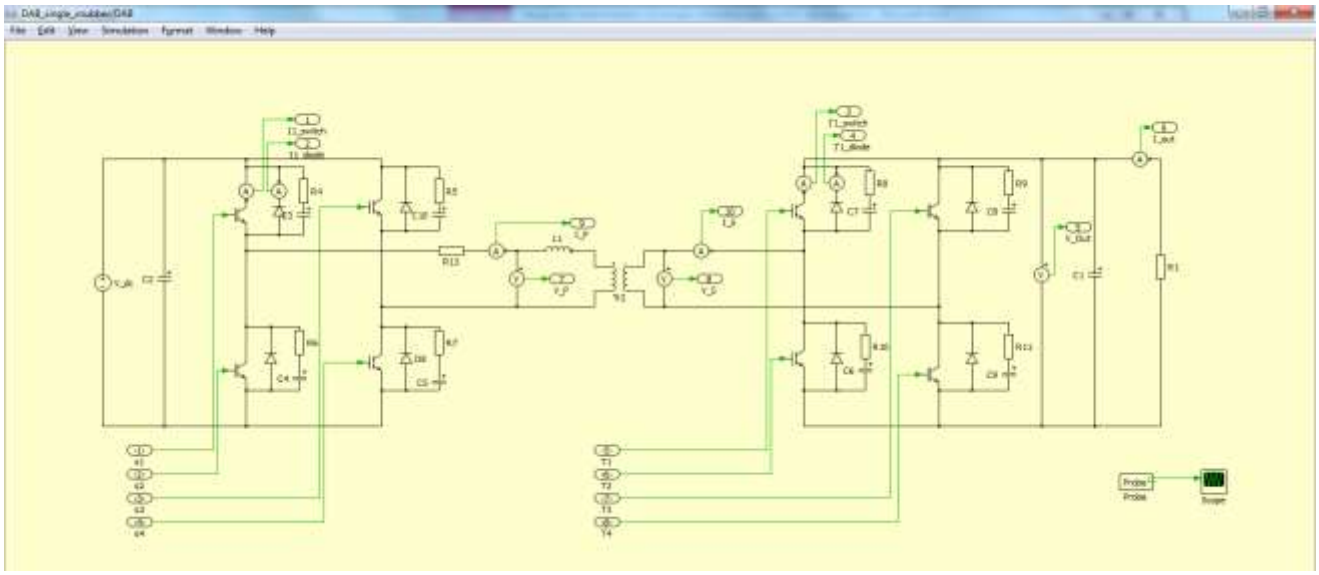

Fig. 3.8: Single phase Dual Active Bridge converter implementation in PLECS

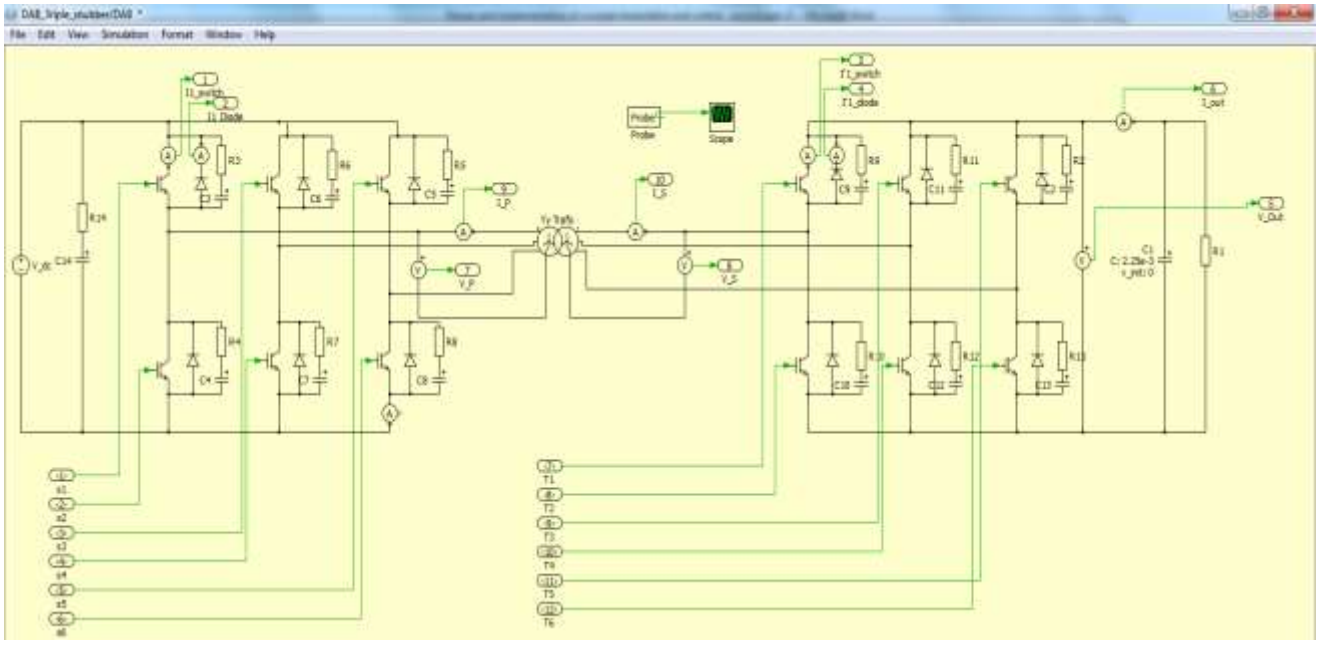

Fig. 3.9: Three phase Dual Active Bridge converter implemented in PLECS

As mentioned earlier, the simulation has been done for one case study as well. The characteristics of the simulated converter in this case study are presented in Table 3.10.

Table 3.10: The characteristics of the desired single and three phase DAB converter components

	Single phase DAB	***Three phase DAB***
Component	***Data***	***Data***
IGBT switches	V_{CEO} =1.2 V	V_{CEO} =1.2 V
Diode	V_F =1.75 V	V_F =1.75 V
Output capacitor	C=1.5e-4	C=1.5e-4
Input capacitor	C=2.25e-6	C=2.25e-6
Transformer	[1 2], L=4e-6	[1 2], L=4e-6
Rout	It depends on the needed power,	It depends on the needed power,

The value of the output capacitor is calculated to be 1.5e-4 practically in the simulation which gives less than 0.01 voltage ripple for the desired voltage but it can be determined theoretically as well. The value of the transformer is also approximated based on the other report just as a value for one possible high frequency transformer. (Fazli and Mobarrez, 2012: 62).

3.3 Experimentally Implementation of the Dual Active Bridge

This section can be divided into the dual active bridge hardware setup and the dSPACE controller setup for the mentioned converter.

3.3.1 dSPACE controller setup

As mentioned in the theoretical section, the DS 1103 controller has been used in this thesis. The master PPC on the DS1103 which controls the I/O bit units is also used to send the TTL signal to the converter. Eight bits have been used to make signals for eight switches of the single phase converter, four signals for the inverter bridge and four ones for the rectifier bridge.(for three phase DAB converter is 12 signals for twelve switches totally). I/O digital Connection on the DS1103 can be seen in Figure 2.4.

As mentioned in the theory section, the first step is to make a Simulink file for signals. The signals block in Simulink should be connected to RTI block interface which is shown in Figure 3.10 for the single phase DAB converter and in Figure 3.11 for the three phase DAB converter.

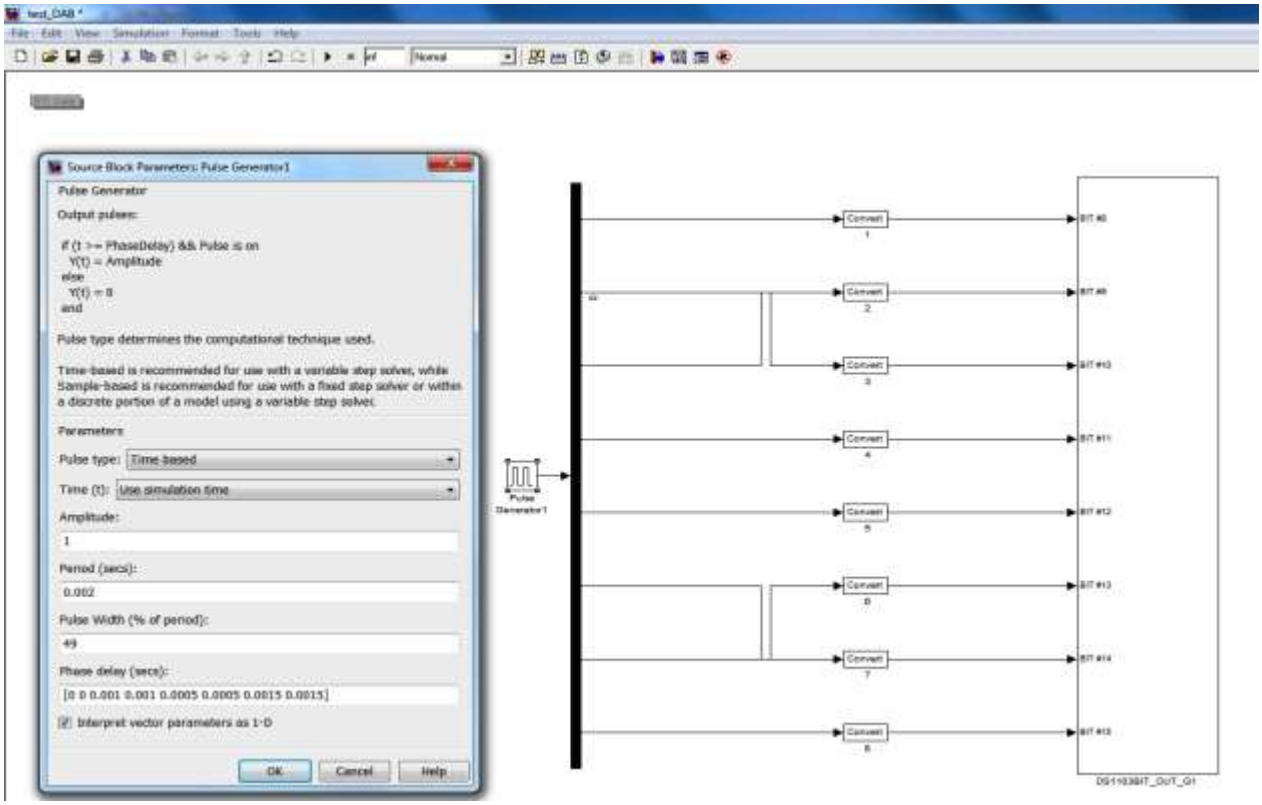

Fig. 3.10: The Simulink model of the controlling signals

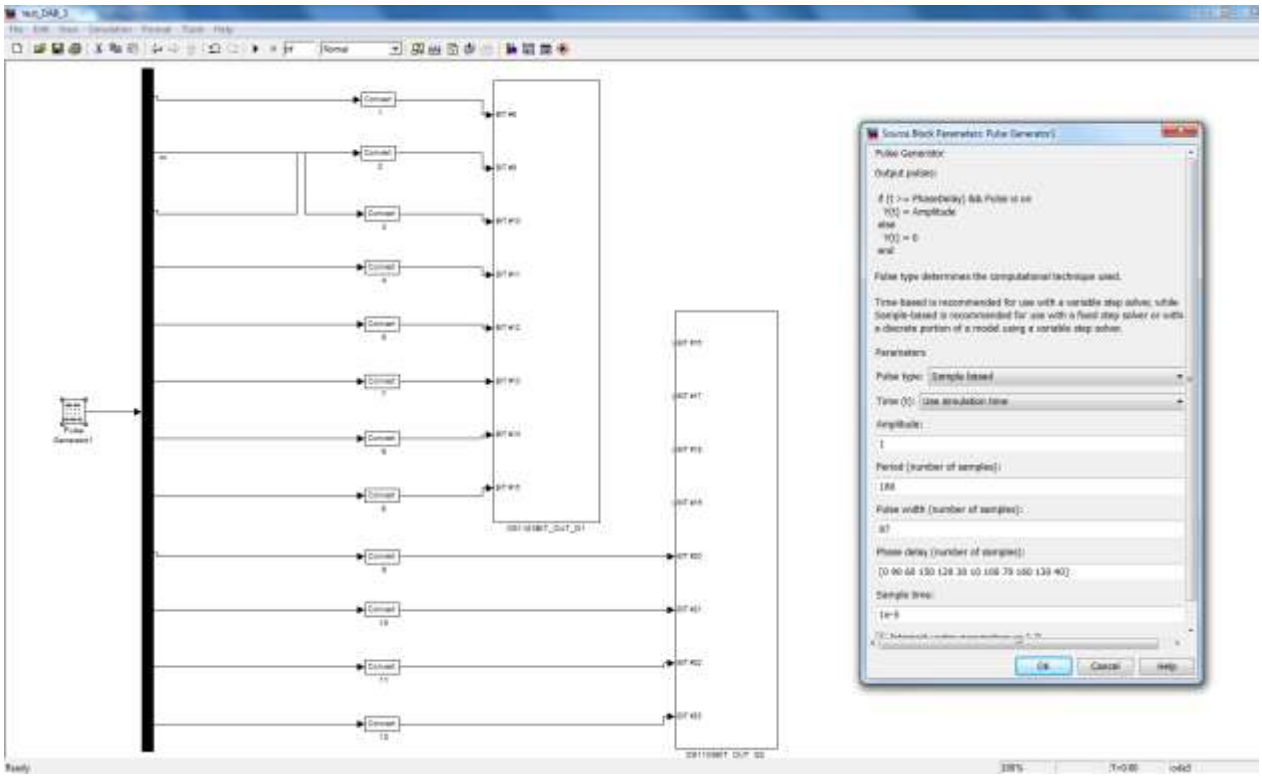

Fig. 3.11: The Simulink model of the controlling signals

As can be seen in Figure 3.10, one signal generator, generate eight signals for the eight switches. As mentioned in the simulation section, there is 180 degrees phase shift between the switches 1, 4 and 2, 3 and also between 5,8 and 6,7. The duty cycle is set to 49% in order to avoid a short circuit in the switches. Figure 3.11 shows that, in the same way as for the single phase DAB converter, one signal generator, generate twelve signals for twelve switches in the three phase dual active bridges. Due to the reason that each I/O block in the RTI library generates 8 bits, two I/O blocks have been used to generate the 12 needed signals. There should also be the phase shift between the signals of the inverter and the rectifier bridge which is variable according to the desired parameters. All signals are set in one signal generator block as a matrix in the phase delay section. The period is also set which determines the frequency of the signals. The output of the signal generator is converted by the conversion block to 1 and 0 bits which is readable by the I/O bit interface block. The reason of the conversion is that the output of the signal generator is a double type data which should be converted to the Boolean data (1 and 0) in order to be understandable for the bit Block. A double amount more than 0 represent a 1 in the Boolean which generates High TTL digital output and a double amount less or equal to zero represent a 0 in the Boolean type which generates a low TTL digital output as shown in Table 3.11.

Table 3.11: Relation between the digital output and the input of the block

Simulink Input	With data typing	Digital output(TTL)
>0 (double) <=0 (double)	1 (Boolean) 0 (Boolean)	High Low

The bit block is the RTI interface which connects and converts the signal to the physical converters by using the DS1103 board. The output of the DS1103 board which can be seen in Figure 2.4 is connected to the dual active bridge converter.

3.3.2 Dual Active Bridge setup

In this thesis the dual active bridge converter is the combination of the one prepared three-phase inverter which is connected to the output of the other prepared three-phase inverter which represents the rectifier by using a 50 Hz single phase transformer (and a 50 Hz three phase transformer). The whole setup can be seen in Figure 3.13. For the single phase dual active bridge just four switches out of 6 switches of each inverter have been used. In other word, just one phase of the three-phase inverter has been used. The characteristics of the inverter are mentioned in Table 3.12.

Table 3.12: The characteristics of the inverter of the available Dual active bridge

Component	***Data***
IGBT switches	8
Diodes	8
Input capacitor	C=2.25e-3
Parallel Resistance	156e3

The technical details of inverters can be found in Appendix 3.

The gate drive connection of the inverter has 8 TTL inputs. Each pair represents one high and low TTL voltage. Figure 3.12 shows the inside of the whole inverter. As can be seen, each IGBT package consists of two IGBT switches. The input TTL signal number 1 on the connection board of the gate drive belongs to the IGBT package number one. The TTL input which is written as 1T belongs to the IGBT package number one top switch and 1B belongs to the IGBT package number one bottom switch. Each IGBT package has been signed by different colors. In order to use the inverter as a single-phase inverter, there is a need to just use two IGBT packages which consist of four switches totally. So, four signals from the output of the DS1103 board are connected to the gate drive of inverter one and four signals from DS1103 are connected to the gate drive of inverter two which is used as a rectifier.

The input of inverter one has been supplied by the DC voltage source and its output is connected to the primary side of the single-phase transformer (in three phase DAB converter is connected to the primary side of the three phase transformer). Then, the secondary side of the transformer is connected to the AC input of the other inverter (to use it as a rectifier) and the DC output of the rectifier is connected to the variable load.

It should be noticed that the outputs of the secondary side of the transformer should be connected to the input of the rectifier in a correct order; otherwise it can damage the capacitor of the rectifier.

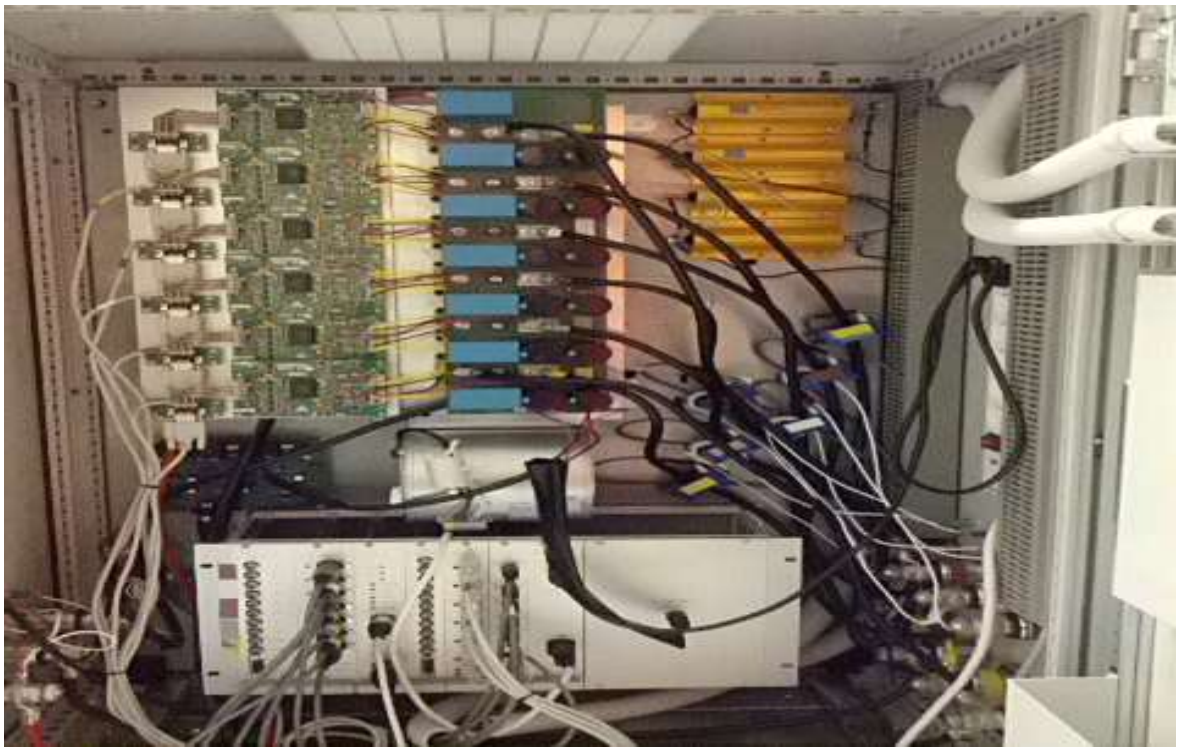

Fig. 3.12: The inside of the inverter of the DAB converter

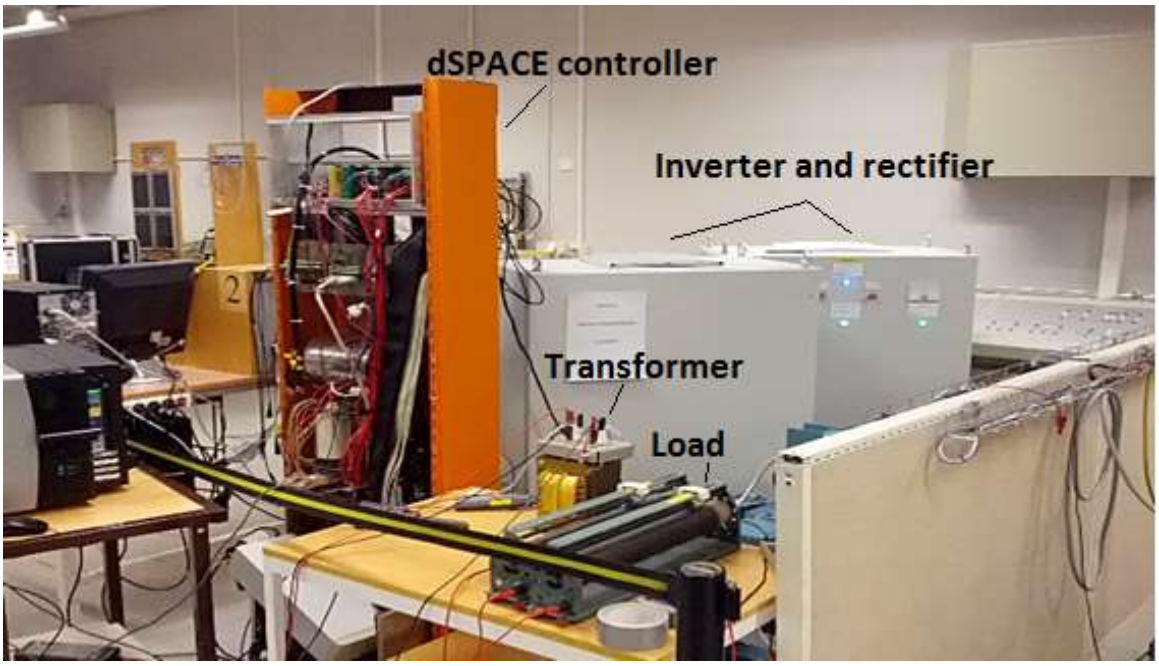

Fig. 3.13: The view of the whole setup

4 Analysis

4.1 Analysis of simulation results

The simulation has been done for both the single and three phase dual active bridge converter. The simulations which are done can be categorized into two parts. In the first part, simulations have been done for the desired high power and frequency as a case study. In the second part, simulations have been done based on the converters and transformers which are available in the laboratory. The point is that, due to the lack of a high frequency transformer and limitation of the transformer and dSPACE controller, it's not possible to implement the Dab converter for a high frequency and high power in the laboratory. In the following sections, the simulation results have been analyzed for both single and three phase dual active bridges. The results of the case study simulation are presented in the following section (4.1.1) and the result of the second part of simulation are presented and discussed together with the experimental results in the experimental Section 4.2.

4.1.1 Single phase dual active bridge simulation

As mentioned earlier, since the aim of the simulation is to show the waveform of both the primary and secondary sides of the DABs transformer, both voltage and current waveforms are shown in Figure 4.1 for the desired output power which is 2 MW.

The desired parameters which are implemented on the case study DAB converter are given in Table 4.1.

Table 4.1: Desired characteristics of the converter

	Value
Input voltage	3KV
Output voltage	6KV
Switching Frequency	5 kHz
Output Power	2 MW
Transformer ratio	2

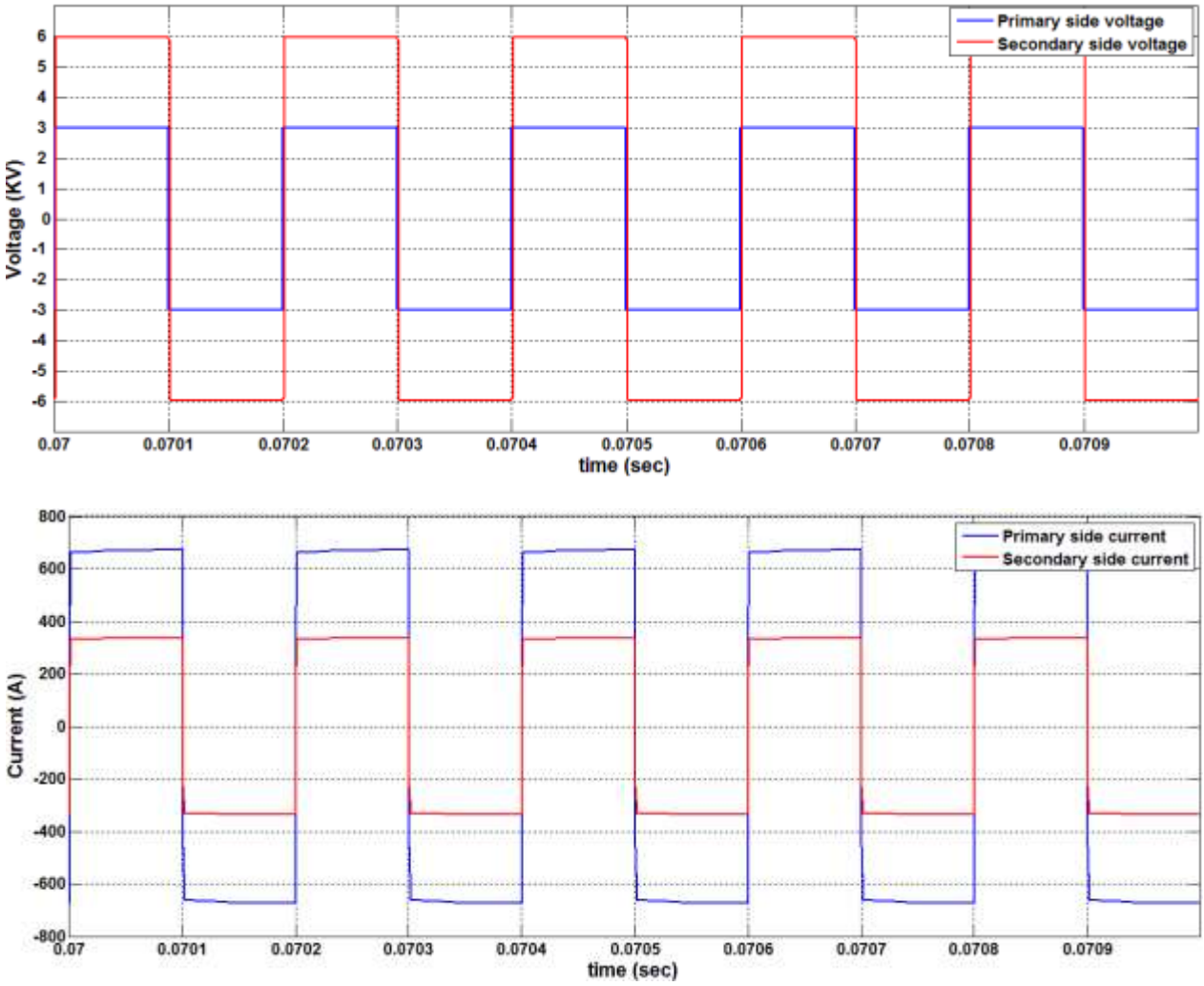

Fig. 4.1 The primary and secondary voltage and currents of transformer for desired power level

As can be seen in this figure, both the primary and secondary voltage and current waveforms are square wave. This is due to the little phase shift (about 2.4 degrees) between the bridges of the DAB converter which should be implemented in order to reach the desired power level. This little phase shift cannot be seen in Figure 4.1.

Both the primary and secondary current and voltage waveforms of the transformer are also investigated for the phase shift of 90 degree between the two bridges which gives the maximum output power according to (2.1). As can be seen in Figure 4.2 the current waveforms looks trapezoidal which is due to the 90 degrees phase shift between the two bridges of the converters and the effect of inductance of the transformer. The ripple of the secondary side voltage of the transformer is due to the low output capacitor in comparison to the high current in this test.

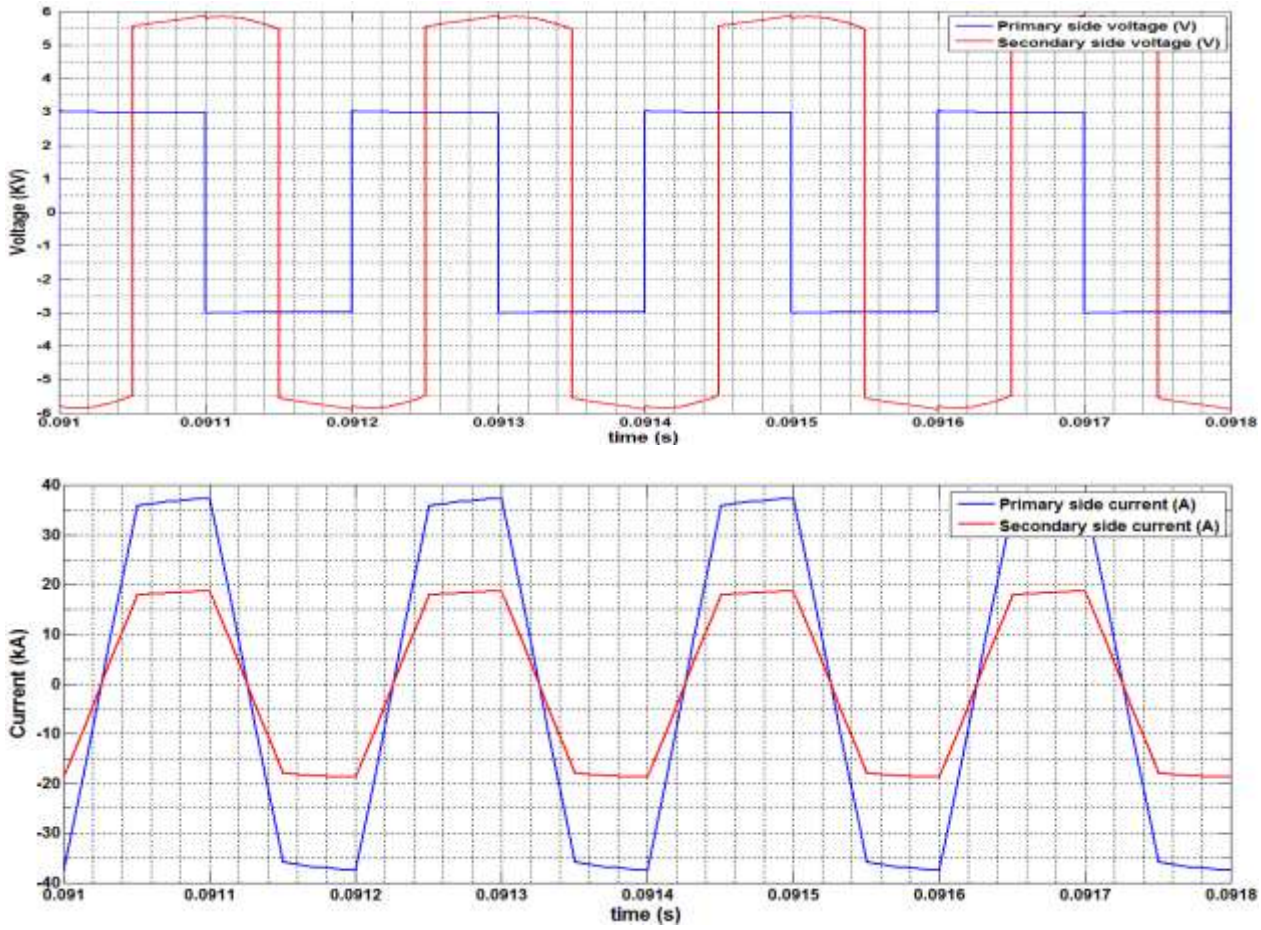

Fig 4.2 The primary and secondary currents and voltages of the transformer for the maximum power in the steady state

As can be seen in Figure 4.3, Section A shows the phase shift between the primary and secondary voltages of transformer in the converter. The current has been accelerated with a high slope since there is a high difference between the primary and secondary voltages of the transformer according to (4.1).

$$i(\theta) = \left[\frac{V_{in} + \frac{V_{out}}{n}}{\omega L}\right]\theta + i(0) \qquad (4.1)$$

In Section B, The current still has been increased because of the higher voltage levels of the primary side than the secondary side. The relation can be seen in (4.2).

$$i(\theta) = \left[\frac{V_{in} - \frac{V_{out}}{n}}{\omega L}\right](\theta - \phi) + i(\phi) \qquad (4.2)$$

In Sections C and D, both currents have been decreased but the slope of reduction in Section C is lower than in Section D which is due to the reason that the voltage difference between the primary and secondary sides are lower in Section C than in Section D.

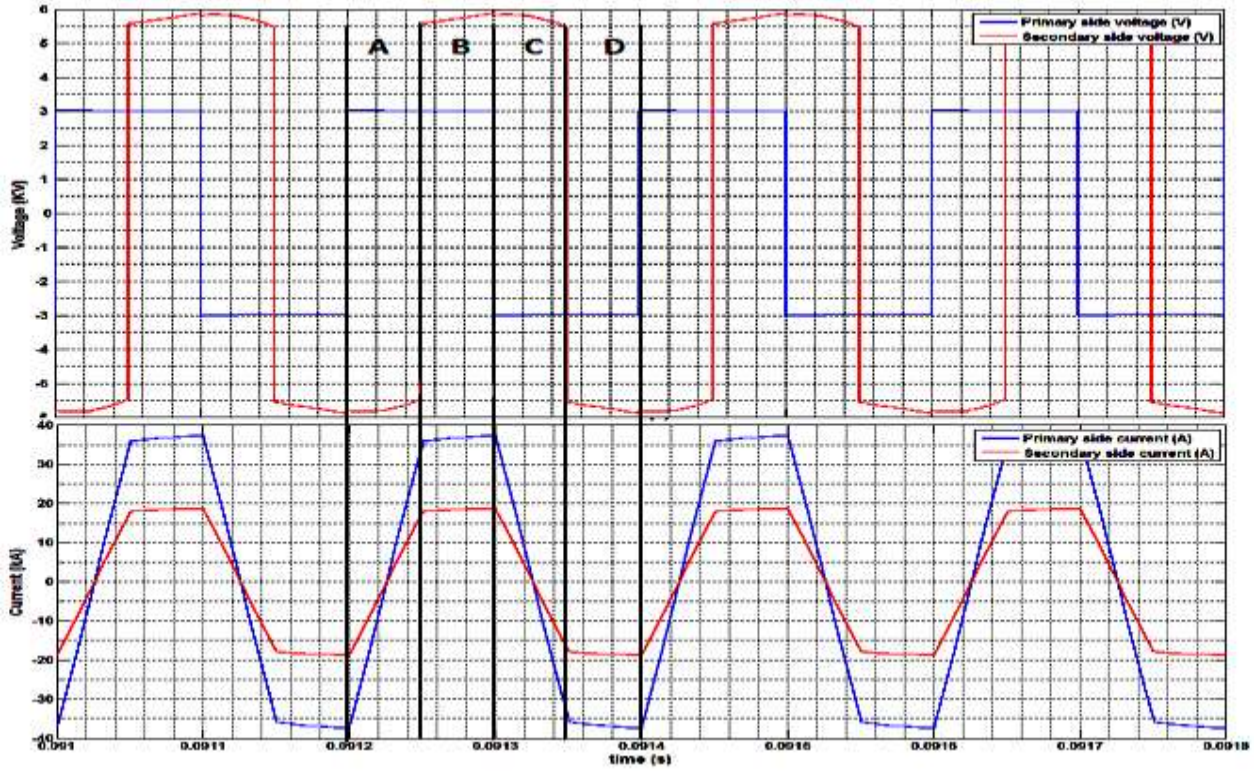

Fig. 4.3 The primary and secondary voltages and currents of transformer for the desired output power

As mentioned in the theory part and in the zero voltage switching section, one aim of the thesis is to achieve soft switching in the converter as well. Figure 4.4 show that soft switching for the turning on state of the switches has been reached.

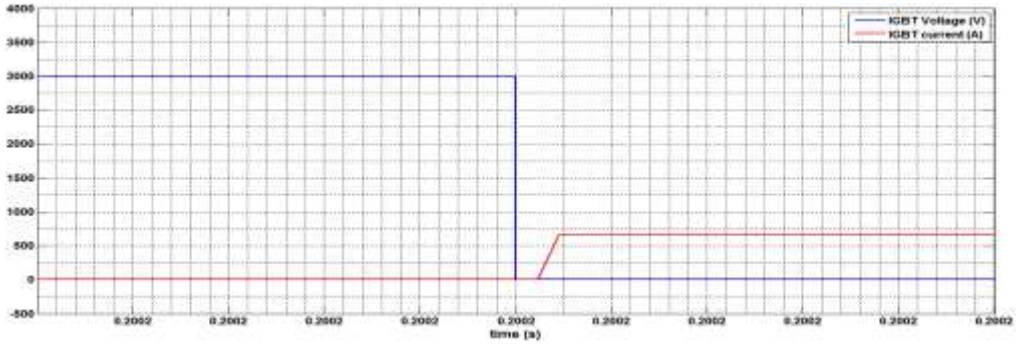

Fig. 4.4 The voltage and current waveforms of the switches in soft switching

It can be seen that the voltage across the switches become zero before the conduction state of the switches start. In order to have soft switching during the turn off state of switches, it's necessary to use

the snubber capacitor. The snubber capacitor value should be calculated based on the turn-off time, rising-time of the voltage and falling-time of the current in the IGBT. Due to the limitation of PLECS which does not get any value for the turn-off time of the IGBT, it's not possible to see the turn off soft switching in the voltage and current waveforms of the simulated DAB converter but in the laboratory, the overvoltage snubber capacitor has been designed for the DAB converter which is discussed later.

4.1.2 Three phase dual active bridge simulation

In the same way as the single phase dual active bridge, the three phase DAB converter has been simulated with the same desired parameters. Figure 4.5 shows the primary and secondary waveforms of the transformer for the same transferred power of 2MW.

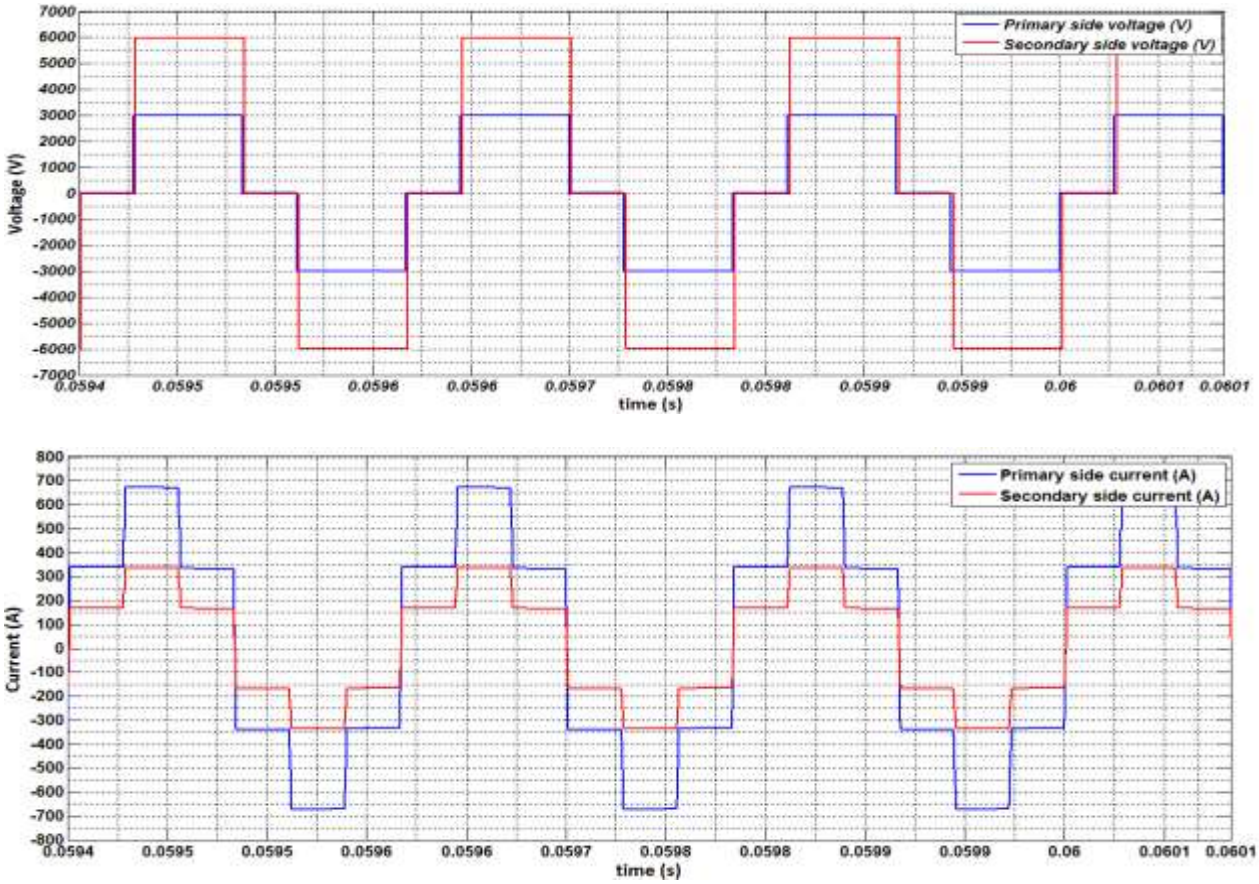

Fig. 4.5 The primary and secondary voltages and currents of a transformer for the desired output power

A test has been done for the phase shift of 90 degrees as well leads to maximum transferred power. It should be noted that this maximum transferred power is not realistic due to the limitation of the switches

and transformer and it's just presented to show the possible different waveforms of the three phase dual active bridge converter.

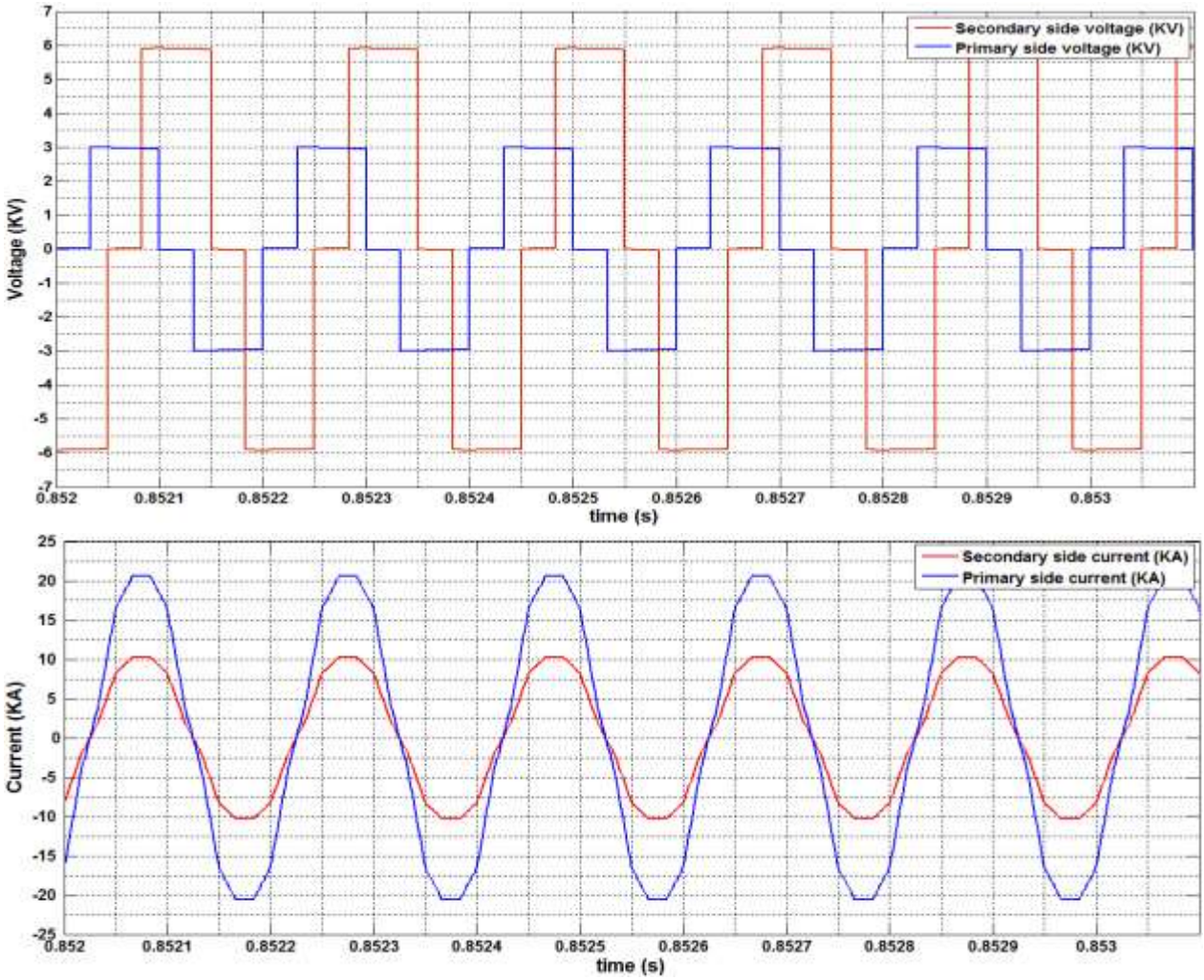

Fig. 4.6 The primary and secondary voltages and currents of transformer for maximum power

As can be seen in Figure 4.6, the current waveforms have been changed due to 90 degrees phase shift between the primary and secondary bridges of the DAB converter. It should be noted that the voltage waveforms are belong to $V_{L\text{-}L}$ in this figure.

4.2 Analysis of the Experimental Results

In this section, both the simulation and experimental results and waveforms are presented and discussed for the implemented dual active bridge converter in the laboratory. It should be noted that just the simulation has been done for the case study of the DAB converter with the desired output power which was analyzed and discussed in the previous section. Here in this section, the aim is just to analyze the implemented DAB converter which is available in the laboratory.

4.2.1 Single phase dual active bridge experimental results

In this section, results and figures of a practical implementation of the single phase DAB converter are presented and discussed. As mentioned, some tests have been done for several frequencies and for different level of voltages. The parameters values of different tests which have been done can be seen in Table 4.2.

Table 4.2: The parameters value of all five tests

	Test 1	Test 2	Test 3	Test 4	Test 5
Frequency (Hz)	50	50	100	500	1000
$V_{in\ (V)}$	30	80	20	15	30
$V_{out\ (V)}$	54	144	36	27	54
$R_{L\ (\Omega)}$	25.5	41.5	27	48.6	101
Power (W)	114	500	48	15	28.8
Phase shift (sec)	0.0005	0.0003	0.0005	0.0005	0.0002

The mentioned output power in this table is determined by (2.1). The resistance load can also be calculated by following formula for the desired output power and voltage.

$$R = \frac{V_o^2}{P_o} \tag{4.1}$$

The relation between the phase shift based on the time and phase shift in radian is as follows.

$$\emptyset = \left(\frac{x}{\pi}\right)\frac{T}{2} \tag{4.2}$$

The phase shift which is mentioned in Table 4.2 is based on the time (Ø in formula).

The experimental results are given in Table 4.3 for all five tests.

Table 4.3: The experimental results for DAB converter for five tests

Test	1	2	3	4	5
Frequency(Hz)	50	50	100	500	1000
V_{in} (V)	30	80	20	15	30
V_{out} (V)	48	134	30	20	40
R_L (Ω)	25.5	41.5	27	48.6	100
Power (W)	90	432	33.3	8.2	16
Phase shift (s)	0.0005	0.0003	0.0005	0.0005	0.0002

The given output voltage and power values are based on the measurement of the implemented DAB converter in the laboratory. As can be seen in Table 4.2, there is a 6-10 V voltage drop for the different tests.

In next sections, the voltage and current waveforms for each test are presented and discussed separately.

A. Analysis of the single phase DAB at 50 Hz

Two tests have been done for the frequency of 50 Hz for different input voltages and different phase shifts. The voltage and current waveforms of the first test can be seen in Figure 4.7.

As shown in Figure 4.7, there is 0.0005 sec phase shift between the primary and secondary voltage waveforms of the transformer which shows that the dual active bridge works in a desired way. The output voltage is supposed to be 54 V based on the ideal calculations, but it reaches to 48 V due to the voltage drops through the switches, diodes and transformer.

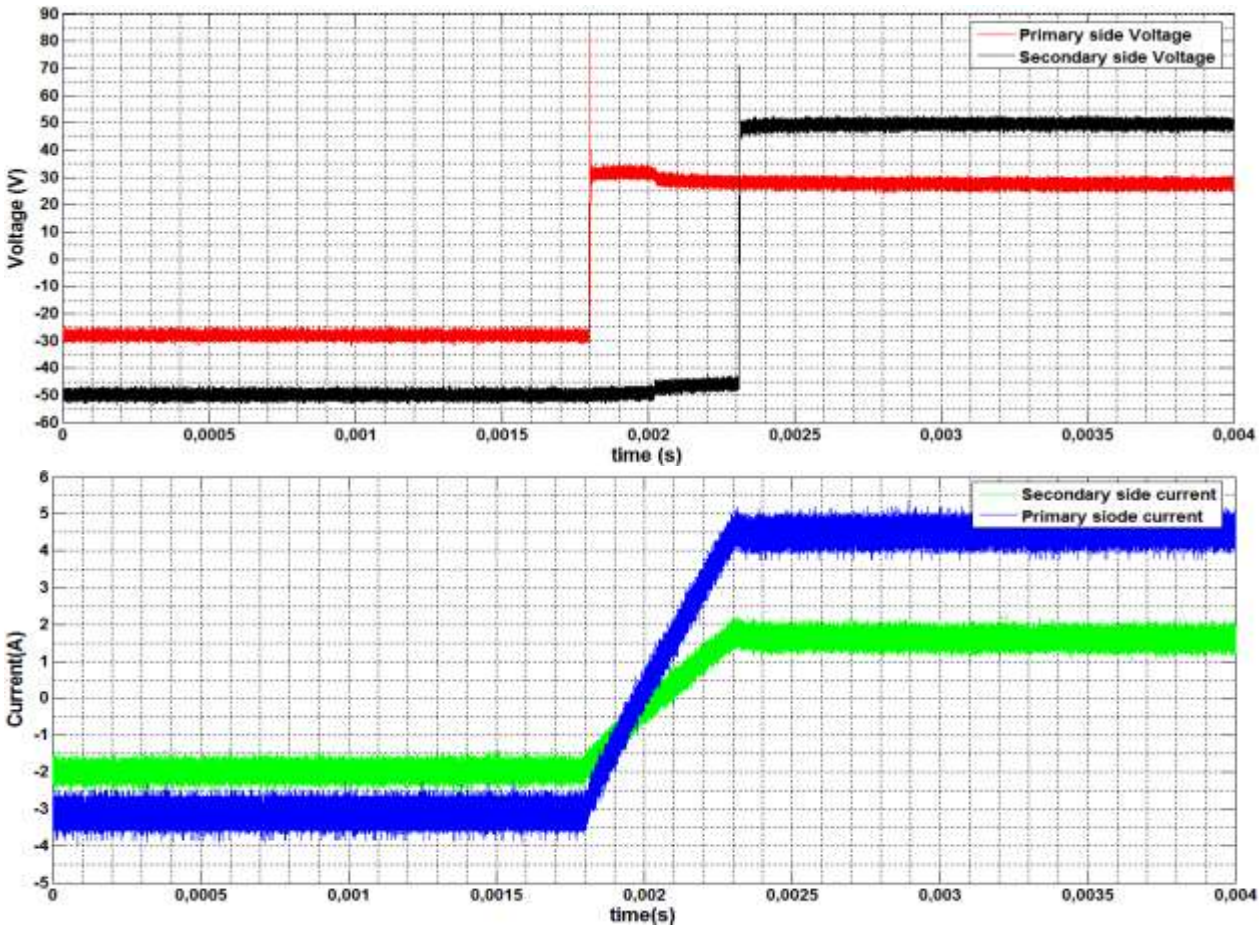

Fig. 4.7: The voltage and current wave forms of DAB converter for test one

Figure 4.8 shows a half period of test two which has been done at a frequency of 50 Hz but for the higher voltage and power.

As can be seen here, the current waveforms have a rapid rise during the phase shift time between the voltages of the primary and secondary side of the transformer. The output voltage should be 144 V according to (2.1), but due to the voltage drops of switches, diodes and transformer it becomes 134 V

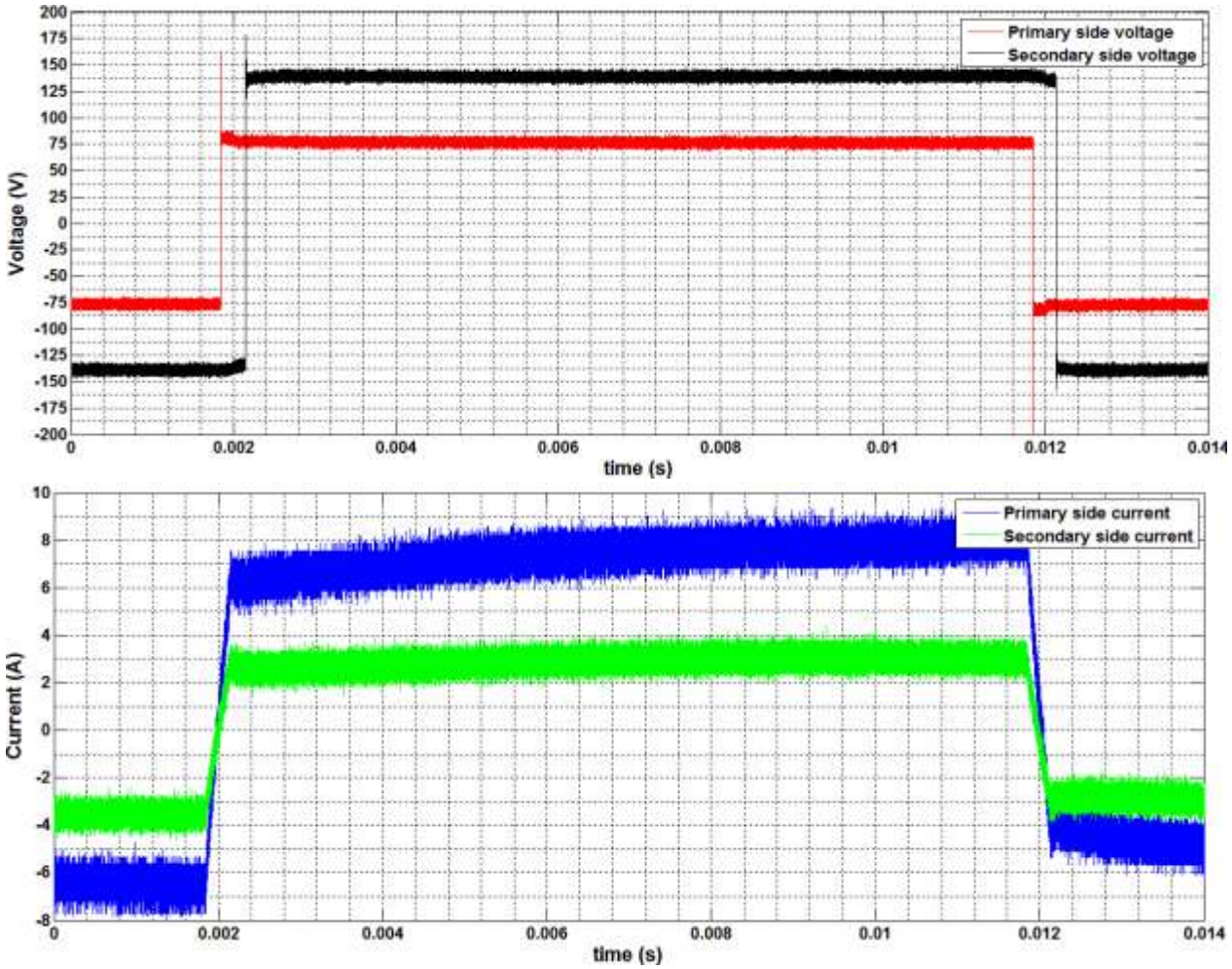

Fig. 4.8: The voltage and current waveforms of DAB converter in test 2

Switching overvoltage can be seen in the voltage waveforms of both tests 1 and 2. This phenomenon is due to the lack of snubber capacitor in the available converters.

B. Analysis of the single phase DAB at 100 Hz

A test has also been done at a frequency of 100 HZ but lower power has been considered due to the limitation of the 50 HZ transformer. Figure 4.9 shows the voltage and current waveforms.

As can be seen in Figure 4.9, there is a drop in the voltage waveforms during the phase shift. This phenomenon is due to the forward voltage drop of both diodes and IGBTs in the converter. As mentioned earlier, both the diode and IGBTs have forward voltage drop which is 1.1 and 0.9 for diodes and IGBTS respectively according to the technical detail of the IGBT package in the catalog. It should be noted that this forward voltage value can be vary with temperature and selection of PE module and temperatures of the case.

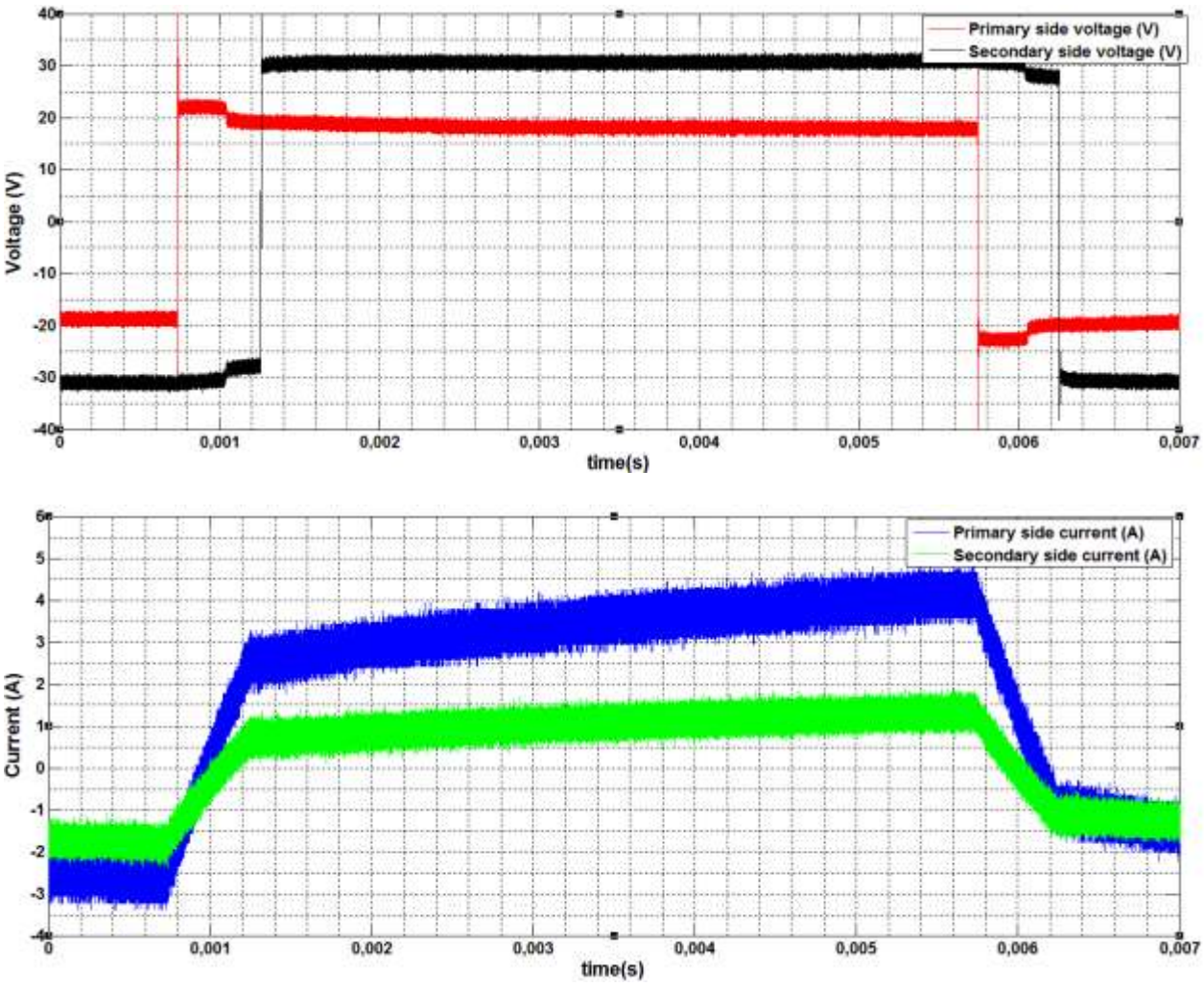

Fig. 4.9: The voltage and current waveforms of the DAB converter in the test three

As can be seen here, the output voltage has reached 30V while according to (2.1) it was determined to be 36 V which shows 6V voltage drops.

C. Analysis of the single phase DAB at 500 Hz

The same test has also been done at a frequency of 500 Hz but again a low power has been considered in order to avoid the situation which can warm a 50 Hz transformer. Figure 4.10 shows the voltage and current waveforms.

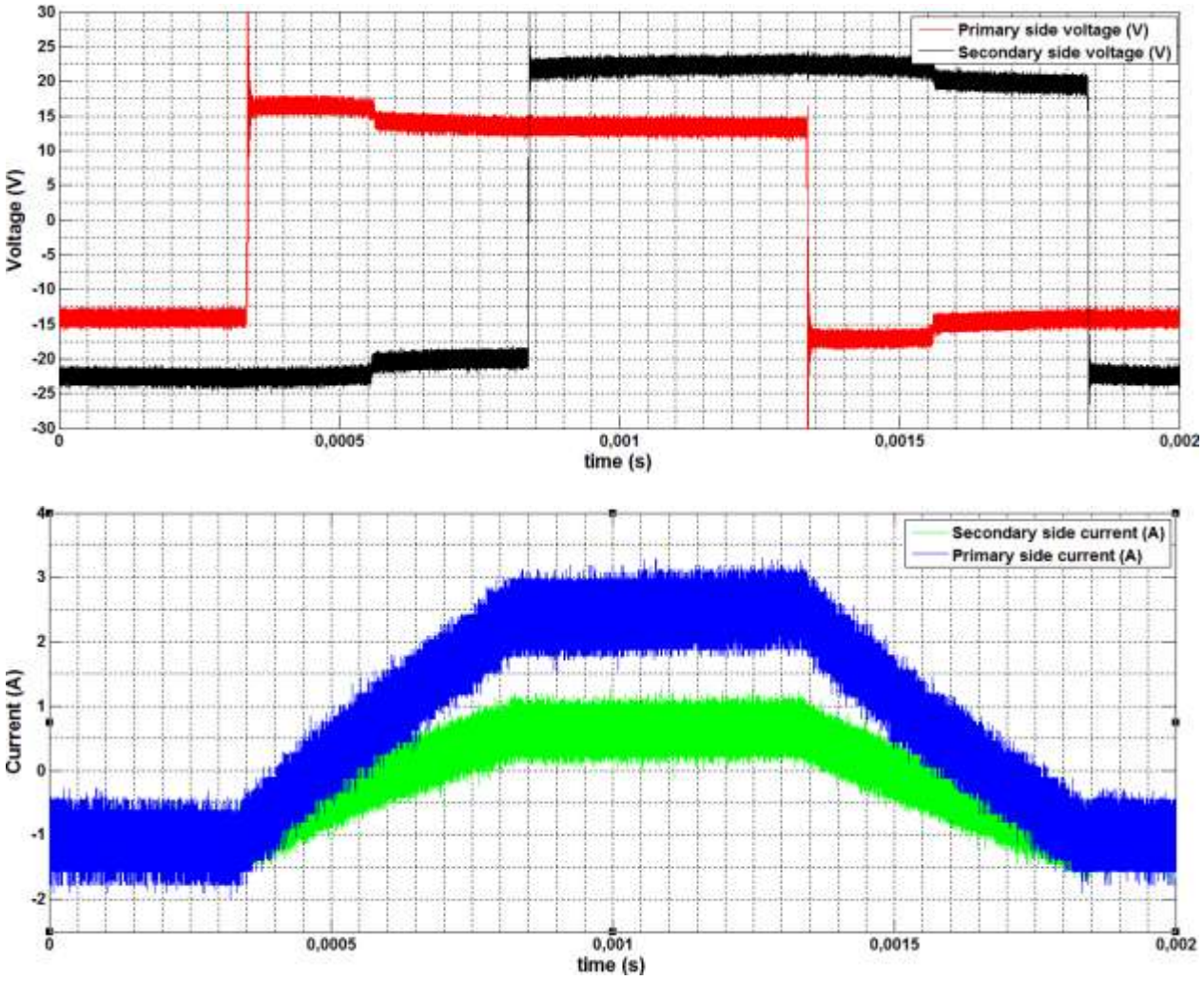

Fig. 4.10: The voltage and current waveforms of the DAB converter in test four

As can be seen in Figure 4.10, the voltage drop of the voltage waveforms is clearer here. The phase shift is completely clear in this test. Due to the frequency of 500 Hz and using the 50 Hz transformer, the losses in this test are higher than the previous tests. It will be discussed more in the loss calculation section.

D. Analysis of the single phase DAB at 1 KHz

In the last steps of the project, a better accuracy for the dSPACE controller is achieved by optimizing the Simulink code for dSPACE which makes it possible to increase the frequency up to 1 KHz. This test has been done after installing snubber capacitors on the converters so it gives over-shoot free waveforms which can be seen in Figure 4.11.

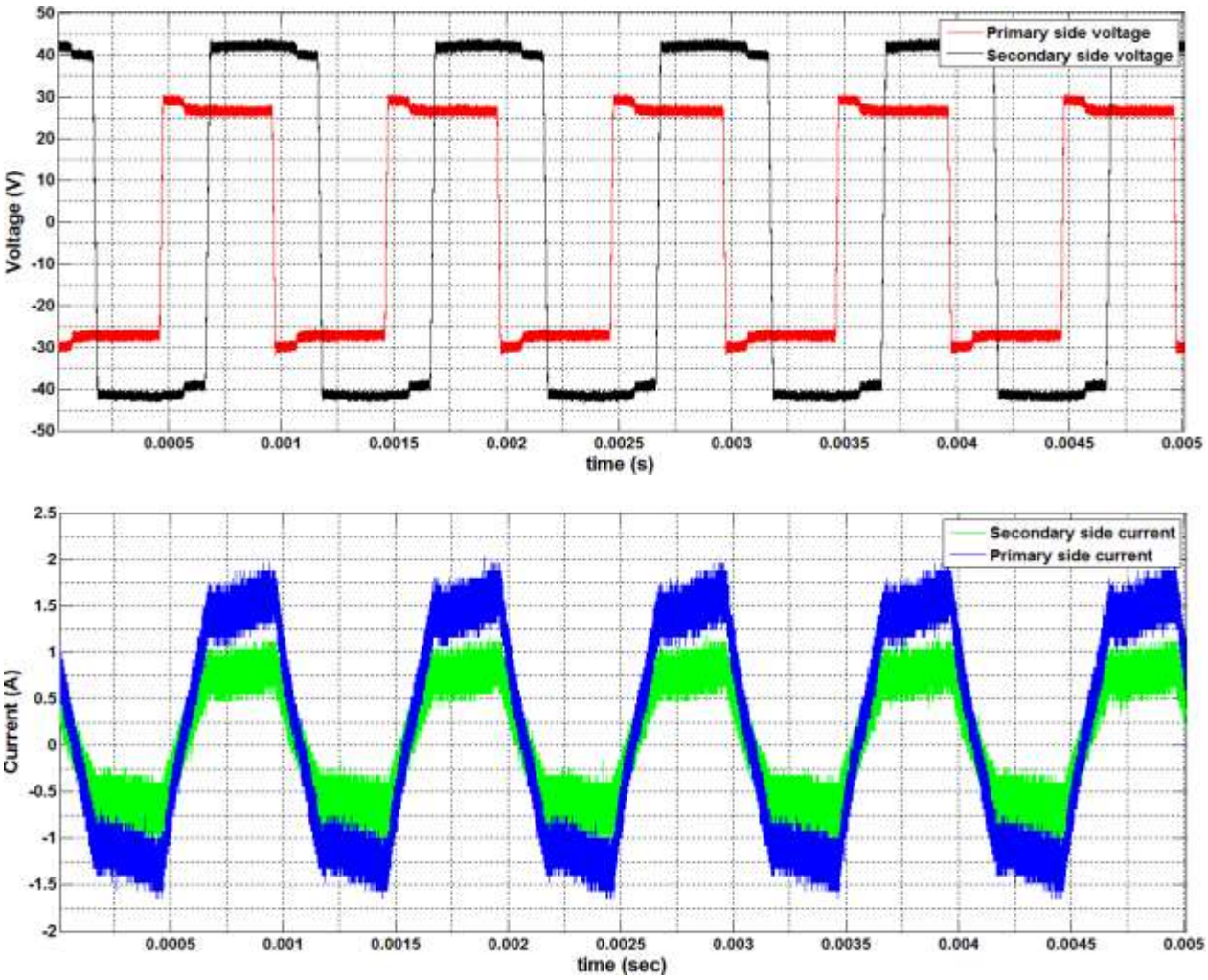

Fig. 4.11: The voltage and current waveforms of the DAB converter in test five

As can be seen in Figure 4.11, there is no switching overvoltage in the voltage waveforms which is due to the usage of overvoltage snubber capacitor in this test. The comparison between the DAB with and without snubber capacitor is discussed later.

4.2.2 The three phase dual active bridge experimental results

In the same way as for the single phase dual active bridge converter, some tests have been done for different frequencies and powers for the three phase dual active bridges. The results of the theoretical calculation by using (2.3) and (2.4) are presented in Table 4.4.

Table 4.4: The parameters value of all three tests

	Test 1	Test 2	Test 3
Frequency (Hz)	55	55	555
$V_{in\ (V)}$	50	125	50
$V_{out\ (V)}$	86.5	216	86.5
$R_{L\ (\Omega)}$	25	31	25
Power (W)	300	1500	300
Phase shift	1e-4	1e-4	1.1e-4

It should be noted that, these results are completely ideal and based on the theoretical formulas. Table 4.5 gives the experimental results for these three tests.

Table 4.5: The experimental results for DAB converter for five tests

	Test 1	Test 2	Test 3
Frequency (Hz)	55	55	555
$V_{in\ (V)}$	50	125	50
$V_{out\ (V)}$	70	194	68.5
$R_{L\ (\Omega)}$	25	31	25
Power (W)	196	1214	187.5
Phase shift	1e-4	1e-4	1.1e-4

In the following steps, the results for each test are discussed.

A. The analysis of the three phase DAB at 55.55 Hz

The first and second tests are done for a frequency of 55 Hz. The reason of choosing 55 Hz instead of 50 Hz is the timing details of the dSPACE controller. In case of using 50 Hz, the time period become 0.02 which is not dividable by three and six while different phase shifts of 30, 60 and so on should be implemented between the trigger time of the three phase inverter and rectifier bridges. Due to the limitation of the dSPACE controller, it is better to choose a time period which can be dividable by three and six which can increase the accuracy of test. The time period which is selected is 0.018 which is equal to the frequency of 55.55 Hz.

The first test has been done using low voltage of 50 V in order to reach the power of 300 W. According to (2.3) a phase shift of 2 degrees (equal to the phase shift of 1e-4 sec) has been implemented between the two bridges in order to reach to this power. The voltage and current waveforms can be seen in Figure 4.12.

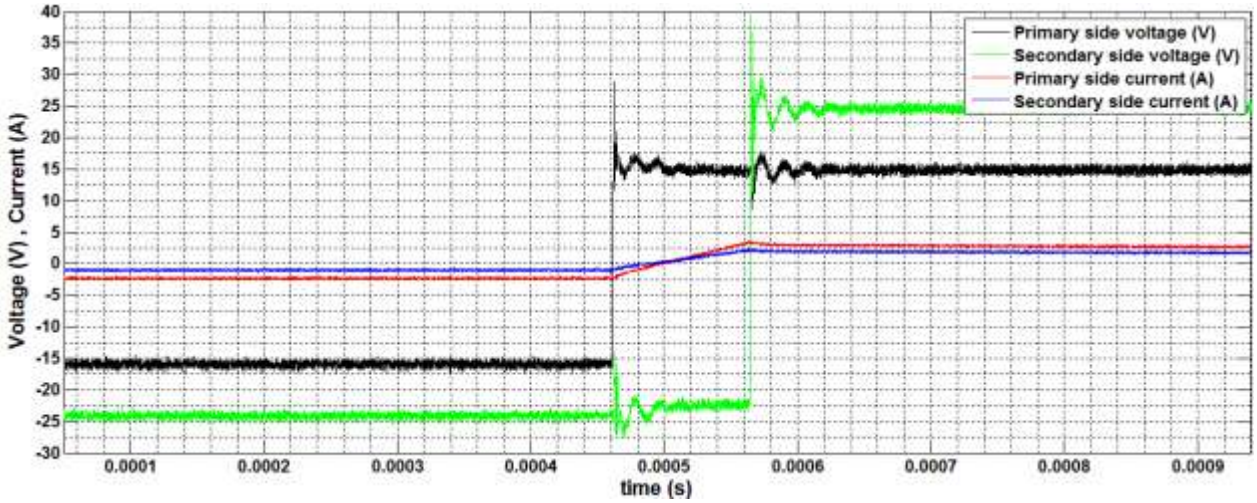

Fig. 4.12: The primary and secondary voltage and currents waveforms of the transformer at 55 Hz

The phase shift of 1e-4 second can be seen in this figure which is the desired phase shift. The switching overvoltage can also be seen in the voltage waveforms of the both primary and secondary sides. As mentioned earlier, the overvoltage snubber capacitor is needed to avoid switching overvoltage. In Section 4.2.3, the three phase DAB converter by using snubber capacitor has been analyzed and discussed.

.

B. The analysis of the three phase DAB at 55.55 Hz for higher power

The second test has been done for the frequency of 55 HZ and for the highest possible power which is 1.5 KW. The limitation is due to the transformer and dSPACE controller. Figure 4.13 shows the voltage and current waveforms of both the primary and secondary side of transformer.

As can be seen in this figure, a phase shift of 1e-4 is implemented between two sides of transformers. The switching overvoltage is considerable in this figure and is about 100 V. the reason is that the available converters don't have snubber capacitor. This problem has been fixed later by using overvoltage snubber capacitor and the results have been analyzed and discussed later.

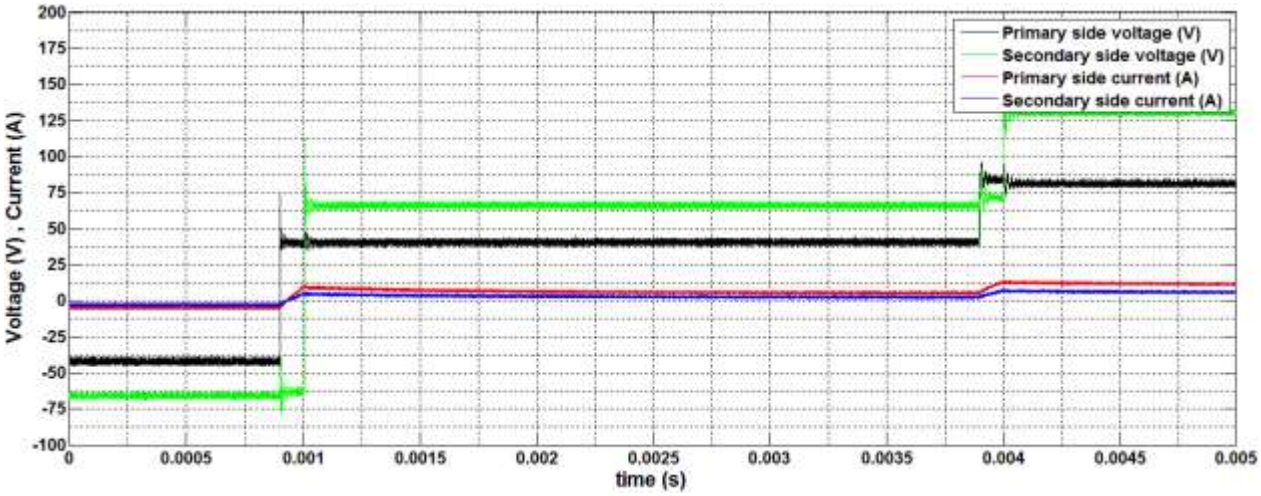

Fig. 4.13: The primary and secondary voltage and currents waveforms of the transformer in the frequency of 55 Hz and for maximum possible power

According to Table 4.3 and 4.4, and by comparing the output power results, it can be concluded that there is about 22 V voltage drop through the switches, diodes and transformers

C. The analysis of the three phase DAB at 555.55 Hz

The aim of this test is to reach the maximum possible frequency. As it was discussed earlier and in the single phase DAB converter, a maximum frequency of 1 KHz has been reached by using the dSPACE controller. Due to reason that 12 signals should be used in order to control the switches of the three phase DAB converter, the highest frequency which can be reached is 555 Hz. The reason is that the dSPACE digital implementation speed is decreased when more I/O digital bits are used. The low power is considered due to the unavailability of the high frequency transformer. The reason is that the high power led to the high

current and at high frequency the skinny effect happens through the winding of the transformer which increases the resistance of the wire and led to the high loss. The available transformer has an iron core and for a high frequency it can be overheated and damaged. Due to this reason, a test has been done for 555 Hz and low transferred power. The voltage and current waveforms can be seen in Figure 4.14.

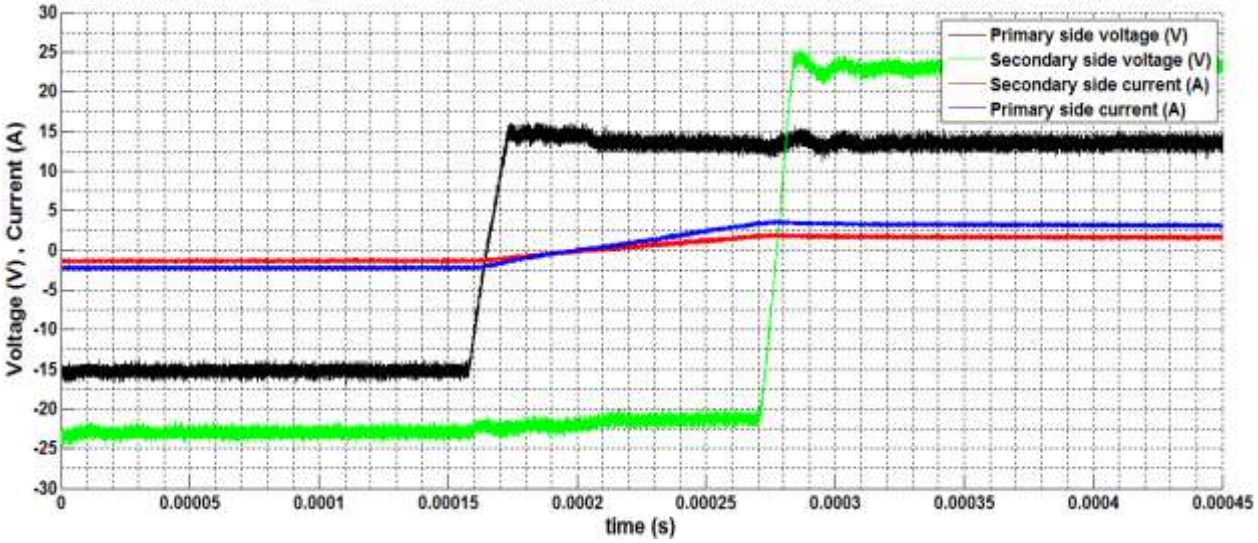

Fig. 4.14: The primary and secondary voltage and currents waveforms of the transformer in the frequency of 555 Hz

According to this figure, a phase shift of 1.1e-4 has been implemented between the two bridges of the DAB converter. This test has been done after installing the snubber capacitor on the DAB converter and due to this; no switching overvoltage can be seen in the voltage waveforms.

4.2.3 Analysis of three phase DAB converter by using snubber capacitor

As can be seen in the figures in the previous sections, the voltage waveforms for the both single and three phase dual active bridge converter have switching overvoltages. In order to avoid the switching overvoltage, a snubber capacitor should be used as mentioned in the previous sections. According to the calculation which has been done earlier and the tests which have been done, the value of 330 nF has been selected for the inverter bridge switches and the 180 nF has been used for the switches of the rectifier bridge. Other values for snubber capacitor are also tested.

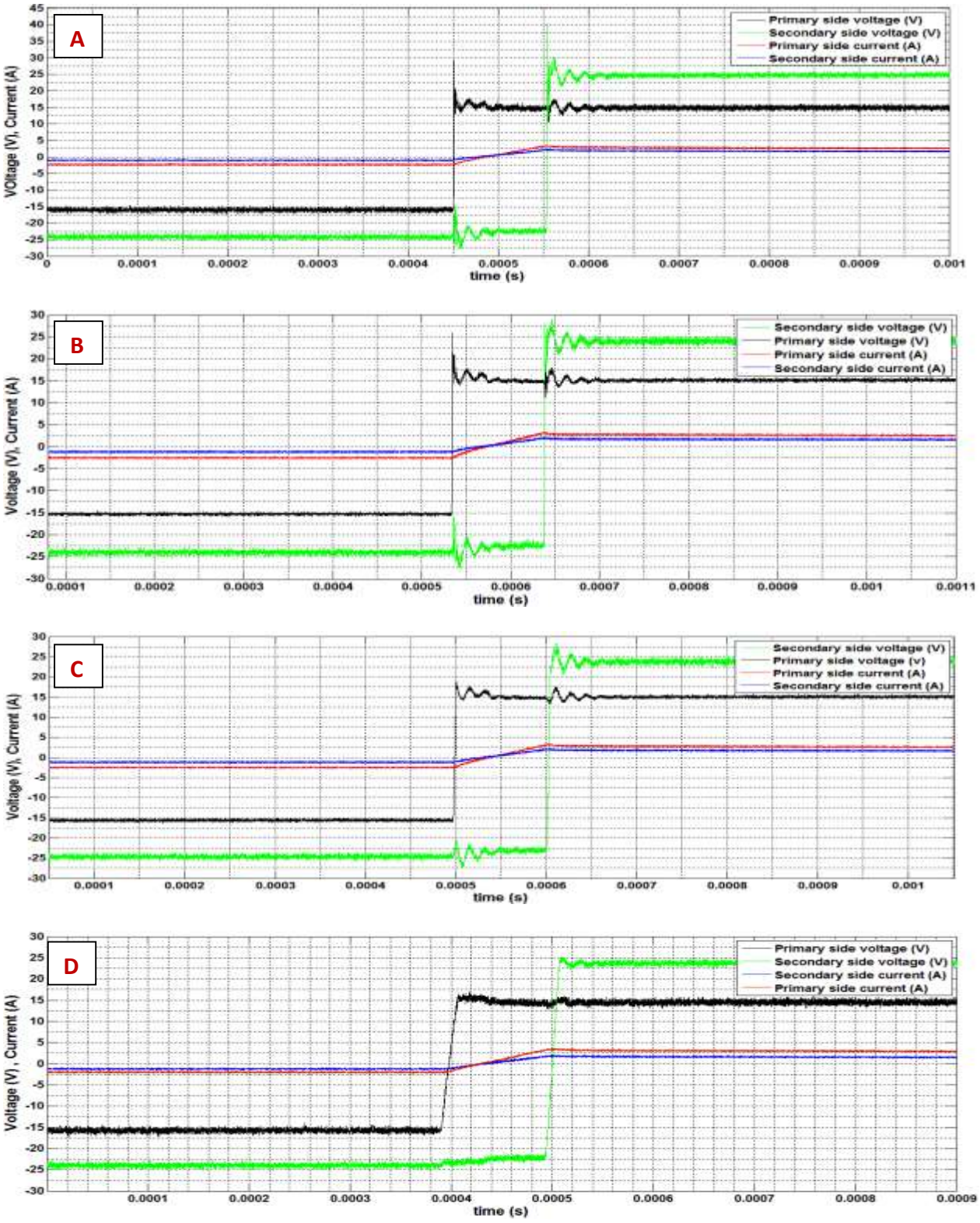

Figure 4.15: The primary and secondary voltage and current waveforms for the first test by using snubber capacitor with the value of A) no snubber capacitor B) 6.8 nF C) 68 nF and D) 330 nF

Figure 4.15 shows the switching overvoltage for the first test with different values of snubber capacitor. Table 4.6 shows the different values of snubber capacitor which are used.

Table 4.6: The different value of the used snubber capacitor

Test	The value of snubber capacitor in Inverter bridge	In Rectifier bridge
D	330 nF	180 nF
C	68 nF	47 nF
B	6.8 nF	3.3 nF

Figure 4.16 and 4.17 Show the comparison between the DAB converter with and without installed capacitor for both single and three phase dual active bridge respectively.

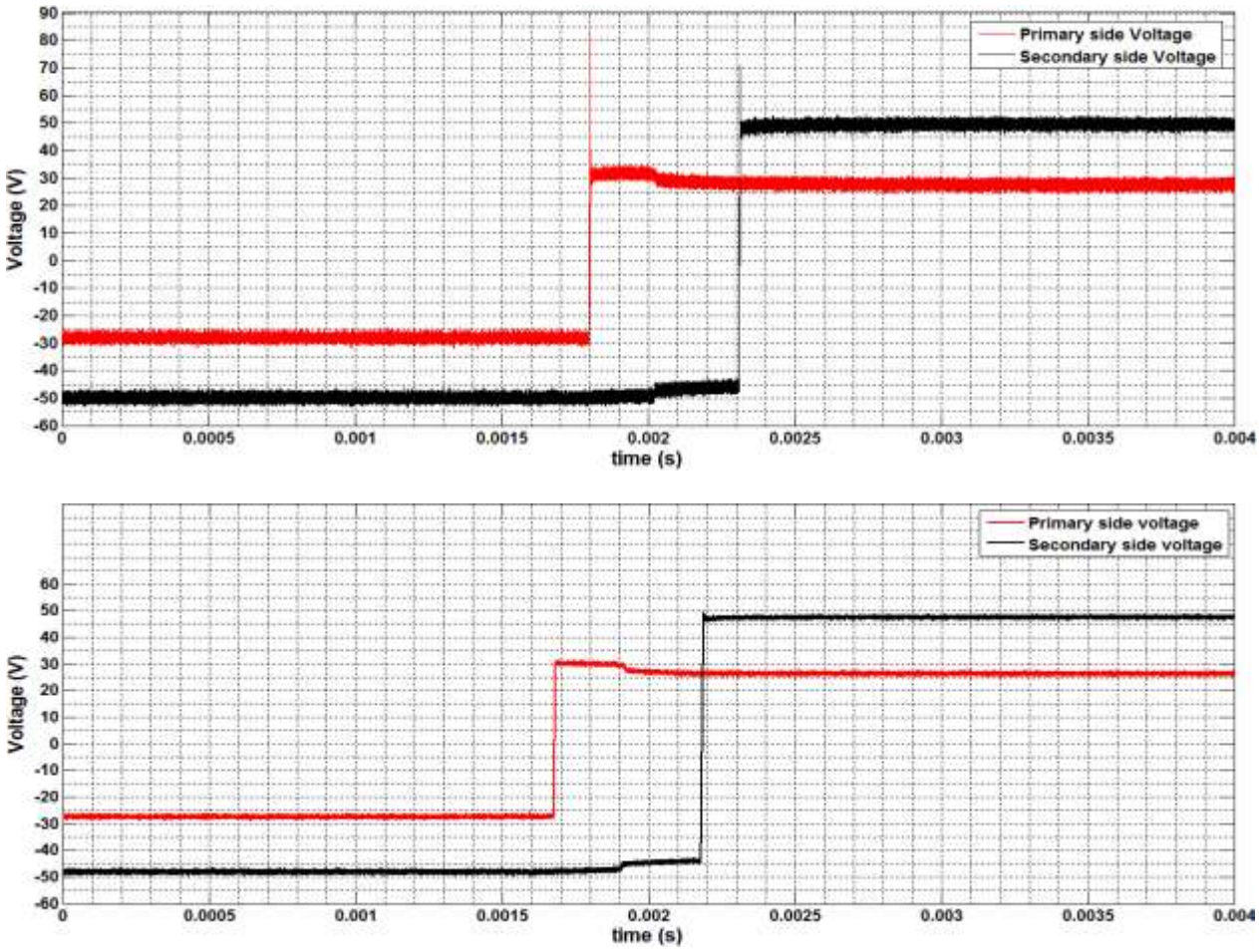

Fig. 4.16: The primary and secondary voltage waveforms for the first test of the single phase DAB converter with (down) and without snubber capacitor (up)

As can be seen in Figure 4.16 which belongs to the first test of the single phase dual active bridge converter for a frequency of 50 Hz, there is about 45 V switching overvoltage in the voltage waveform of the primary side. The second figure shows the voltage waveforms of the same test by using snubber capacitor. It's clear that the switching overvoltage is completely removed. It should be mentioned that, although the overvoltage has been avoided by using the snubber capacitor, the switching losses is transferred to the loss through the IGBTs resistance which is in parallel to the snubber capacitor.

Figure 4.17 shows the comparison for the three phase DAB converter with and without snubber capacitor. As can be seen in this figure, there is the switching overvoltage of 15 Volts in both primary and secondary sides which have been removed by using the snubber capacitor.

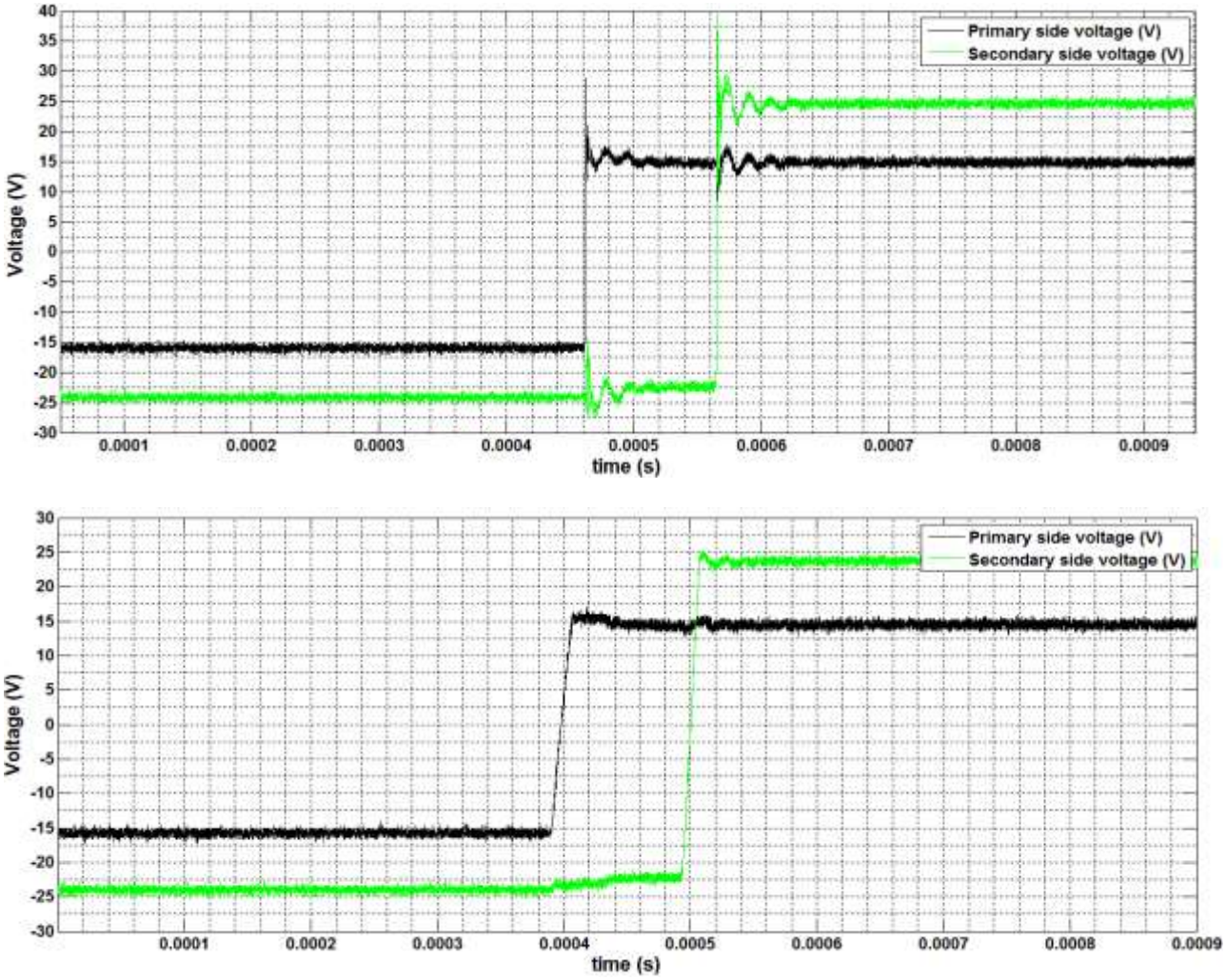

Fig. 4.17: The primary and secondary voltage waveforms for the first test of the three phase DAB converter with (down) and without snubber capacitor (up)

As can be seen in Figure 4.17 down, the slope of primary side voltage in rising time is considerably different compared to the one in the upper figure which is due to the instantaneous rate of voltage change over

time, or the rate of change of voltage (volts per second increase or decrease) at a specific point in time according to

$$I_c = C\frac{dv}{dt} \tag{4.3}$$

4.3 Loss calculation for both the single and three phase DAB converter

The aim of this section is to calculate the losses for both the single and three phase DAB converters for all tests. The loss calculation have been done theoretically, based on the simulation results and also based on the experimental results. First step to calculate the losses for all tests is to get some data from the switch data sheets. The used datasheets are available in Appendix 2. Figure 4.18 and the following calculation show how the needed value can be calculated from the data sheet.

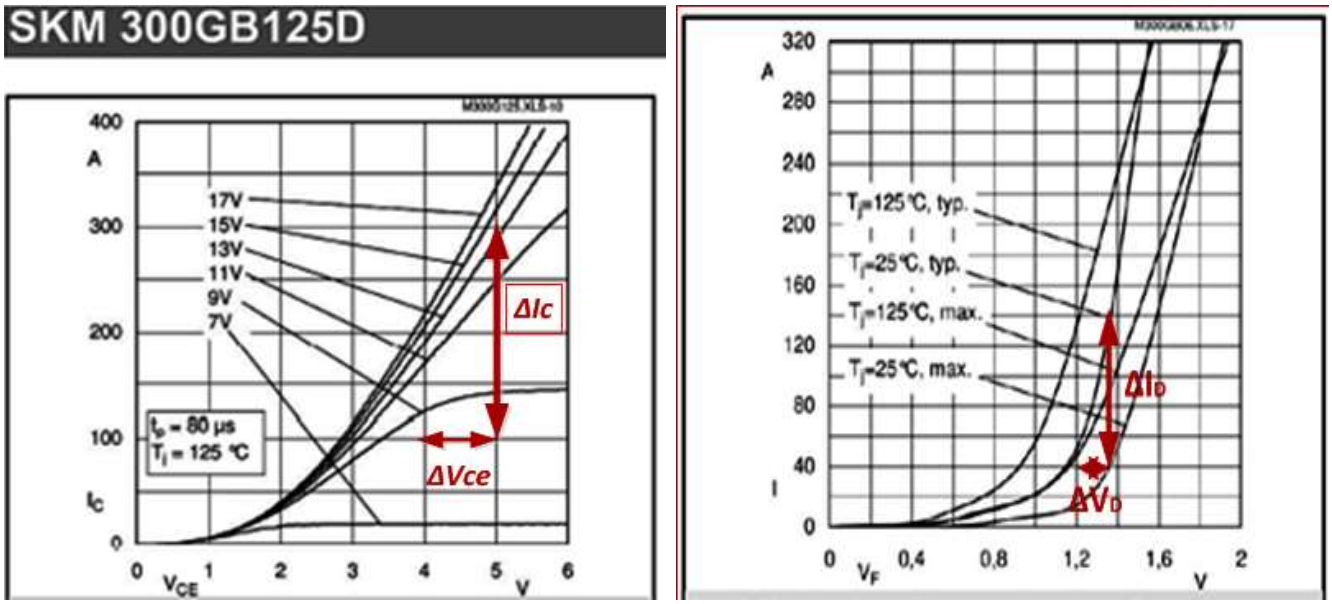

Figure 4.18: Typical output characteristics for the SEMIKRON IGBT (left) and diode (right) from the datasheet

$$V_{CE} = 15\ V$$
$$r_C = \frac{\Delta\ V_{CE}}{\Delta\ I_C} = \frac{1}{200} = 5m\Omega$$
$$V_{CE0} = 0.9V$$

$$\text{Qrr} = 18 + 23 = 41\mu\text{C} \rightarrow \text{E}_{\text{onD}} = \frac{1}{4} 41 \frac{Vdc}{2} 10^{-6} = \frac{41Vdc}{8000} mWs$$
$$r_D(25c) = \frac{\Delta\ V_D}{\Delta\ I_D} = \frac{0.1}{100} = 1m\Omega$$
$$V_{D0} = 1.1V$$

As it was discussed before, there is no switching turn on losses in this project, so the formula can be rewritten as,

$$P_T = P_{CT} + P_{swT} = V_{CE0}.I_{cav} + r_C.I^2_{crms} + E_{offT}.f_{sw} \quad (4.4)$$
$$P_D = P_{CD} + P_{swD} = V_{D0}.I_{Dav} + r_D.I^2_{Drms} + E_{onD}.f_{sw} \quad (4.5)$$

4.3.1 Loss calculation for the first test of the single phase DAB converter

The loss calculation has been done for the first test. The ideal output power can be calculated by (2.1).

$$\mathrm{P_o} = \frac{V_i^2}{\omega L}\left(\frac{\mathrm{V_o}}{nV_i}\right)\emptyset\left(1-\frac{\emptyset}{\pi}\right) = 114w$$

In order to calculate the current, the current formula for the leakage inductance of the transformer can be used. The current of switches are the same as the inductance current.

$$V_L = Vin - \frac{Vout}{n} = L\frac{di}{dt} \rightarrow i(t) = -\frac{\frac{Vout}{n}-Vin}{L}t + i_0 \qquad (4.6)$$

The above formula shows that the current has the linear relation which can be seen in Figure 4.19 as well. So, the current equation can be calculated as follow:

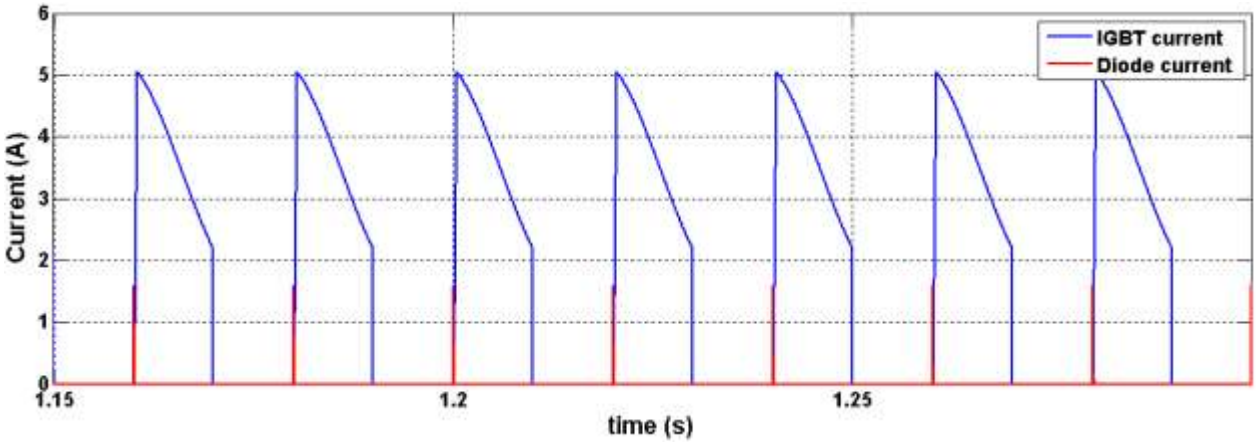

Figure 4.19: The IGBT and diode currents of switches S1 for the first test

$$i(t) = -\frac{i_{max}-i_{min}}{T_{on}}t + i_{max} \qquad (4.7)$$

And the I_{rms} can be calculated by the following calculation:

$$T_{on} = DT$$

$$i(t) = -\frac{i_{max}-i_{min}}{T_{on}}t + i_{max} \rightarrow I_{rms} = \sqrt{\frac{1}{T}\int_0^{T_{on}} i(t)^2 dt} = \sqrt{\frac{1}{T}\int_0^{T_{on}}\left(-\frac{i_{max}-i_{min}}{T_{on}}t + i_{max}\right)^2 dt}$$

$$= \sqrt{\frac{1}{T}\int_0^{T_{on}}\left(\left(\frac{i_{max}-i_{min}}{T_{on}}\right)^2 t^2 + {i_{max}}^2 - 2i_{max}\frac{i_{max}-i_{min}}{T_{on}}t\right)dt}$$

$$= \sqrt{\frac{1}{T}\left(\left(\frac{i_{max}-i_{min}}{T_{on}}\right)^2 \frac{{T_{on}}^3}{3} + {i_{max}}^2.T_{on} - 2i_{max}\frac{i_{max}-i_{min}}{T_{on}}\frac{{T_{on}}^2}{2}\right)}$$

$$= \sqrt{\frac{T_{on}}{T}\left(\frac{(i_{max}-i_{min})^2}{3} + {i_{max}}^2 - i_{max}(i_{max}-i_{min})\right)} =$$

$$\rightarrow I_{rms} = \frac{1}{\sqrt{6}}\sqrt{{i_{max}}^2 + {i_{min}}^2 + i_{max}i_{min}} \quad (4.8)$$

and the I_{Cav} can be calculated by

$$I_{cav} = \frac{I_{max}+I_{min}}{2}.\frac{T_{onsw}}{T} = \frac{I_{max}+I_{min}}{2}D \quad (4.9)$$

and the diode has the following relations

$$I_{Drms} = \sqrt{\frac{T_{onD}}{T}\left(\frac{(i_{max})^2}{3}\right)} = I_{Dmax}\sqrt{\frac{T_{onD}}{3T}} \quad (4.10)$$

$$I_{Dav} = \frac{I_{Dmax}+0}{2}.\frac{T_{onD}}{T} = T_{onD}\frac{I_{Dmax}}{2T} \quad (4.11)$$

I_{max} and I_{min} can be calculated by using the output current, input current and the leakage inductance current formula but the problem is that the calculation is ideal since no losses is considered in the calculation. So, in order to have the more accurate value for them, the simulation results can be used which is shown in Figure 4.19.

According to (2.7-2.16), the switching and conduction losses can be calculated for both the IGBT and diode:

$$P_T = P_{CT} + P_{swT} = V_{CE0}I_{cav} + r_C I_{crms}^2 + E_{offT}f_{sw}$$

$$\rightarrow P_T = 0.9\frac{I_{max}+I_{min}}{2}D + \frac{5\times10^{-3}}{6}\left({i_{max}}^2 + {i_{min}}^2 + i_{max}i_{min}\right) + \frac{5\times20}{450}\times10^{-3}\times50$$

$$\rightarrow P_T = 0.9\frac{5+2.2}{4} + \frac{5\times10^{-3}}{6}(5^2 + 2.2^2 + 5\times2.2) + \frac{5}{450}$$

$$= 1.62 + 0.03403 + 0.0111 = 1.66513\,W$$

$$P_D = P_{CD} + P_{swD} = V_{D0}I_{Dav} + r_D I_{Drms}^2 + E_{onD}f_{sw}$$

$$\rightarrow P_D = 1.1\frac{I_{Dmax}}{2}\frac{Ton_D}{T} + 10^{-3}\frac{T_{onD}}{3T}{I_{Dmax}}^2 + \frac{41Vi}{8}\times10^{-6}\times50$$

$$\rightarrow P_D = 1.1\frac{1.6}{2}\frac{0.13\times10^{-3}}{2\times10^{-2}} + 10^{-3}\frac{0.13\times10^{-3}}{6\times10^{-2}}1.6^2 + \frac{41\times30}{8}\times10^{-6}\times50$$

$$= 5.72\times10^{-3} + 0.00555\times10^{-3} + 7.6875\times10^{-3} = 13.413\,mW$$

$$Ploss_{sw} = 8(P_D + P_T) = 8(1.66513 + 13.413\times10^{-3}) = 13.428\,W$$

The copper and iron losses for the single phase transformer can be calculated by (2.17-2.19) and using the value of the table 3.5-3.7.

$$P_{CU} = RI_{rms}^2 = \frac{R}{6}\left({i_{max}}^2 + {i_{min}}^2 + i_{max}i_{min}\right) = \frac{0.31}{6}(5^2 + 2.2^2 + 5 \times 2.2) = 2.11\ W$$

The transformer iron loss is calculated by using the open circuit test for the single phase transformer which was mentioned before. So,

$$R_C = \frac{{V_{oc}}^2}{P_{oc}} = \frac{63^2}{7.7} \cong 516\Omega$$

$$V_{eff} = V_{in} - 2 * V_{sw} - R_T I = 30 - 2 * 0.9 - (0.31 + 0.1)\frac{5 + 2.2}{2} = 26.724$$

The effective voltage across the transformer is calculated above. The V_{sw} here is the voltage drop of the two IGBTs and the R_T is the resistance of the IGBT.

The transformer has the square wave voltage waveform which contains many harmonics. In order to have an accurate calculation, the harmonics of the waveform should be analyzed and then the core resistance can be calculated for the different frequencies in order to calculate the core losses. Due to the complex calculation, just the fundamental voltage has been considered and its magnitude has been considered equal to the magnitude of the square wave voltage.

$$P_{core} = \frac{{V_{eff(rms)}}^2}{R_C} = \frac{\left(\frac{26.724}{\sqrt{2}}\right)^2}{516} = 0.692\ W$$

$$\rightarrow P_{LossT} = P_{core} + P_{CU} = 0.692 + 2.11 = 2.802\ W$$

Since the total cabling is not clear, the length of the cabling is approximated to be about 6m for each phase. By using the data form Table 3.5, the cabling losses can be calculated.

$$P_{Cable} = RI_{rms}^2 = \frac{2R}{6}\left({i_{max}}^2 + {i_{min}}^2 + i_{max}i_{min}\right) = \frac{2 \times 6 \times 0.05}{6}(5^2 + 2.2^2 + 5 \times 2.2) = 4.0424$$

$$\mathrm{PLoss_{total}} = \mathrm{Ploss_{sw}} + \mathrm{P_{LossT}} + \mathrm{P_{Cable}} = 13.428 + 2.802 + 4.0424 = 20.314\ \mathrm{W}$$

As it can be seen, the theoretical total losses for the first test are about 20W.

The total losses for the simulation is calculated below,

$$\mathrm{PLoss_{total}} = \mathrm{P_{in}} - \mathrm{P_{Out}} = V_{dc}I_{ave} - \mathrm{P_{Out}} = 30 \times \frac{5 + 2.2}{2} - 92.5 = 15.5\ \mathrm{W}$$

The value of I_{max} and I_{min} has be obtained from Figure 4.20.

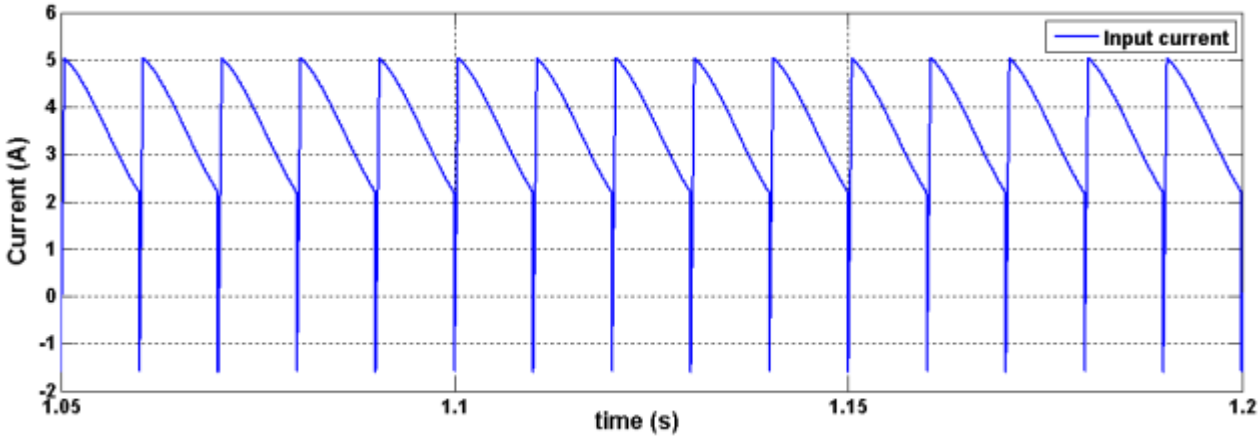

Figure 4.20: The input current of the DAB converter for the first test

As it can be seen, the total loss for the simulation results is lower which is due to the neglecting of the cable losses, core losses and switching losses in the simulation.

$$\mathrm{PLoss_{total}} = \mathrm{P_{in}} - \mathrm{P_{Out}} = V_{dc} I_{ave} - \mathrm{P_{Out}} = 30 \times \frac{5.2 + 2.4}{2} - 90 = 24\ \mathrm{W}$$

I_{ave} has been calculated from *the* I_{rms} of the primary side of the transformer since there was no data for the input current.

The total losses for the experimental results are calculated above. As calculations show, the losses for the experimental results is higher than the theoretically calculated losses which can be due to the resistance of the capacitor, connection resistance, temperature varying and the environmental noises or some approximation which has been done in the theoretical calculation.

4.3.2 Loss calculation for the second test of the single phase DAB converter

The same calculation as the first test has been done for the second test as well.

$$\mathrm{P_o} = \frac{V_i^2}{\omega L}\left(\frac{\mathrm{V_o}}{nV_i}\right)\emptyset\left(1-\frac{\emptyset}{\pi}\right) = 500w$$

The current has been changed linearly between the I_{max} and I_{min} ,as it is shown in Figure 4.21.

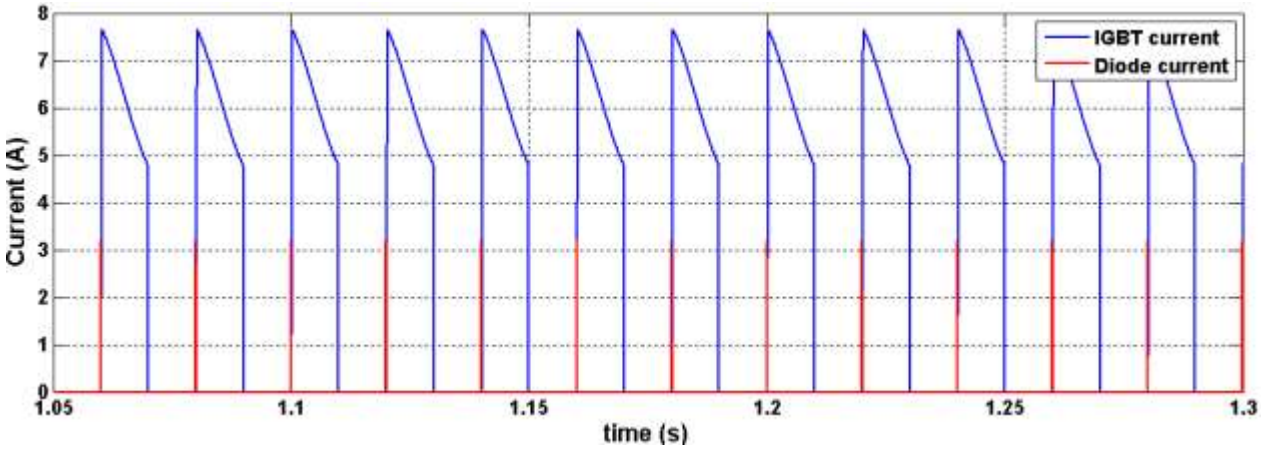

Figure 4.21: The IGBT and diode currents of switches S1 for the second test

The other calculation is as follows as the same as for the first test:

$$P_T = P_{CT} + P_{swT} = V_{CE0}I_{cav} + r_C I_{crms}^2 + E_{offT}f_{sw}$$

$$\rightarrow P_T = 0.9\frac{I_{max}+I_{min}}{2}D + \frac{5\times10^{-3}}{6}\left({i_{max}}^2 + {i_{min}}^2 + i_{max}i_{min}\right) + \frac{7.65\times20}{450}10^{-3}\times50$$

$$\rightarrow P_T = 0.9\frac{7.65+4.78}{4} + \frac{5\times10^{-3}}{6}(7.65^2 + 4.78^2 + 7.65\times4.78) + \frac{7.65}{450}$$

$$= 2.79675 + 0.09828 + 0.017 = 2.91203\,W$$

$$P_D = P_{CD} + P_{swD} = V_{D0}I_{Dav} + r_D I_{Drms}^2 + E_{onD}f_{sw}$$

$$\rightarrow P_D = 1.1\frac{I_{Dmax}}{2}\frac{Ton_D}{T} + 10^{-3}\frac{T_{onD}}{3T}{I_{Dmax}}^2 + \frac{41Vi}{8}\times10^{-6}\times50$$

$$\rightarrow P_D = 1.1\frac{3.2}{2}\frac{0.12\times10^{-3}}{2\times10^{-2}} + 10^{-3}\frac{0.12\times10^{-3}}{6\times10^{-2}}3.2^2 + \frac{41\times80}{8}\times10^{-6}\times50$$

$$= 10.56\times10^{-3} + 0.02048\times10^{-3} + 20.5\times10^{-3} = 31.08048\,mW$$

$$Ploss_{sw} = 8(P_D + P_T) = 8(2.91203 + 31.08048 \times 10^{-3}) = 23.545\,W$$

Transformer copper loss:

$$P_{CU} = RI_{rms}^2 = \frac{R}{6}\left({i_{max}}^2 + {i_{min}}^2 + i_{max}i_{min}\right) = \frac{0.31}{6}(7.65^2 + 4.78^2 + 7.65 \times 4.78) = 6.093W$$

Transformer iron loss:

$$V_{eff} = 80 - 2 * 0.9 - (0.31 + 0.1)\frac{7.65 + 4.78}{2} = 76.65\,V$$

$$P_{core} = \frac{{V_{eff(rms)}}^2}{R_C} = \frac{\left(\frac{76.65}{\sqrt{2}}\right)^2}{516} = 5.693\,W$$
$$\rightarrow P_{LossT} = P_{core} + P_{CU} = 5.693 + 6.093 = 11.786\ W$$

Cable loss:

$$P_{Cable} = RI_{rms}^2 = \frac{2R}{6}\left({i_{max}}^2 + {i_{min}}^2 + i_{max}i_{min}\right) = \frac{0.6}{6}(7.65^2 + 4.78^2 + 7.65 \times 4.78) = 11.8\,W$$

$$\mathrm{PLoss_{total}} = \mathrm{Ploss_{sw}} + \mathrm{P_{LossT}} + \mathrm{P_{Cable}} = 23.545 + 11.786 + 11.8 = 47.245\ \mathrm{W}$$

Simulation:

$$\mathrm{PLoss_{total}} = \mathrm{P_{in}} - \mathrm{P_{Out}} = \mathrm{V_{dc}I_{ave}} - \mathrm{P_{Out}} = 80 \times \frac{7.65 + 4.78}{2} - 465.9 = 31.3\mathrm{W}$$

Experimentally:

$$\mathrm{PLoss_{total}} = \mathrm{P_{in}} - \mathrm{P_{Out}} = V_{dc}I_{ave} - \mathrm{P_{Out}} = 80 \times \frac{5.05 + 7.05}{2} - 432 = 52\ \mathrm{W}$$

4.3.3 Loss calculation for the third test of the single phase DAB converter

$$\mathrm{P_o} = \frac{V_i^2}{\omega L}\left(\frac{\mathrm{V_o}}{nV_i}\right)\emptyset\left(1-\frac{\emptyset}{\pi}\right) = 48w$$

Figure 4.22 shows the IGBT and diode current of switches S1 which have the linear relations.

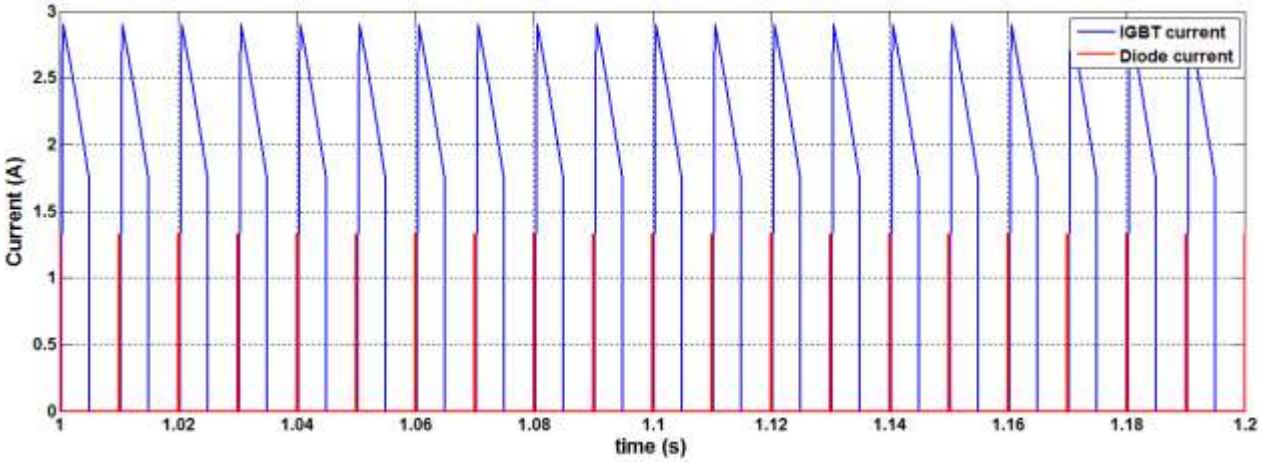

Figure 4.22: The IGBT and diode currents of switches s1 for the third test

$$P_T = P_{CT} + P_{swT} = V_{CE0}I_{cav} + r_C I_{crms}^2 + E_{offT}f_{sw}$$
$$\rightarrow P_T = 0.9\frac{I_{max}+I_{min}}{2}D + \frac{5\times10^{-3}}{6}\left({i_{max}}^2 + {i_{min}}^2 + i_{max}i_{min}\right) + \frac{2.9\times20}{450}10^{-3}\times100$$
$$\rightarrow P_T = 0.9\frac{2.9+1.73}{4} + \frac{5\times10^{-3}}{6}(2.9^2 + 1.73^2 + 2.9\times1.73) + \frac{2.9}{450}$$
$$= 1.04175 + 0.01368 + 0.013 = 1.06843\,W$$

$$P_D = P_{CD} + P_{swD} = V_{D0}I_{Dav} + r_D I_{Drms}^2 + E_{onD}f_{sw}$$
$$\rightarrow P_D = 1.1\frac{I_{Dmax}}{2}\frac{Ton_D}{T} + 10^{-3}\frac{T_{onD}}{3T}{I_{Dmax}}^2 + \frac{41Vi}{8}\times10^{-6}\times100$$
$$\rightarrow P_D = 1.1\frac{1.335}{2}\frac{0.16\times10^{-3}}{2\times10^{-2}} + 10^{-3}\frac{0.16\times10^{-3}}{6\times10^{-2}}1.335^2 + \frac{41\times20}{8}\times10^{-6}\times100$$
$$= 5.874\times10^{-3} + 0.0048\times10^{-3} + 10.25\times10^{-3} = 16.1288\,mW$$

$$Ploss_{sw} = 8(P_D + P_T) = 8(1.06843 + 16.1288\times10^{-3}) = 8.6765\,W$$

Transformer copper loss:

$$P_{CU} = R.I_{rms}^2 = \frac{0.31}{6}\left({i_{max}}^2 + {i_{min}}^2 + i_{max}i_{min}\right) = \frac{0.31}{6}(2.9^2 + 1.73^2 + 2.9 \times 1.73) = 0.8484\ W$$

Transformer iron loss:

The problem here is that the frequency is not 50 Hz. The core loss which has been calculated by the open circuit test of the transformer is for the frequency of the 50 Hz which is the frequency of the local network voltage. The relation between the core resistance and frequency is complex and depends on the core parameters and materials which is not the focus of this project. The relation can be approximated in a way that the core resistance and the frequency have the inverse relationship (by ignoring the magnitude of the eddy loss in comparison to the hysteresis loss).

$$V_{eff} = 20 - 2 * 0.9 - (0.31 + 0.1)\frac{2.9 + 1.73}{2} = 17.25\ V$$

$$P_{core} = \frac{{V_{eff(rms)}}^2}{R_C} = \frac{\left(\frac{17.25}{\sqrt{2}}\right)^2}{\frac{516}{2}} = 0.577\ W$$

$$\rightarrow P_{LossT} = P_{core} + P_{CU} = 0.577 + 0.8484W = 1.4254\ W$$

Cable loss:

$$P_{Cable} = RI_{rms}^2 = \frac{0.6}{6}\left({i_{max}}^2 + {i_{min}}^2 + i_{max}i_{min}\right) = \frac{0.6}{6}(2.9^2 + 1.73^2 + 2.9 \times 1.73) = 1.6842\ W$$

$$\mathrm{PLoss_{total}} = \mathrm{Ploss_{sw}} + \mathrm{P_{LossT}} + \mathrm{P_{Cable}} = 8.6765 + 1.4254 + 1.6842 = 11.7861\ W$$

Simulation:

$$\mathrm{PLoss_{total}} = \mathrm{P_{in}} - \mathrm{P_{Out}} = V_{dc}I_{ave} - \mathrm{P_{Out}} = 20 \times \frac{2.9 + 1.73}{2} - 36.75 = 9.55\ W$$

Experimentally:

$$\mathrm{PLoss_{total}} = \mathrm{P_{in}} - \mathrm{P_{Out}} = V_{dc}I_{ave} - \mathrm{P_{Out}} = 20 \times \frac{3.2 + 1.8}{2} - 33.3 = 16.7\ W$$

4.3.4 Loss calculation for the fourth test of the single phase DAB converter

$$\mathrm{P_o} = \frac{V_i^2}{\omega L}\left(\frac{\mathrm{V_o}}{nV_i}\right)\emptyset\left(1-\frac{\emptyset}{\pi}\right) = 15w$$

Figure 4.23 shows the linear relation for the IGBT and diode current.

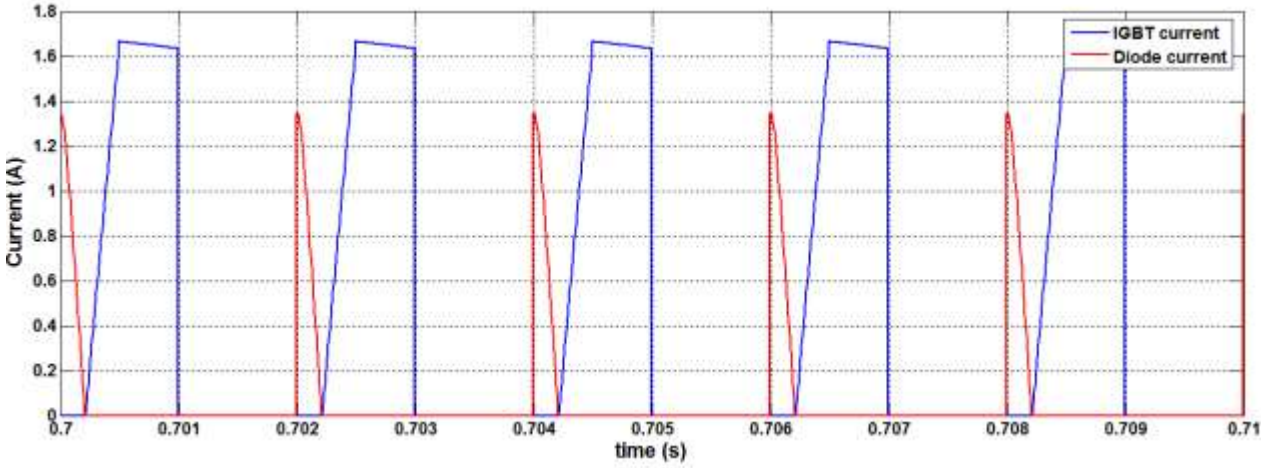

Figure 4.23: The IGBT and diode current of switches S1 for the fourth test

$$i_1(t) = \frac{i_{max}}{t_1}t$$

$$i_2(t) = \frac{i_{min}-i_{max}}{(t_2-t_1)}(t-t_1)+i_{max}$$

$$I_{rms1} = \sqrt{\frac{1}{T_{on}}\left(\int_0^{t1} i_1(t)^2dt + \int_0^{t1} i_2(t)^2dt\right)} = \sqrt{\frac{1}{T_{on}}\left(\int_0^{t1}\left(\frac{i_{max}}{t_1}t\right)^2 dt + \int_{t1}^{t2}\left(\frac{i_{min}-i_{max}}{(t_2-t_1)}(t-t_1)+i_{max}\right)^2 dt\right)}$$

$$= \sqrt{\frac{1}{T_{on}}\left(\frac{i_{max}}{t_1}\right)^2\frac{{t_1}^3}{3} + \frac{1}{T_{on}}\left(\left(\frac{i_{max}-i_{min}}{t_2-t_1}\right)^2\frac{(t_2-t_1)^3}{3} + {i_{max}}^2.(t_2-t_1) - 2i_{max}\frac{i_{max}-i_{min}}{(t_2-t_1)}\frac{(t_2-t_1)^2}{2}\right)}$$

$$= \sqrt{\frac{t_1}{T_{on}}\frac{{i_{max}}^2}{3} + \frac{t_2-t_1}{T_{on}}\left(\frac{(i_{max}-i_{min})^2}{3} + {i_{max}}^2 - i_{max}(i_{max}-i_{min})\right)}$$

$$= \sqrt{\frac{t_1}{3T_{on}}{i_{max}}^2 + \frac{t_2-t_1}{3T_{on}}\left({i_{max}}^2 + {i_{min}}^2 + i_{max}i_{min}\right)}$$

$$= \sqrt{\frac{0.0003}{3\times 0.0008}1.67^2 + \frac{0.0007}{3\times 0.0008}(1.67^2 + 1.64^2 + 1.64\times 1.67)} = 1.6569\ A$$

$$I_{cav} = \frac{I_{max}}{2}\frac{t_1}{T} + \frac{I_{max}+I_{min}}{2}.\frac{(t_2-t_1)}{T} = \frac{1.67}{2}\frac{0.0003}{0.002} + \frac{1.67+1.64}{2}.\frac{0.0007}{0.002} = 0.7045\ A$$

$$I_{Drms} = \frac{i_{max}}{\sqrt{3}} = \frac{1.35}{\sqrt{3}} = 0.78\ A$$
$$I_{Dav} = \frac{I_{max} + 0}{2}.\frac{T_{onD}}{T} = T_{onD}\frac{I_{max}}{2T} = \frac{0.0002}{0.002}\frac{1.35}{2} = 0.0675\ A$$

$$P_T = P_{CT} + P_{swT} = V_{CE0}I_{cav} + r_C I_{crms}^2 + E_{offT}f_{sw}$$
$$\rightarrow P_T = 0.9 \times 0.7045 + 5 \times 10^{-3} \times 1.6569^2 + \frac{1.67 \times 20}{450}10^{-3} \times 500$$
$$\rightarrow P_T = 0.63405 + 13.73 \times 10^{-3} + \frac{16.7}{450} = 0.68489\ W$$

$$P_D = P_{CD} + P_{swD} = V_{D0}I_{Dav} + r_D I_{Drms}^2 + E_{onD}f_{sw}$$
$$\rightarrow P_D = 1.1 \times 0.0675 + 10^{-3} \times 0.78^2 + \frac{41 \times 15}{8} \times 10^{-6} \times 500$$
$$= 74.25 \times 10^{-3} + 0.6084 \times 10^{-3} + 38.4375 \times 10^{-3} = 113.2959\ mW$$

$$Ploss_{sw} = 8(P_D + P_T)$$
$$= 8(0.68489 + 113.2959 + \times 10^{-3}) = 6.385\ W$$

Transformer copper loss:

$$P_{CU} = RI_{rms}^2 = 0.31 \times 1.436^2 = 0.63924976\ W$$

Transformer iron loss:

$$V_{eff} = 15 - 2 * 0.9 - (0.31 + 0.1)1.245 = 12.69\ V$$
$$P_{core} = \frac{V^2}{R_C} = \frac{\left(\frac{12.69}{\sqrt{2}}\right)^2}{\frac{515}{10}} = 1.56\ watt$$
$$\rightarrow P_{LossT} = P_{core} + P_{CU} = 1.56 + 0.639 = 2.199\ W$$

Cable loss:

$$P_{Cable} = RI_{rms}^2 = \frac{0.6}{2} \times 1.436^2 + \frac{0.6}{2}\left(\frac{1.436}{1.8}\right)^2 = 0.8088\ W$$

$$PLoss_{total} = Ploss_{sw} + P_{LossT} + P_{Cable} = 6.385 + 2.199 + 0.8088 = 9.39\text{W}$$

Simulation:

$$I_{ave} = \frac{1.67}{2}\frac{0.0005}{0.001} + \frac{1.67 + 1.64}{2}\frac{0.0005}{0.001} = 1.245\ A$$

$$\mathrm{PLoss_{total}} = \mathrm{P_{in}} - \mathrm{P_{Out}} = V_{dc} I_{ave} - \mathrm{P_{Out}} = 15 \times 1.245 - 11.5 = 7.175\mathrm{W}$$

Experimentally:

$$I_{ave} = \frac{1.8}{2}\frac{0.0005}{0.001} + \frac{2 + 1.8}{2}\frac{0.0005}{0.001} = 1.4\ A$$

$$\mathrm{PLoss_{total}} = \mathrm{P_{in}} - \mathrm{P_{Out}} = V_{dc} I_{ave} - \mathrm{P_{Out}} = 15 \times 1.4 - 8.2 = 12.8\mathrm{W}$$

4.3.5 Loss calculation for the fifth test of the single phase DAB converter

$$\mathrm{P_o} = \frac{V_i^2}{\omega L}\left(\frac{\mathrm{V_o}}{nV_i}\right)\emptyset\left(1-\frac{\emptyset}{\pi}\right) = 28.8\ W$$

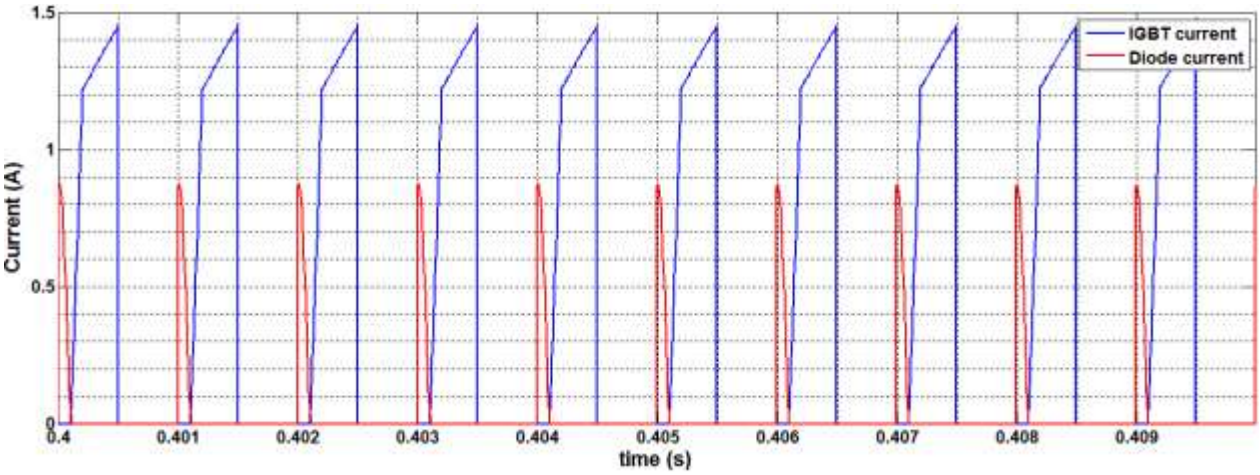

Figure 4.24: The IGBT and diode currents of switches S1 for the fifth test

The value of the I_{max} and I_{min} can be read from Figure 4.24.

$$I_{rms} = \sqrt{\frac{t_1}{3T_{on}}{i_{min}}^2 + \frac{t_2 - t_1}{3T_{on}}\left({i_{max}}^2 + {i_{min}}^2 + i_{max}i_{min}\right)}$$

$$= \sqrt{\frac{0.0001}{3\times 0.0004}1.18^2 + \frac{0.0003}{3\times 0.0004}\left(1.47^2 + 1.18^2 + 1.18\times 1.47\right)} = 1.143\ A$$

$$I_{cav} = \frac{i_{min}}{2}\frac{t_1}{T} + \frac{I_{max}+I_{min}}{2}.\frac{(t_2-t_1)}{T} = \frac{1.18}{2}\frac{0.0001}{0.001} + \frac{1.18+1.47}{2}.\frac{0.0003}{0.001} = 0.4565\ A$$

$$I_{Drms} = \frac{i_{Dmax}}{\sqrt{3}} = \frac{0.89}{\sqrt{3}} = 0.51384\ A$$

$$I_{Dav} = \frac{I_{Dmax}+0}{2}.\frac{T_{onD}}{T} = T_{onD}\frac{I_{Dmax}}{2T} = \frac{0.0001}{0.001}\frac{0.89}{2} = 0.0445\ A$$

$$P_T = P_{CT} + P_{swT} = V_{CE0}I_{cav} + r_C I_{crms}^2 + E_{offT}f_{sw}$$

$$\rightarrow P_T = 0.9\times 0.4565\ + 5\times 10^{-3}\times 1.143 + \frac{1.47\times 20}{450}10^{-3}\times 1000$$

$$\rightarrow P_T = 0.41085 + 5.715\times 10^{-3} + \frac{29.4}{450} = 0.4819\ W$$

$$P_D = P_{CD} + P_{swD} = V_{D0}I_{Dav} + r_D I_{Drms}^2 + E_{onD}f_{sw}$$

$$\rightarrow P_D = 1.1\times 0.0445\ + 10^{-3}\times 0.51384^2 + \frac{41\times 30}{8}\times 10^{-6}\times 1000$$

$= 48.95 \times 10^{-3} + 0.264 \times 10^{-3} + 153.75 \times 10^{-3} = 202.964\ mW$

$Ploss_{sw} = 8(P_D + P_T)$
$= 8(0.4819 + 202.964 \times 10^{-3}) = 5.4789\ W$

Transformer copper loss:

$P_{CU} = RI_{rms}^2 = 0.31 \times 1.143^2 = 0.405\ W$

Transformer iron loss:

$$I_{in(ave)} = \frac{1.18}{2}\frac{0.0002}{0.0005} + \frac{1.18 + 1.47}{2}\frac{0.0003}{0.0005} = 1.031\ A$$

$$V_{eff} = 30 - 2 * 0.9 - (0.31 + 0.2)1.031 = 27.6742\ V\ V$$

$$P_{core} = \frac{{V_{eff(rms)}}^2}{R_C} = \frac{\left(\frac{27.6742}{\sqrt{2}}\right)^2}{\frac{516}{20}} = 14.84\ W$$

$$\rightarrow P_{LossT} = P_{core} + P_{CU} = 18 + 0.405 = 18.405\ W$$

Cable loss:

$$P_{Cable} = RI_{rms}^2 = \frac{0.6}{2} \times 1.143^2 + \frac{0.6}{2}\left(\frac{1.143}{1.8}\right)^2 = 0.5137\ W$$

$$\mathrm{PLoss_{total}} = \mathrm{Ploss_{sw}} + \mathrm{P_{LossT}} + \mathrm{P_{Cable}} = 5.4789 + 14.84 + 0.5137 = 20.83\ \mathrm{W}$$

Simulation:

$$\mathrm{PLoss_{total}} = \mathrm{P_{in}} - \mathrm{P_{Out}} = V_{dc}I_{ave} - \mathrm{P_{Out}} = 30 \times 1.031 - 18.5 = 12.43\mathrm{W}$$

Experimentally:

$$I_{ave} = \frac{1.5}{2}\frac{0.0002}{0.0005} + \frac{1.5 + 1.65}{2}\frac{0.0003}{0.0005} = 1.345$$

$$\mathrm{PLoss_{total}} = \mathrm{P_{in}} - \mathrm{P_{Out}} = V_{dc}I_{ave} - \mathrm{P_{Out}} = 30 \times 1.345 - 16 = 24.35\ \mathrm{W}$$

4.3.6 Loss calculation for the first test of the three phase DAB converter

$$P_o = \frac{V_i^2}{\omega L}\left(\frac{V_o}{nV_i}\right)\emptyset\left(1-\frac{\emptyset}{\pi}\right) = 300W$$

According to the Figure 4.25, the current can be considered in the three level of I_{max}, I_{min} and 0.

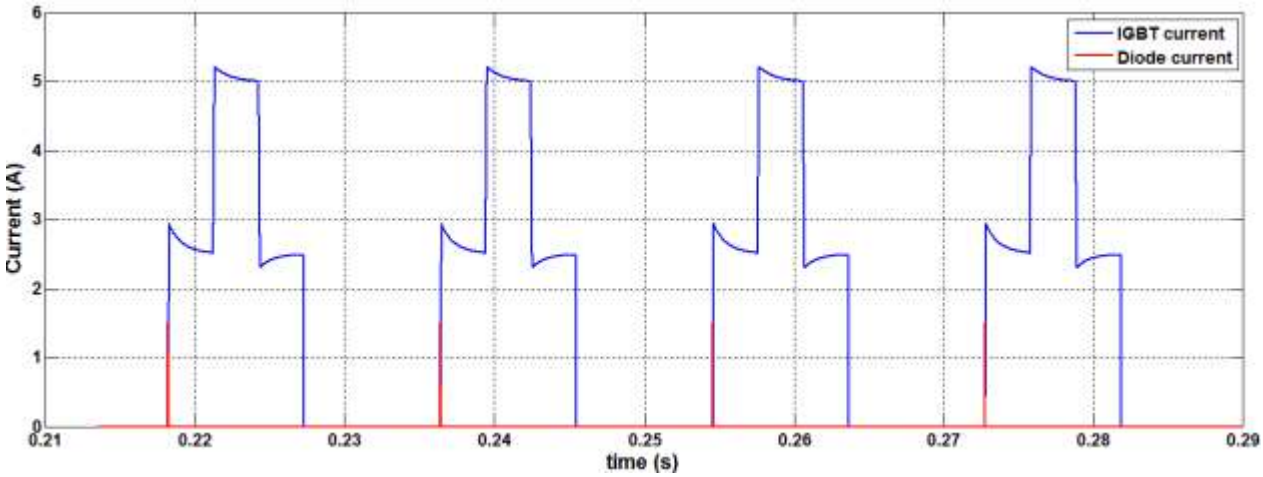

Figure 4.25: The IGBT and diode currents of switches S1 for the first test of the three phase DAB converter

$$\rightarrow I_{rms} = \sqrt{\frac{1}{T}\int_0^{t_1} i_1(t)^2 dt + \frac{1}{T}\int_{t_1}^{t_2} i_2(t)^2 dt + \frac{1}{T}\int_{t_2}^{t_3} i_3(t)^2 dt}$$

$$= \sqrt{\frac{t_1}{T}{i_{min1}}^2 + \frac{t_2-t_1}{T}{i_{max}}^2 + \frac{t_3-t_2}{T}{i_{min2}}^2}$$

$$= \sqrt{\frac{T_{on}}{T}\frac{{i_{min1}}^2 + {i_{max}}^2 + {i_{min2}}^2}{3}} = \sqrt{\frac{{i_{min1}}^2 + {i_{max}}^2 + {i_{min2}}^2}{6}} = \sqrt{\frac{2.6^2 + 5.1^2 + 2.45^2}{6}} = 2.542\ A$$

$$I_{cav} = \frac{t_1 i_{min1} + (t_2-t_1)i_{max} + (t_3-t_2)i_{min2}}{T_{on}} \cdot \frac{T_{on}}{T} = \frac{i_{min1} + i_{max} + i_{min2}}{3}\frac{T_{on}}{T}$$

$$= \frac{i_{min1} + i_{max} + i_{min2}}{6} = \frac{2.6 + 5.1 + 2.45}{6} = 1.692\ A$$

$$I_{Drms} = I_{Dmax}\sqrt{\frac{T_{onD}}{3T}} = 1.5\sqrt{\frac{0.00005 \times 55}{3}} = 0.0454$$

$$I_{Dav} = \frac{I_{max} + 0}{2} \cdot \frac{T_{onD}}{T} = T_{onD}\frac{I_{Dmax}}{2T} = 1.5\frac{0.00005 \times 55}{2} = 0.0021\ A$$

$$P_T = P_{CT} + P_{swT} = V_{CE0} I_{cav} + r_C I_{crms}^2 + E_{offT} f_{sw}$$
$$\rightarrow P_T = 0.9 \times 1.692 + 5 \times 10^{-3} \times 2.542^2 + \frac{5.1 \times 20}{450} 10^{-3} \times 55$$
$$\rightarrow P_T = 1.5228 + 0.03231 + 0.0125 = 1.56761\ W$$

$$P_D = P_{CD} + P_{swD} = V_{D0} I_{Dav} + r_D I_{Drms}^2 + E_{onD} f_{sw}$$
$$\rightarrow P_D = 1.1 \times 0.0021 + 10^{-3} \times 0.0454^2 + \frac{41 \times 50}{8} \times 10^{-6} \times 55$$
$$\rightarrow P_D = 2.31 \times 10^{-3} + 0.0021 \times 10^{-3} + 14.094 \times 10^{-3} = 16.4061 \times 10^{-3}\ mw$$

$$Ploss_{sw} = 12(P_D + P_T) = 12(1.56761 + 16.4061 \times 10^{-3}) = 19.0082\ W$$

Transformer copper loss:

$$P_{CU} = 3RI_{rms}^2 = 3 \times 0.5 \times 2.542^2 = 11.1925\ W$$

Transformer iron loss:

$$R_{C(50Hz)} = \frac{{V_{oc}}^2}{P_{oc}} = \frac{63^2}{6} \cong 661.5\Omega \rightarrow R_{C(55Hz)} = \frac{R_{C(50Hz)}}{\frac{55}{50}} = 601.4\Omega$$
$$V_{eff} = 50 - 2 * 0.9 - (0.4 + 0.1)5 = 45.2\ V$$
$$P_{core} = 3\frac{{V_{eff(rms)}}^2}{R_C} = 3\frac{\left(\frac{45.2}{\sqrt{2}}\right)^2}{601.4\Omega} = 5.096\ W$$

$$\rightarrow P_{LossT} = P_{core} + P_{CU} = 5.096 + 11.1925 = 16.288\ W$$

Cable loss:

$$P_{Cable} = 3RI_{rms}^2 = 3 \times (0.1 \times 5.1^2 + 0.2 \times 2.542^2) = 11.68\ W$$

$$\mathrm{PLoss_{total}} = \mathrm{Ploss_{sw}} + \mathrm{P_{LossT}} + \mathrm{P_{Cable}} = 19.008 + 16.288 + 11.68 = 46.96\ \mathrm{W}$$

In order to calculate the input power for the simulation results, the input current of the converter is needed. Figure 4.26 shows the waveform of the input current for the converter. The average value of the current has been calculated and been used in order to calculate the input power.

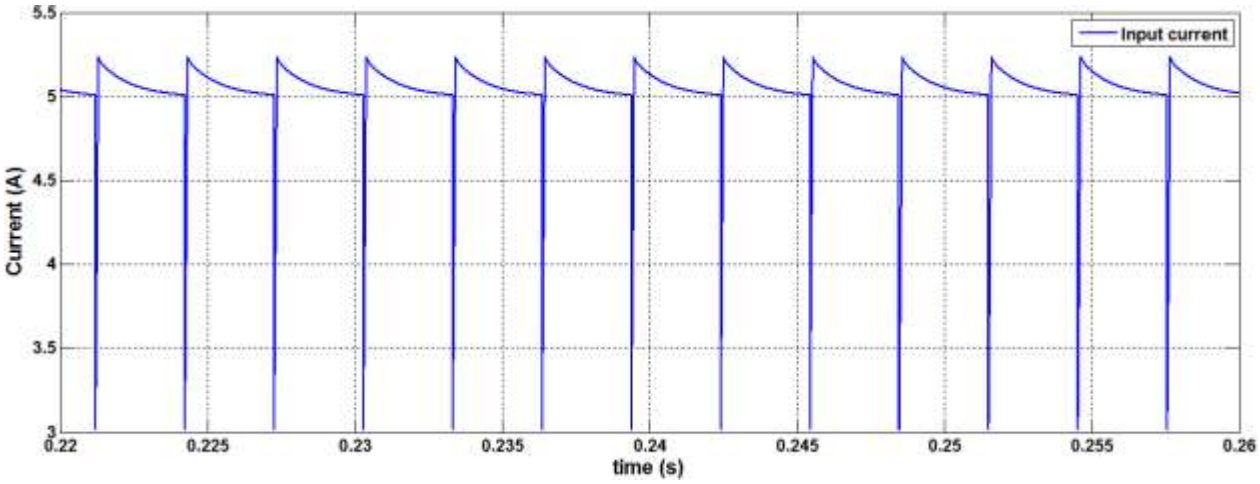

Figure 4.26: The input current of the converter for the first test of the three phase DAB converter

Simulation:

The I_{ave} can be calculated from Figure 4.26.

$$\mathrm{PLoss_{total}} = \mathrm{P_{in}} - \mathrm{P_{Out}} = \mathrm{V_{dc}I_{ave}} - \mathrm{P_{Out}} = 50 \times 5.1 - 213 = 37\ \mathrm{W}$$

Experimentally:

$$\mathrm{PLoss_{total}} = \mathrm{P_{in}} - \mathrm{P_{Out}} = V_{dc}I_{ave} - \mathrm{P_{Out}} = 50 \times 5 - 196 = 54\ \mathrm{W}$$

4.3.7 Loss calculation for the second test of the three phase DAB converter

$$\mathrm{P_o} = \frac{V_i^2}{\omega L}\left(\frac{\mathrm{V_o}}{nV_i}\right)\emptyset\left(1-\frac{\emptyset}{\pi}\right) = 1500W$$

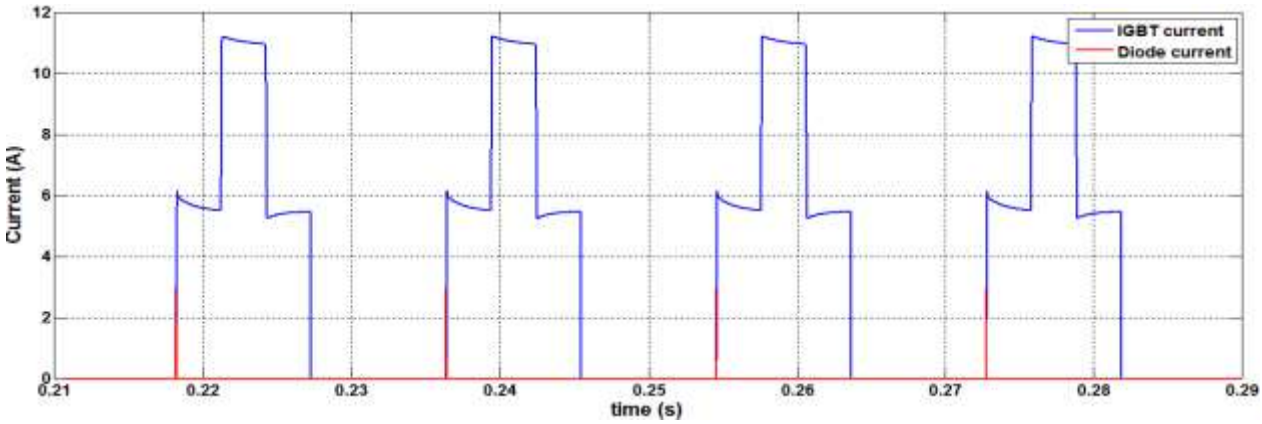

Figure 4.27: The IGBT and diode currents of switches S1 for the second test of the three phase DAB converter

Figure 4.27 shows the IGBT and diode current for the second test.

$$I_{rms} = \sqrt{\frac{{i_{min1}}^2 + {i_{max}}^2 + {i_{min2}}^2}{6}} = \sqrt{\frac{5.7^2 + 11^2 + 5.4^2}{6}} = 5.5174\ A$$

$$I_{cav} = \frac{i_{min1} + i_{max} + i_{min2}}{6} = \frac{5.7 + 11 + 5.4}{6} = 3.683\ A$$

$$I_{Drms} = I_{Dmax}\sqrt{\frac{T_{onD}}{3T}} = 3\sqrt{\frac{0.00005 \times 55}{3}} = 0.0908\ A$$

$$I_{Dav} = T_{onD}\frac{I_{Dmax}}{2T} = 3\frac{0.00005 \times 55}{2} = 0.0042\ A$$

$$P_T = P_{CT} + P_{swT} = V_{CE0}I_{cav} + r_C I_{crms}^2 + E_{offT}f_{sw}$$

$$\rightarrow P_T = 0.9 \times 3.683 + 5 \times 10^{-3} \times 5.5174^2 + \frac{11 \times 20}{450}10^{-3} \times 55$$

$$\rightarrow P_T = 3.3147 + 0.1522 + 0.0269 = 3.4938$$

$$P_D = P_{CD} + P_{swD} = V_{D0}I_{Dav} + r_D I_{Drms}^2 + E_{onD}f_{sw}$$

$$\rightarrow P_D = 1.1 \times 0.0042 + 10^{-3} \times 0.0908^2 + \frac{41 \times 125}{8} \times 10^{-6} \times 55$$

$$\rightarrow P_D = 4.62 \times 10^{-3} + 0.0083 \times 10^{-3} + 35.235 \times 10^{-3} = 39.8633 \times 10^{-3}\ mW$$

$$Ploss_{sw} = 12(P_D + P_T) = 12(3.4938 + 39.8633 \times 10^{-3}) = 42.404\ W$$

Transformer copper loss:

$$P_{CU} = 3RI_{rms}^2 = 3 \times 0.5 \times 5.5174^{\,2} = 45.66\,W$$

Transformer iron loss:

$$V_{eff} = 125 - 2 * 0.9 - (0.4 + 0.1)11 = 117.7\,V$$

$$P_{core} = 3\frac{V_{eff(rms)}^{\,2}}{R_C} = 3\frac{\left(\frac{117.7}{\sqrt{2}}\right)^2}{601.4\Omega} = 34.553\,W$$

$$\rightarrow P_{LossT} = P_{core} + P_{CU} = 34.553 + 45.66 = 80.215\ W$$

Cable loss:

$$P_{Cable} = 3RI_{rms}^2 = 3 \times (0.1 \times 11.1^2 + 0.2 \times 5.5174^2) = 55.228\,W$$

$$\mathrm{PLoss_{total}} = \mathrm{Ploss_{sw}} + \mathrm{P_{LossT}} + \mathrm{P_{Cable}} = 42.404 + 80.215 + 55.228 = 177.53\ \mathrm{W}$$

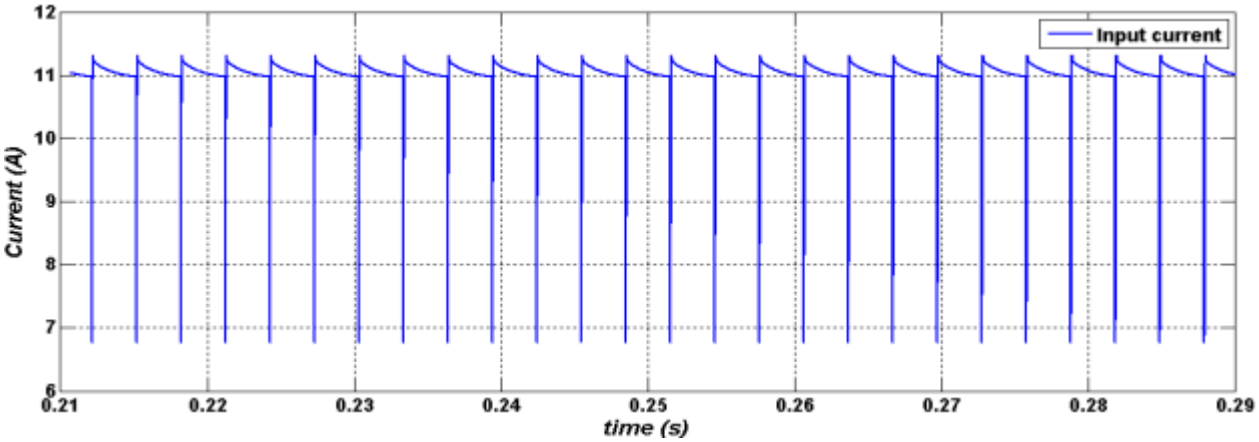

Figure 4.28: The input current of the Converter for the second test

Simulation:

The I_{ave} value can be read from figure 4.28.

$$\mathrm{PLoss_{total}} = \mathrm{P_{in}} - \mathrm{P_{Out}} = \mathrm{V_{dc}I_{ave}} - \mathrm{P_{Out}} = 125 \times 11.1 - 1222 = 165.5\mathrm{W}$$

Experimentally:

$$\mathrm{PLoss_{total}} = \mathrm{P_{in}} - \mathrm{P_{Out}} = V_{dc}I_{ave} - \mathrm{P_{Out}} = 125 \times 11.2 - 1214 = 186.5\ \mathrm{W}$$

In this test, just the switching loss is not considered for the simulation. That's the reason that the value of the losses for the simulation results and theoretical calculation is closer to each other. The core losses of the transformer are considered like a parallel resistance with the primary side of the transformer.

4.3.8 Loss calculation for the third test of the three phase DAB converter

$$\mathrm{P_o} = \frac{V_i^2}{\omega L}\left(\frac{\mathrm{V_o}}{nV_i}\right)\emptyset\left(1-\frac{\emptyset}{\pi}\right) = 300W$$

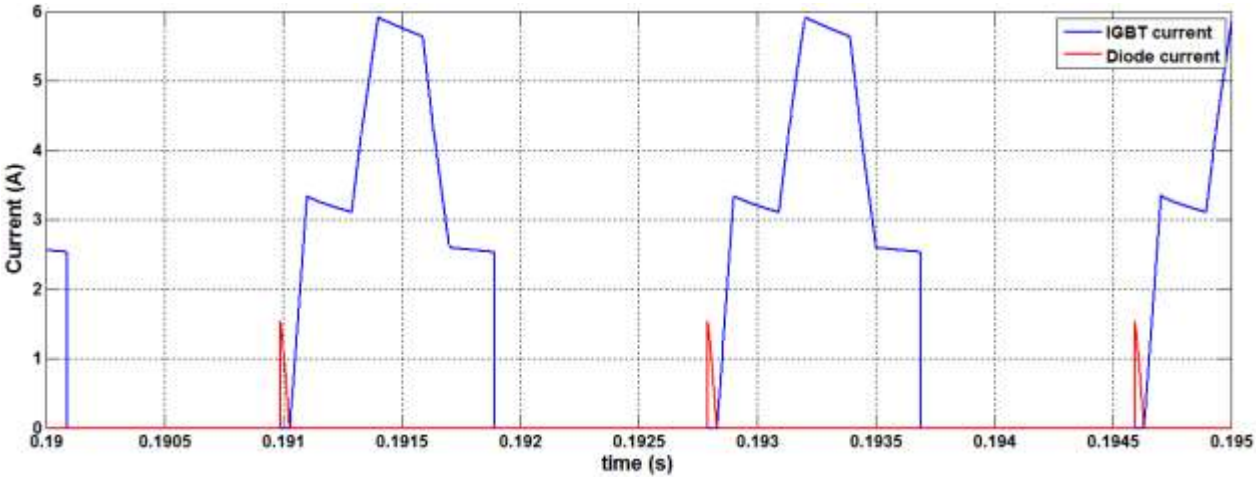

Figure 4.29: The IGBT and diode currents of switches S1 for the third test of the three phase DAB converter

I_{min} and I_{max} for the following calculation can be achieved from Figure 4.29.

$$I_{rms} = \sqrt{\frac{{i_{min1}}^2 + {i_{max}}^2 + {i_{min2}}^2}{6}} = \sqrt{\frac{3.2^2 + 5.8^2 + 2.55^2}{6}} = 2.898\ A$$

$$I_{cav} = \frac{i_{min1} + i_{max} + i_{min2}}{6} = \frac{3.2 + 5.8 + 2.55}{6} = 1.925\ A$$

$$I_{Drms} = I_{Dmax}\sqrt{\frac{T_{onD}}{3T}} = 1.5\sqrt{\frac{0.00005 \times 555}{3}} = 0.1443\ A$$

$$I_{Dav} = T_{onD}\frac{I_{Dmax}}{2T} = 1.5\frac{0.00005 \times 555}{2} = 0.0208\ A$$

$$P_T = P_{CT} + P_{swT} = V_{CE0}I_{cav} + r_C I_{crms}^2 + E_{offT}f_{sw}$$
$$\rightarrow P_T = 0.9 \times 1.925 + 5 \times 10^{-3} \times 2.898^2 + \frac{5.8 \times 20}{450}10^{-3} \times 555$$
$$\rightarrow P_T = 1.7325 + 0.042 + 0.1431 = 1.9176\ W$$

$$P_D = P_{CD} + P_{swD} = V_{D0}I_{Dav} + r_D I_{Drms}^2 + E_{onD}f_{sw}$$
$$\rightarrow P_D = 1.1 \times 0.0208 + 10^{-3} \times 0.1443^2 + \frac{41 \times 50}{8} \times 10^{-6} \times 555$$
$$\rightarrow P_D = 22.88 \times 10^{-3} + 0.021 \times 10^{-3} + 142.219 \times 10^{-3} = 165.12 \times 10^{-3}\ mW$$

$$Ploss_{sw} = 12(P_D + P_T) = 12(1.9176 + 165.12 \times 10^{-3}) = 24.993\ W$$

Transformer copper loss

$$P_{CU} = 3RI_{rms}^2 = 3 \times 0.4 \times 2.898^2 = 10.078\ W$$

Transformer iron loss

$$V_{eff} = 50 - 2 * 0.9 - (0.4 + 0.1)5.75 = 45.325\ V$$

$$P_{core} = 3\frac{V_{eff(rms)}{}^2}{R_C} = 3\frac{\left(\frac{45.325}{\sqrt{2}}\right)^2}{\frac{601.4}{10}\Omega} = 51.239\ W$$

$$\rightarrow P_{LossT} = P_{core} + P_{CU} = 51.239 + 10.078 = 61.317\ \ W$$

Cable loss:

$$P_{Cable} = 3RI_{rms}^2 = 3 \times (0.1 \times 5.75^2 + 0.2 \times 2.898^2) = 14.958\ W$$

$$\mathrm{PLoss_{total}} = \mathrm{Ploss_{sw}} + \mathrm{P_{LossT}} + \mathrm{P_{Cable}} = 24.993 + 61.317 + 14.958 = 101.268\ \mathrm{W}$$

Simulation:

By using Figure 4.30, the input power can be calculated for the simulation result.

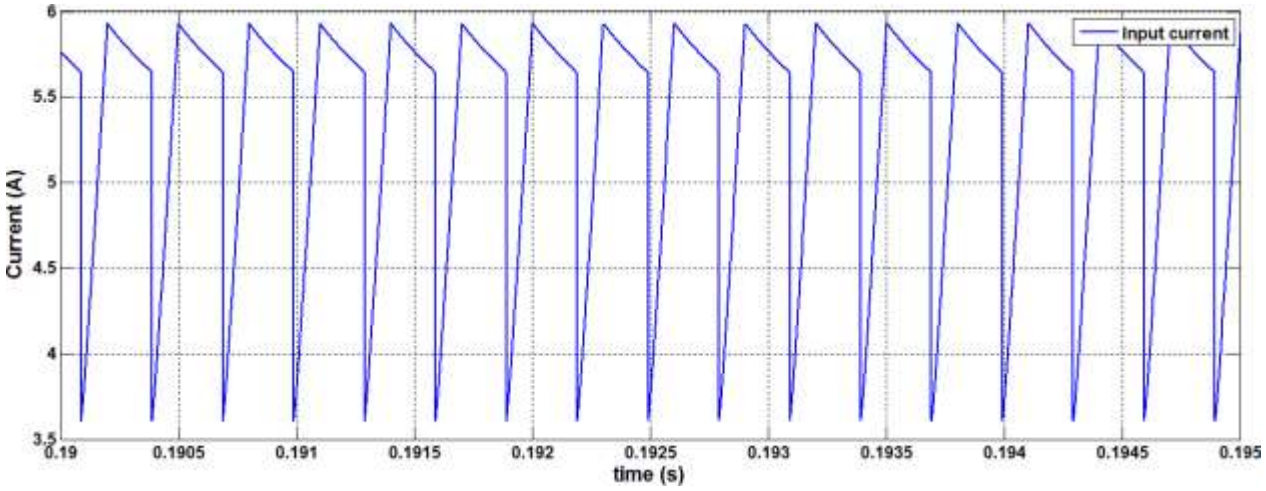

Figure 4.30: The input current of the converter for the third test

$$\mathrm{PLoss_{total}} = \mathrm{P_{in}} - \mathrm{P_{Out}} = \mathrm{V_{dc}I_{ave}} - \mathrm{P_{Out}} = 50 \times 5.6 - 204.5 = 76\mathrm{W}$$

Experimentally:

$$\mathrm{PLoss_{total}} = \mathrm{P_{in}} - \mathrm{P_{Out}} = V_{dc}I_{ave} - \mathrm{P_{Out}} = 50 \times 5.9 - 187.5 = 107.5\ \mathrm{W}$$

Calculation shows 107.5 W losses in this test. In comparison to the first test with the same input voltage and same output voltage and power, the losses in test 3 are higher. Since the switching frequency in test 3 is 10 times higher, it's reasonable that the total loss become higher as well. It should be noted that a 50 Hz three phase transformer also can led to the higher losses when it operates at 555 Hz in comparison to the 55 Hz.

4.4 Comparison between Simulation and Experimental Results

In addition to the theoretical results based on (2.1),(2.2),(2,3) and (2.4) for both single and three phase dual active bridges converter, which are presented in Table 4.1 and 4.3 in the previous sections, there are simulation and experimental results as well which are different from the theoretical results. In this section, the simulation and experimental results and waveforms are presented and discussed for both single and three phase DAB converter.

4.4.1 The comparison for the single phase dual active bridge converter

As mentioned earlier, the power of the converter can be calculated by (2.1) based on the implemented phase shift between the two bridges of DAB converter. The formula works for the ideal DAB converter. The forward voltage drops across switches and diodes and also the transformer losses are not considered in this formula. Apart from these ideal results, there are results for both simulation and experimental cases as well which are given in Table 4.7 As mentioned earlier, the voltage drop through the switches and diodes and also resistance losses of the single phase transformer are considered in the simulation but the switching losses and cabling losses of the whole measuring system are ignored due to the limitation of PLECS. This issue and also the accuracy of the measuring devices can make differences between the simulated and experimental results.

Table 4.7: The results of both simulation and experimental implementation

	Simulation					Practically				
Test	1	2	3	4	5	1	2	3	4	5
Frequency(Hz)	50	50	100	500	1000	50	50	100	500	1000
V_{in} (V)	30	80	20	15	30	30	80	20	15	30
V_{out} (V)	48.5	140	31.5	23	43	48	134	30	20	40
R_L (Ω)	25.5	41.47	27	46	101	25.5	41.5	27	48.6	100
Power (W)	92.5	472	36.75	11.5	18.5	90	432	33.3	8.2	16
Phase shift (s)	5e-4	3e-4	5e-4	5e-4	2e-4	5e-4	3e-4	5e-4	5e-4	2e-4
Losses (W)	15.5	31	9.5	7.1	12.4	24	52	16.7	12.8	24.3

All five tests have been done by simulation also and all the results for both simulation and experimental parts can be seen in Table 4.7. According to this table, the results are nearly the same for the simulation and experimental case. The phase shifts are almost the same for both experimental and simulation and also the ideal results. Tables 4.7 show that there is a 7 V voltage drops in all tests but the exact value depends on the on-time of IGBTS and diodes in each test. The voltage drop in the experimental case is a little different compared to the simulation and is in the range of 6-10 V. This can be caused by the different forward voltage drops of diodes and IGBTs at the different power level and also the losses in the real transformer since all devices in the simulation are ideal.

Differences can also be due to the limitation and accuracy of measurement instruments in the laboratory while all measurement instruments in the simulation are ideal.

In order to make a better comparison, both simulation and experimental voltage waveforms of test two are shown in Figure 4.31.

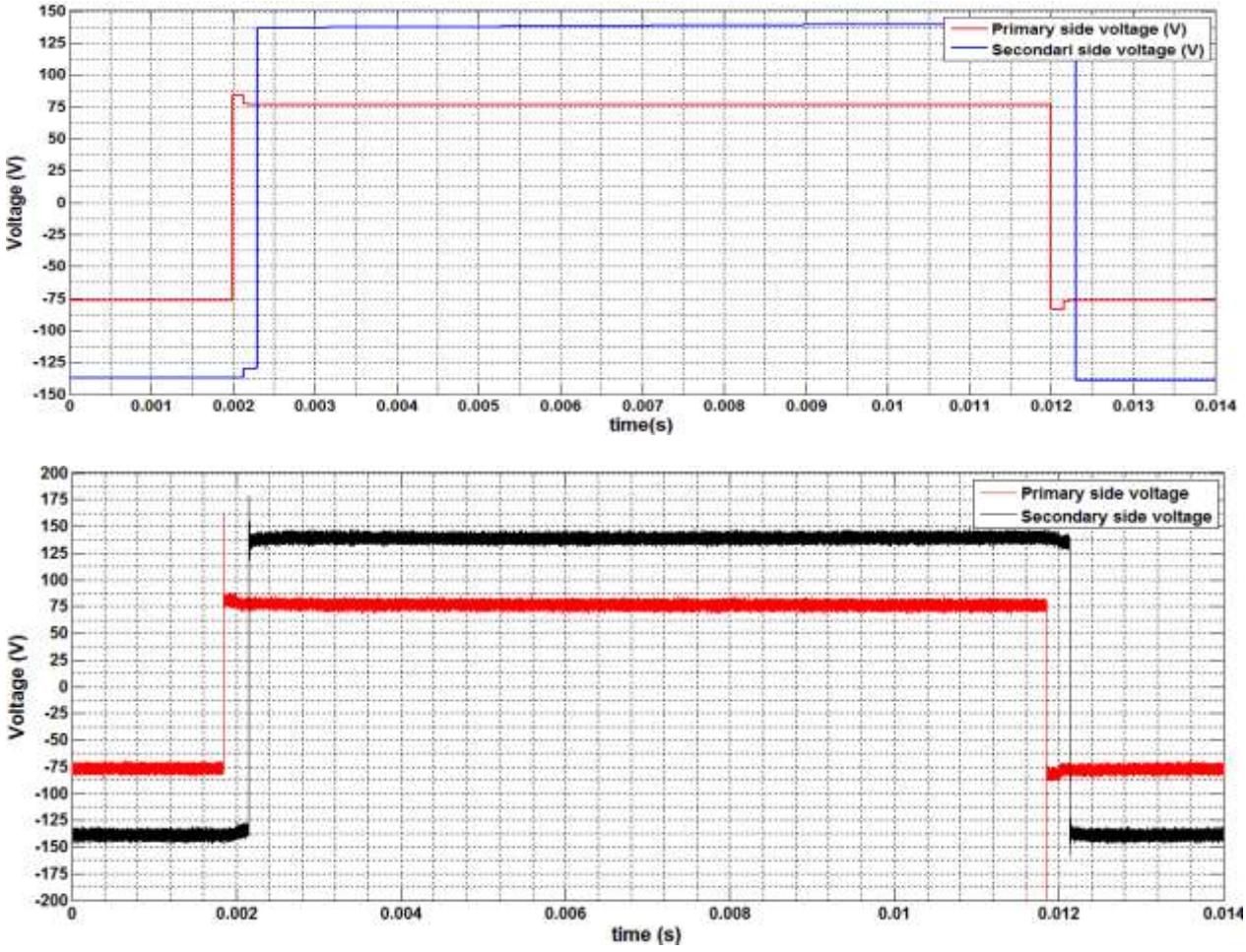

Fig. 4.31: Voltage waveforms of the DAB converter in both simulation (top) and experimental (down)

As can be seen in Figure 4.31, both simulated and experimental waveforms have approximately the same form and also the same phase shift. The voltage levels are the same as well. Moreover, the drop during the phase shift period which was discussed earlier exists in both the simulation and experimental waveforms.

In order to make the other comparison, both simulation and experimental current waveforms of test two are also shown in Figure 4.32.

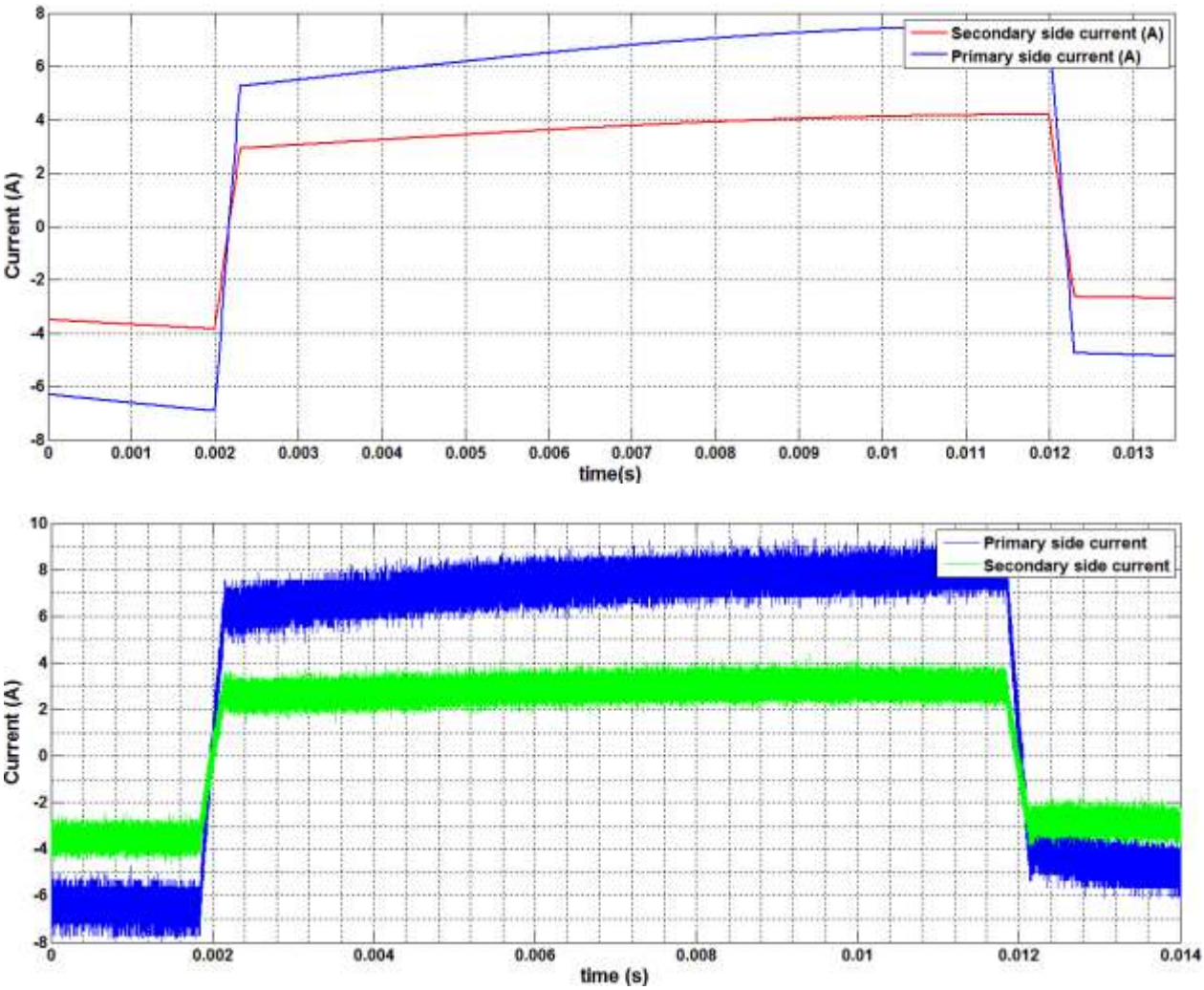

Fig. 4.32: Current waveforms of the DAB converter in both simulation (top) and experimental (down)

As can be seen in this figure, both simulation and experimental waveforms have the same form approximately. Just there is little difference in the current level rising time which is due to the difference between the inductance of the real DAB converter and the simulated DAB converter according to.

$$i(\theta) = \left[\frac{V_{in} + \frac{V_{out}}{n}}{\omega L}\right]\theta + i(0) \tag{4.4}$$

where, *n* is defined as the ratio of the transformer in the converter. [1]

Since the inductance of the real DAB converter can't be measured exactly, there is a little difference between the inductance of the simulated DAB converter and the real one which makes a difference between the current levels of the waveforms in Figure 4.32.

4.4.2 The comparison for the three phase dual active bridge converter

As mentioned earlier, three tests have been done for the three phase dual active bridges. The first test is for the frequency of 55 Hz but in low power of 300 W. In the second test, the frequency is the same but the output power has been increased up to 1.5 KW. The limitation function for increasing the power are transformer, DC voltage source and dSPACE controller as well. the dSPACE controller limitation doesn't allow to choose a phase shift less than 2 degrees due to its digital implementation time. The DC voltage source current limitation is 10 A and the transformer current limitation is the same. The DC voltage source can generate a higher voltage up to 600 V but in this case a lower phase shift should be implemented by dSPACE controller in order to keep the current below 10 A which is not possible by considering the mentioned limitation of a dSPACE controller. Simulation has been done for all three tests in order to compare the results with the experimental tests. Table 4.8 shows the simulation and experimental results for all three tests.

Table 4.8: The simulation and experimental results of three tests on three phase DAB converter

	Simulation			Practically		
Test	1	2	3	1	2	3
Frequency(Hz)	55	55	555	55	55	555
Vin (V)	50	125	50	50	125	50
Vout (V)	73	195	71.5	70	194	68.5
RL (Ω)	25	31.1	25	25	31	25
Power (W)	213	1222	204.5	196	1214	187.5
Phase shift (s)	1e-4	1e-4	1.1e-4	1e-4	1e-4	1.1e-4
Losses (W)	37	165.5	76	54	186.5	107

The voltage and current waveforms of the primary and secondary side of the transformer for both simulation and experimental cases are shown in Figures 4.33, 4.34 and 4.35 for all three tests respectively.

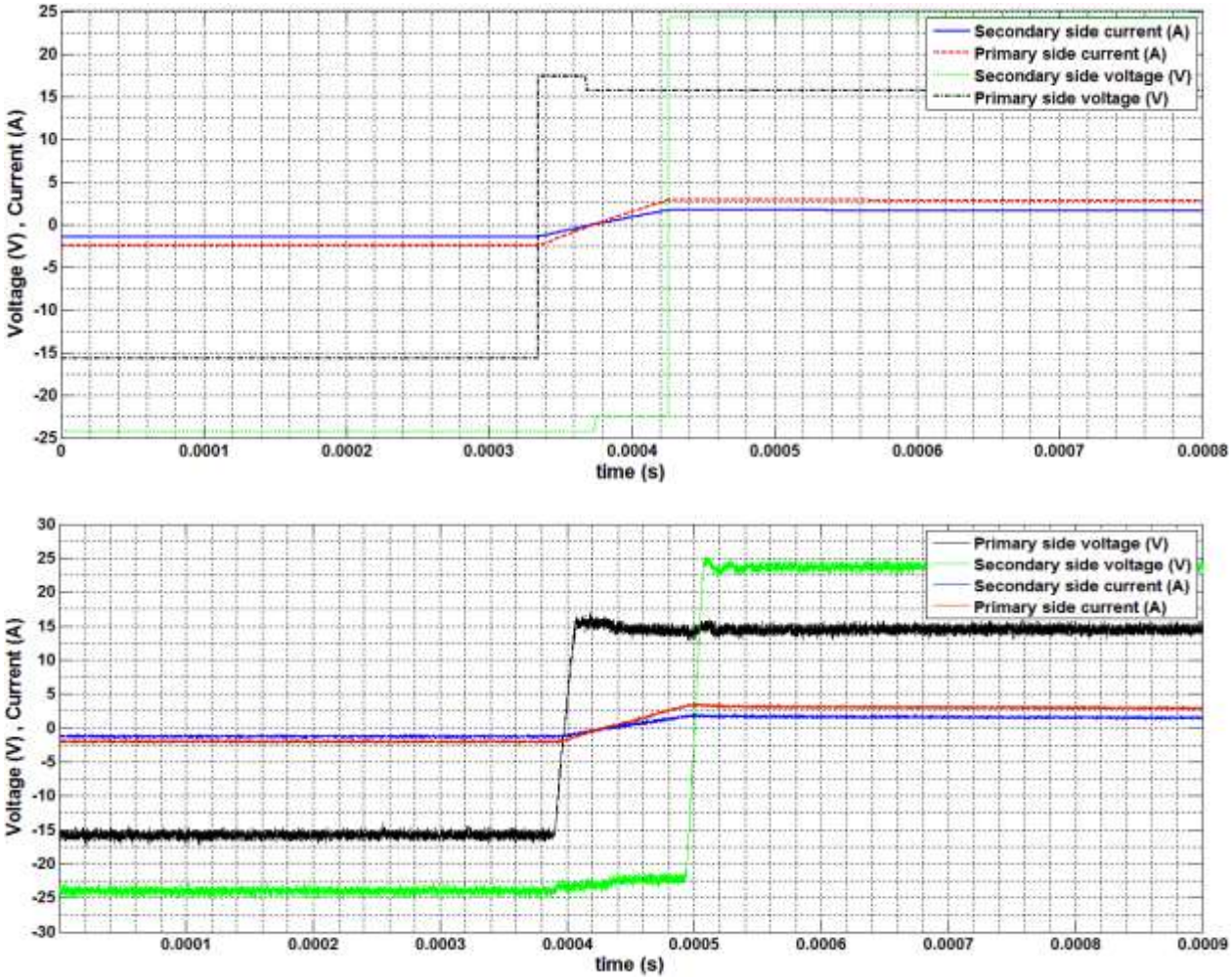

Fig. 4.33: The voltage and current waveforms in both simulation and experimental for test 1

As figures shows, the implemented phase shift is the same in both simulation and experimental waveforms for all three tests. So, the simulation results are verified by the experimental results. It should be noted that the voltage waveforms belong to the phase voltage.

The voltage waveforms for test 2 shows switching overvoltage which is due to the reason that test 2 was done when the DAB converter didn't have snubber capacitor.

The experimental voltage waveforms shows about 1-2 V lower voltage in comparison to the simulated voltage waveforms which can be due to the accuracy of the measurement devices, switching loss which is not considered in simulation and cabling voltage drop which was not considered in the simulation.

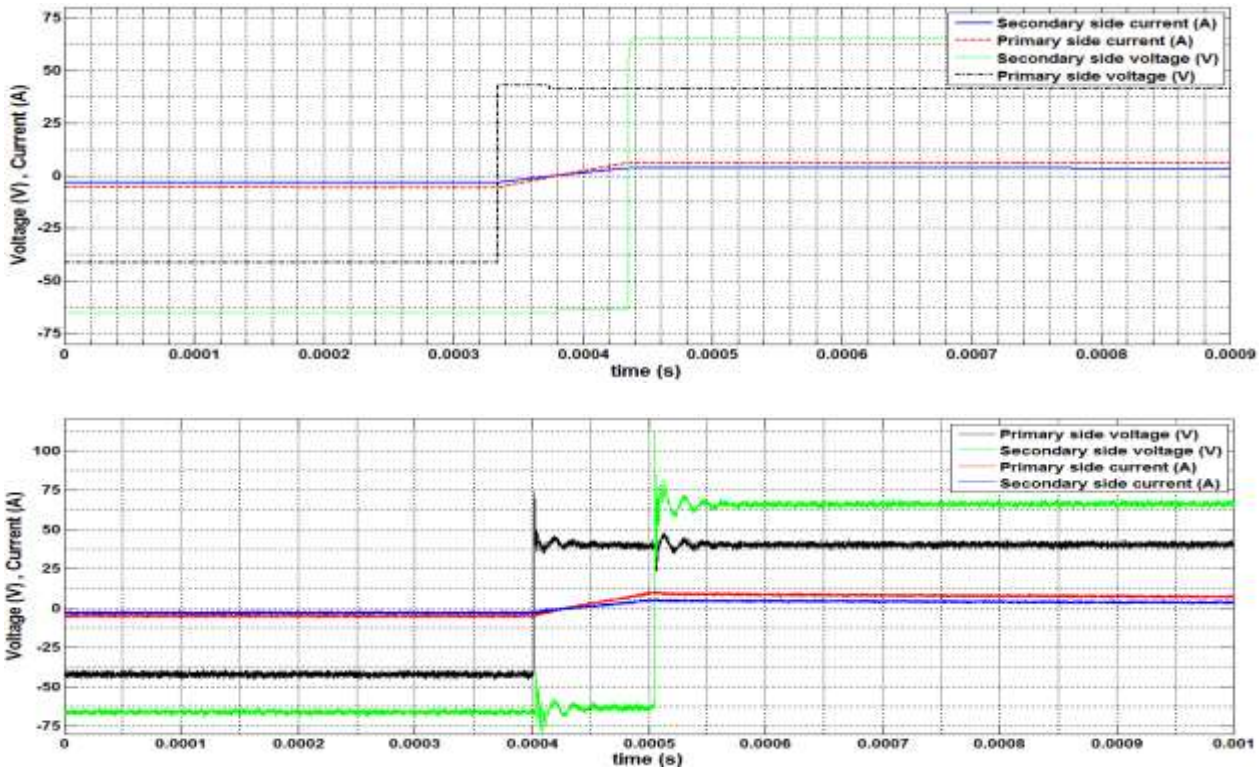

Fig. 4.34: The voltage and current waveforms in both simulation and experimental for test 2

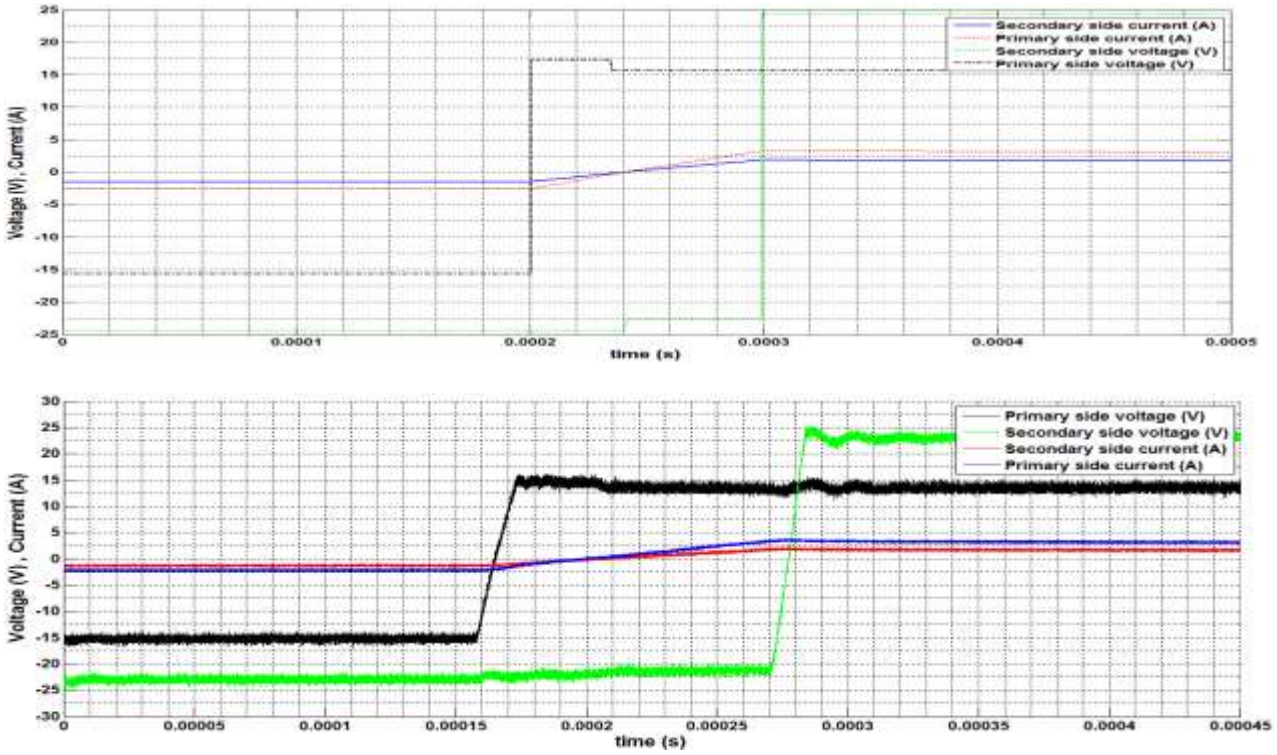

Fig. 4.35: The voltage and current waveforms in both simulation and experimental for test 3

5 Conclusion

Based on the aim of the thesis, the simulated dual active bridge converter has been verified by experimental results of the implemented DAB converter in the laboratory. As can be seen in the comparison section, all waveforms are compatible with each other though there is a little difference between the voltage levels and power losses which are due to the limitation of the measurement in the laboratory and differences between the real and ideal devices in the simulation.

The Single phase Dual active bridge has been implemented and controlled by a dSPACE controller for different frequencies like 50, 100, 500 Hz and 1 KHz. Due to the limitation of the digital implementation of the dSPACE, there is no possibility to control the DAB converter for a frequency of 5 KHz and above. The 50 Hz transformer is also a limitation to reach the higher power for the frequency of 1 KHz.

The three phase dual active bridge is also implemented and controlled by 12 signals from a dSPACE controller for difference frequencies of 55 Hz and 555 Hz. As mentioned earlier, due to the limitation of the controller, it's not possible to increase the frequency. In terms of power, the maximum transferred power of 1.5 KW has been reached.

The effect of the snubber capacitor on the switches is also tested, analyzed and discussed for the single and three phase dual active bridges.

The losses calculation shows that the losses in the three phase Dual active bridge is in the higher level than the single phase dual active bridge converter due to the higher number of switches. The results show that for the higher frequency, losses are increased which can be due to the higher switching losses and also can be due to the 50Hz transformer which is used for the higher frequency.

6 Future Work

The main purpose of this thesis was to implement and control the single and three phase DAB converter by using the dSPACE controller. As mentioned earlier, the dSPACE controller has some limitation in order to implement the little phase shift between two bridges of the DAB converter especially for three phase DAB converter and for high frequency. In this case, one issue for the future work can be to solve this problem and limitation. According to the discussion and investigation which have been done, a DSP can be a good option to be used as a controller for DAB converters.

The other limitation of the current thesis was the lack of high frequency transformer in the laboratory. The second improvement in this case can be designing of the single and three phase high frequency transformers for the DAB converter. In this case, more accurate loss calculation can be done for both the single and three phase DAB converters.

By using the DSP controller and a high frequency transformer with the current available converter in the laboratory, much higher output powers can be reached for both the single and three phase dual active bridges although the available converters also have some limitations in terms of voltage and current level.

The comparison can be done between the single and three phase dual active bridge as well for the exactly same condition for the both converters.

7 References

1. Rik W. A. A. De Doncker, Deepakraj M. Divan, andMustansir H. Kheraluwala," A Three-phase Soft-Switched High-Power-Density dc /dc Converter for High-Power Applications", IEEE Transactions on industry applications, Vol. 27, No. 1, January and February 1991.

2. M. Z. Jacobson, M. A. Delucchi, "Providing all global energy with wind, water, and solar power, Part I:Technologies, energy resources, quantities and areas of infrastructure and materials", Energy Policy 39 (2011), 1154–1169

3. P. Karlsson, M. Bojrup, M. Alaküla and L. Gertmar, "zero voltage switching converters", Industrial electrical Engineering and Automation, Lund university.

4. N. Mohan, T. Undeland, W. P. Robbins, "Power Electronic converters, application and design", John Wiley & sons, 1989

5. B. Zhao, Q. Song, W. Liu, Y. Sun, "Overview of Dual-Active-Bridge Isolated Bidirectional DC-DC Converter for High-Frequency-Link Power-Conversion System", DOI10.1109/TPEL.2013.2289913, IEEE Transactions on Power Electronics

6. M. Fazli, M. Mobarrez, "Design, simulation and evaluation of two different topologies for the 2.4 MW 4/6 kV DC-DC fullbridge converter", Master thesis, Chalmers university, 2012

7. D. Graovac, M. Purschel, "IGBT Power Losses Calculation using the Data-Sheet parameters", Infineon, January 2009

8. SKM 300GB125D, " Semikron IGBT module", Data sheet, SEMIKRON Ltd, 2009

9. DS1103 PPC controller board, " dSPACE controller ", Catalog, dSPACE GmbH, 2013

10. Voltechnotes, "Measuring leakage inductance", Voltech Instruments Ltd, 2001

8 Appendix

Appendix 1: the technical details of the DS 1103 PPC controller board of dSPACE

Technical Details

Parameter		Specification
Processor	PowerPC Type	■ PPC 750GX
	CPU clock	■ 1 GHz
	Cache	■ 32 KB level 1 (L1) instruction cache ■ 32 KB level 1 (L1) data cache ■ 1 MB level 2 (L2)
	Bus frequency	■ 133 MHz
	Temperature sensor	■ Reads actual temperature at the PPC
Memory	Local memory	■ 32 MB application SDRAM as program memory, cached
	Global memory	■ 96 MB communication SDRAM for data storage and data exchange with host
Timer	2 general-purpose timers	■ One 32-bit down counter ■ Reload by software ■ 15-ns resolution
		■ One 32-bit up counter with compare register ■ Reload by software ■ 30-ns resolution
	1 sampling rate timer (decrementer)	■ 32-bit down counter ■ Reload by software ■ 30-ns resolution
	1 time base counter	■ 64-bit up counter ■ 30-ns resolution
Interrupt controller		■ 3 timer interrupts ■ 7 incremental encoder index line interrupts ■ 1 UART (universal asynchronous receiver and transmitter) interrupt ■ 1 CAN interrupt ■ 1 slave DSP interrupt ■ 2 slave DSP PWM interrupts ■ 1 host interrupt ■ 4 external interrupts (user interrupts)
A/D converter	Channels	■ 16 multiplexed channels equipped with 4 sample & hold A/D converters (4 channels belong to one A/D converter. 4 consecutive samplings are necessary to sample all channels belonging to one A/D converter.) ■ 4 parallel channels each equipped with one sample & hold A/D converter ■ Note: 8 A/D converter channels (4 multiplexed and 4 parallel) can be sampled simultaneously.
	Resolution	■ 16-bit
	Input voltage range	■ ±10 V
	Overvoltage protection	■ ±15 V
	Conversion time	■ Multiplexed channels: 1 µs[1] ■ Parallel channels: 800 ns[1]
	Offset error	■ ±5 mV
	Gain error	■ ±0.25%
	Offset drift	■ 40 µV/K
	Gain drift	■ 50 ppm/K
	Signal-to-noise ratio	■ >83 dB
D/A converter	Channels	■ 8 channels
	Resolution	■ 16-bit
	Output range	■ ±10 V
	Settling time	■ 5 µs (14-bit)
	Offset error	■ ±1 mV
	Gain error	■ ±0.5%
	Offset drift	■ 30 µV/K
	Gain drift	■ 25 ppm/K

[1] *Speed and timing specifications describe the capabilities of the hardware components and circuits of our products. Depending on the software complexity, the attainable overall performance figures can deviate significantly from the hardware specifications.*

Parameter		Specification
D/A converter	Signal-to-noise ratio	■ >83 dB
	I_{max}	■ ±5 mA
	$C_{load,max}$	■ 10 nF
Digital I/O	Channels	■ 32-bit parallel I/O ■ Organized in four 8-bit groups ■ Each 8-bit group can be set to input or output (programmable by software)
	Voltage range	■ TTL input/output levels
	$I_{out,max}$	■ ±10 mA
Digital incremental encoder interface	Channels	■ 6 independent channels ■ Single-ended (TTL) or differential (RS422) input (software programmable for each channel)
	Position counters	■ 24-bit resolution ■ Max. 1.65 MHz input frequency, i.e.,fourfold pulse count up to 6.6 MHz ■ Counter reset or reload via software
	Encoder supply voltage	■ 5 V/1.5 A ■ Shared with analog incremental encoder interface
Analog incremental encoder interface	Channels	■ 1 channel ■ Sinusoidal signals: 1 Vpp differential or 11 µApp differential (software programmable)
	Position counters	■ < 5° resolution ■ 32-bit loadable position counter ■ Max. 0.6 MHz input frequency, i.e., fourfold pulse count up to 2.4 MHz
	A/D converter performance	■ 6-bit resolution ■ 10 MSPS
	Encoder supply voltage	■ 5 V/1.5 A ■ Shared with digital incremental encoder interface
CAN interface	Configuration	■ 1 channel based on SAB 80C164 microcontroller ■ ISO DIS 11898-2 CAN high-speed standard
	Baud rate	■ Max. 1 Mbit/s
Serial interface	Configuration	■ TL6C550C single UART with FIFO ■ PLL-driven UART for accurate baud rate selection ■ RS232/RS422 compatibility
	Baud rate	■ Up to 115.2 kBd (RS232) ■ Up to 1 MBd (RS422)
Slave DSP	Type	■ Texas Instruments TMS320F240 DSP
	Clock rate	■ 20 MHz
	Memory	■ 64 Kx16 external code memory ■ 28 Kx16 external data memory ■ 4 Kx16 dual-port memory for communication ■ 32 KB flash memory
	I/O channels[1]	■ 16 A/D converter inputs ■ 10 PWM outputs ■ 4 capture inputs ■ 2 serial ports
	Input voltage range	■ TTL input/output level ■ A/D converter inputs: 0 … 5 V
	Output current	■ Max. ±13 mA
Host interface		■ Plug & Play support ■ Requires a full-size 16-bit ISA slot
Physical characteristics	Physical size	■ 340 x 125 x 45 mm (13.4 x 4.9 x 1.77 in)
	Ambient temperature	■ 0 … 50 °C (32 … 122 °F)
	Cooling	■ Passive cooling
	Power supply	■ +5 V ±5%, 4 A ■ +12 V ±5%, 0.75A ■ -12 V ±5%, 0.25A

[1] *The exact number of I/O channels depends on your configuration and is described in the user documentation.*

Appendix 2: The technical details of the SEMIKRON IGBT and diodes

SKM 300GB125D

SEMITRANS® 3

Ultra Fast IGBT Module

SKM 300GB125D

Features

- NPT - Non punch-through IGBT
- Low inductance case
- Short tail current with low temperature dependence
- High short circuit capability, self limiting
- Fast & soft inverse CAL diodes
- Isolated copper baseplate using DCB Direct Copper Bonding Technology
- Large clearance (10 mm) and creepage distances (20 mm)

Typical Applications*

- Switched mode power supplies at f_{sw} > 20 kHz
- Resonant inverters up to 100 kHz
- Inductive heating
- UPS Uninterruptable power supplies at f_{sw} > 20 kHz
- Electronic welders at f_{sw} > 20 kHz

Absolute Maximum Ratings T_c = 25 °C, unless otherwise specified

Symbol	Conditions		Values	Units
IGBT				
V_{CES}	T_j = 25 °C		1200	V
I_C	T_j = 150 °C	T_{case} = 25 °C	300	A
		T_{case} = 80 °C	210	A
I_{CRM}	I_{CRM}=2xI_{Cnom}		400	A
V_{GES}			± 20	V
t_{psc}	V_{CC} = 600 V; V_{GE} ≤ 20 V; V_{CES} < 1200 V	T_j = 125 °C	10	µs
Inverse Diode				
I_F	T_j = 150 °C	T_{case} = 25 °C	260	A
		T_{case} = 80 °C	180	A
I_{FRM}	I_{FRM}=2xI_{Fnom}		400	A
I_{FSM}	t_p = 10 ms; sin.	T_j = 150 °C	1800	A
Module				
$I_{t(RMS)}$			500	A
T_{vj}			- 40...+ 150	°C
T_{stg}			- 40...+ 125	°C
V_{isol}	AC, 1 min.		4000	V

Characteristics T_c = 25 °C, unless otherwise specified

Symbol	Conditions		min.	typ.	max.	Units
IGBT						
$V_{GE(th)}$	V_{GE} = V_{CE}, I_C = 8 mA		4,5	5,5	6,5	V
I_{CES}	V_{GE} = 0 V, V_{CE} = V_{CES}	T_j = 25 °C		0,1	0,3	mA
V_{CE0}		T_j = 25 °C		1,5	1,75	V
		T_j = 125 °C		1,7		V
r_{CE}	V_{GE} = 15 V	T_j = 25°C		9	10,5	mΩ
		T_j = 125°C		11,5		mΩ
$V_{CE(sat)}$	I_{Cnom} 200 A, V_{GE} 15 V	T_j °C chiplev.		3,3	3,85	V
C_{ies}	V_{CE} = 25, V_{GE} = 0 V	f = 1 MHz		18	24	nF
C_{oes}				2,5	3,2	nF
C_{res}				1	1,3	nF
Q_G	V_{GE} = 0V - +20V			2000		nC
R_{Gint}	T_j = °C			2,5		Ω
$t_{d(on)}$	R_{Gon} = 3 Ω	V_{CC} = 600V		130		ns
t_r		I_C= 200A		40		ns
E_{on}		T_j = 125 °C		16		mJ
$t_{d(off)}$	R_{Goff} = 3 Ω	V_{GE} = ± 15V		460		ns
t_f				30		ns
E_{off}						mJ
$R_{th(j-c)}$	per IGBT				0,075	K/W

SKM 300GB125D

SEMITRANS® 3

Ultra Fast IGBT Module

SKM 300GB125D

Features

- NPT - Non punch-through IGBT
- Low inductance case
- Short tail current with low temperature dependence
- High short circuit capability, self limiting
- Fast & soft inverse CAL diodes
- Isolated copper baseplate using DCB Direct Copper Bonding Technology
- Large clearance (10 mm) and creepage distances (20 mm)

Typical Applications*

- Switched mode power supplies at f_{sw} > 20 kHz
- Resonant inverters up to 100 kHz
- Inductive heating
- UPS Uninterruptable power supplies at f_{sw} > 20 kHz
- Electronic welders at f_{sw} > 20 kHz

Characteristics

Symbol	Conditions		min.	typ.	max.	Units
Inverse Diode						
$V_F = V_{EC}$	I_{Fnom} = 200 A; V_{GE} = 0 V	T_j = 25 °C$_{chiplev.}$		2	2,5	V
		T_j = 125 °C$_{chiplev.}$		1,8		V
V_{F0}		T_j = 25 °C		1,1	1,2	V
		T_j = 125 °C				V
r_F		T_j = 25 °C		4,5	6,5	mΩ
		T_j = 125 °C				mΩ
I_{RRM}	I_F = 200 A	T_j = 125 °C		340		A
Q_{rr}	di/dt = 8000 A/µs			46		µC
E_{rr}	V_{GE} = 0 V; V_{CC} = 600 V					mJ
$R_{th(j-c)D}$	per diode				0,18	K/W
Module						
L_{CE}				15	20	nH
$R_{CC'+EE'}$	res., terminal-chip	T_{case} = 25 °C		0,35		mΩ
		T_{case} = 125 °C		0,5		mΩ
$R_{th(c-s)}$	per module				0,038	K/W
M_s	to heat sink M6		3		5	Nm
M_t	to terminals M6		2,5		5	Nm
w					325	g

This is an electrostatic discharge sensitive device (ESDS), international standard IEC 60747-1, Chapter IX.

* The specifications of our components may not be considered as an assurance of component characteristics. Components have to be tested for the respective application. Adjustments may be necessary. The use of SEMIKRON products in life support appliances and systems is subject to prior specification and written approval by SEMIKRON. We therefore strongly recommend prior consultation of our personal.

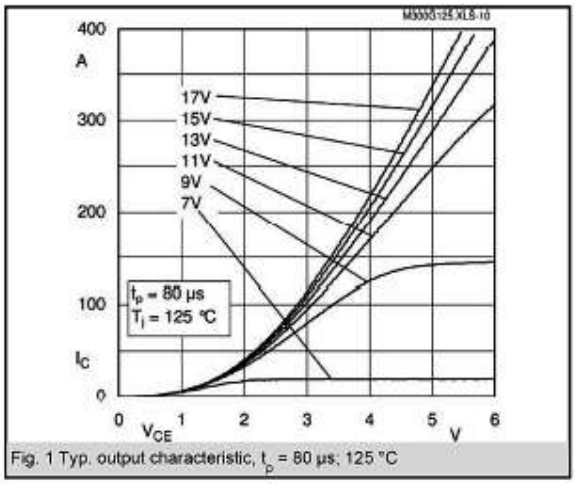

Fig. 1 Typ. output characteristic, t_p = 80 µs; 125 °C

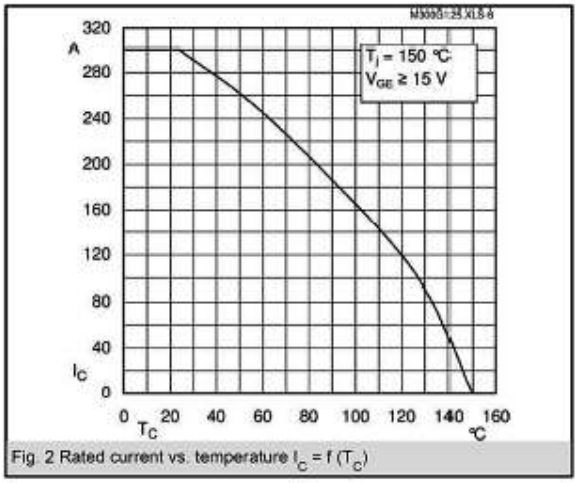

Fig. 2 Rated current vs. temperature $I_C = f(T_C)$

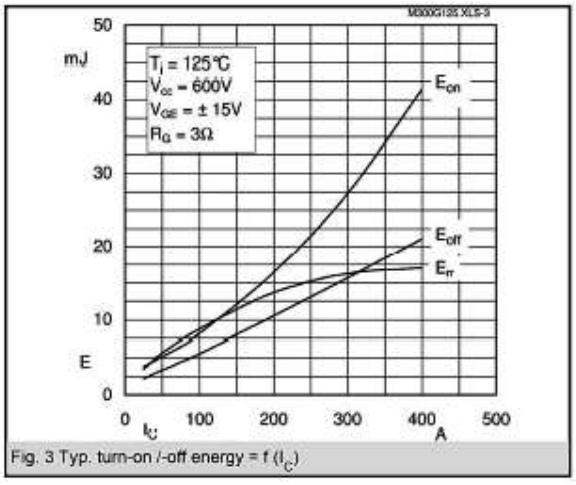

Fig. 3 Typ. turn-on /-off energy = f (I_C)

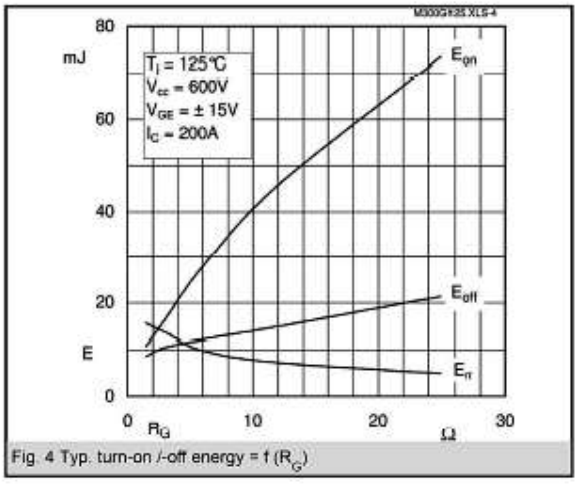

Fig. 4 Typ. turn-on /-off energy = f (R_G)

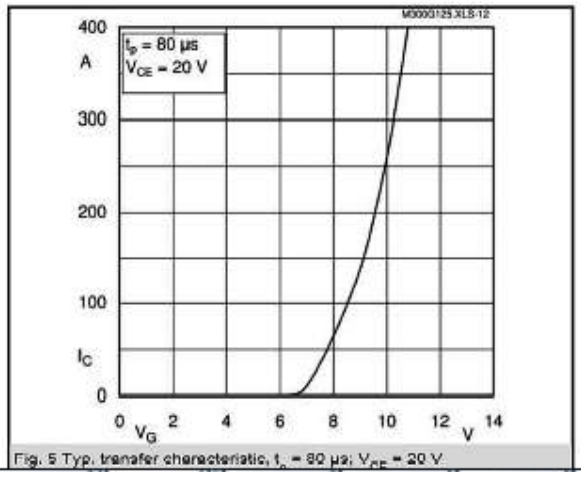

Fig. 5 Typ. transfer characteristic, t_p = 80 µs; V_{CE} = 20 V

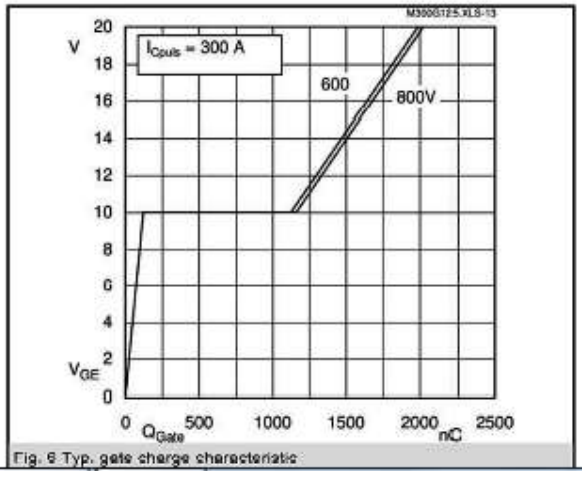

Fig. 6 Typ. gate charge characteristic

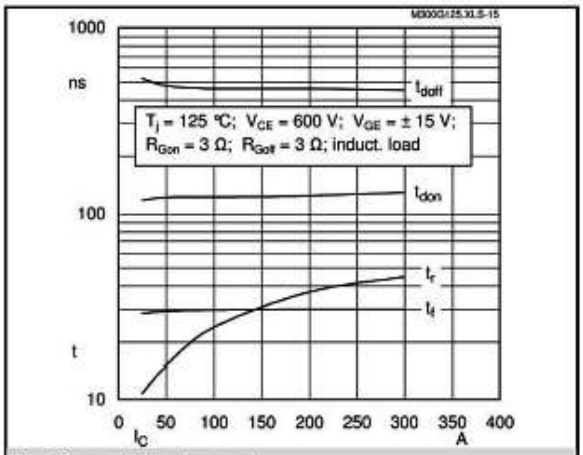

Fig. 7 Typ. switching times vs. I_C

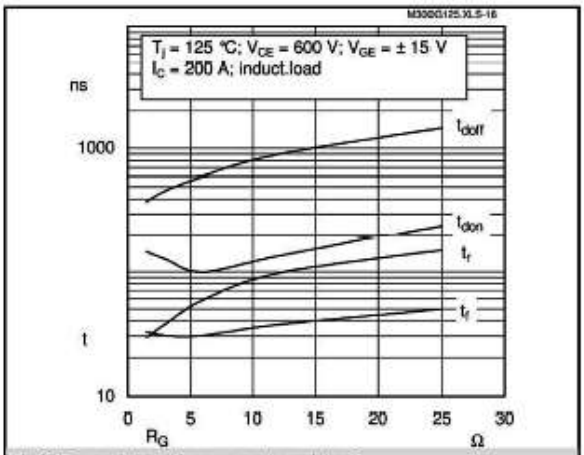

Fig. 8 Typ. switching times vs. gate resistor R_G

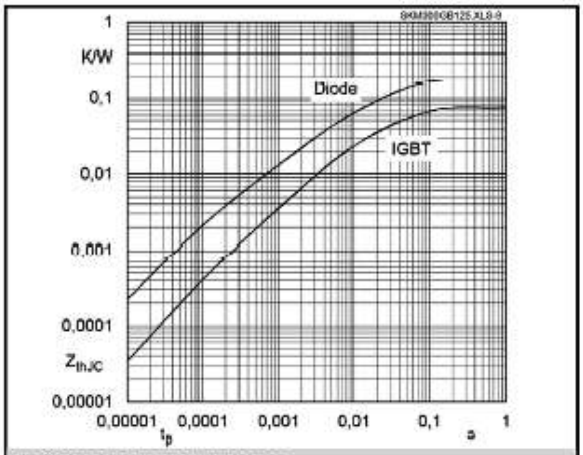

Fig. 9 Transient thermal impedance

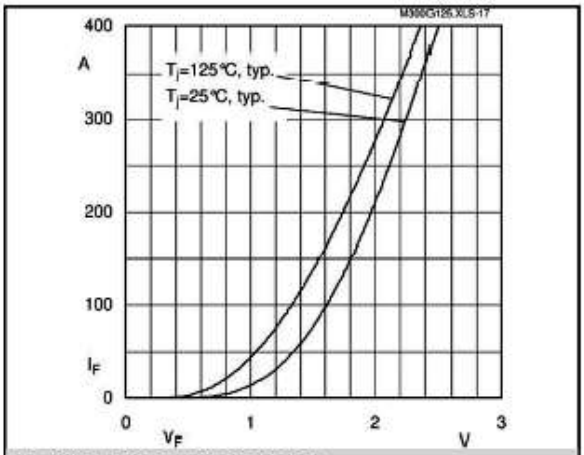

Fig. 10 CAL diode forward characteristic

Appendix 3: The schema of the Converter which is used as a inverter and rectifier